AN ABSTRACT OF THE THESIS OF

Lihan Huang for the degree of Doctor of Philosophy in Food Science and Technology

presented on June 11, 1997. Title: Application of Membrane Filtration to Recover Solids

from Protein Solutions

Signature redacted for privacy.

Abstract approved: _____

Michael T. Morrissey

Water and waste water accounting was conducted in a shore-based surimi

processing plant. A process flow diagram of the plant was developed and sources of

waste water generation were identified. Waste water samples were collected, analyzed,

and characterized. The gutting and first dewatering operations were two major sources

of the solid wastes (COD, BOD_5, and TS), contributing to 60% of total solid wastes. For

every 1 kg of fish processed into frozen surimi, approximately 5.7 L of waste water was

generated. To process 132×10^3 kg of fish, total waste water generated was 750 m^3 per

day, of which 63% (473 m^3) was generated in the washing-dewatering processes.

Ohmic heating was used to coagulate fish proteins and partially purify proteolytic

enzymes in surimi wash water prior to membrane filtration. At temperatures above 60°C,

more than 80% and 90% of protein and TSS, respectively, were removed. Between 30

and 60°C, the proteolytic enzyme activity increased linearly with heating temperature.

Denaturation caused a substantial loss of enzyme activity at temperatures above 60°C.

A laboratory scale plate-and-frame crossflow membrane filtration unit was used

to recover myofibrillar proteins from surimi wash water. Four different microfiltration

membranes were used in the study. It was hypothesized that the development of

membrane fouling was a dynamic process of two distinctive stages. Experimental results showed that the initial membrane fouling process could be modeled by the standard pore blocking law, and the development of fouling continued with a continuous process of cake formation. A new concentration-dependent power law cake resistance model was proposed and verified. The filtration resistance of the cake layer increased with the feed concentration and was found one order in magnitude higher than the initial dominating pore blocking resistance.

Finite element analysis was used to simulate the concentration polarization in ultrafiltration of protein solutions. Protein concentration on the membrane surface and the mass transfer coefficient were accurately predicted. This simulation method may provide a useful tool in engineering analysis and design of a membrane filtration process.

APPLICATION OF MEMBRANE FILTRATION TO RECOVER SOLIDS

FROM PROTEIN SOLUTIONS

By

Lihan Huang

A THESIS

Submitted to

Oregon State University

in partial fulfilment of the requirements for the

degree of

Doctor of Philosophy

Completed June 11, 1997

Commencement June 1998

ACKNOWLEDGMENTS

To my wife,

Ying

and to my daughter,

Meghan

TABLE OF CONTENTS

TABLE OF CONTENTS (Continued)

TABLE OF CONTENTS (Continued)

LIST OF FIGURES

LIST OF FIGURES (Continued)

LIST OF FIGURES (Continued)

LIST OF TABLES

LIST OF TABLES (Continued)

APPLICATION OF MEMBRANE FILTRATION TO RECOVER SOLIDS FROM PROTEIN SOLUTIONS

1. INTRODUCTION

1.1 Issues of Waste Water from the Surimi Industry

Surimi is a Japanese term for washed and dewatered fish mince that is widely used in manufacturing kamoboko or seafood analogs (Lee, 1984). Since it was introduced to North America about 15-20 years ago, the surimi manufacturing industry has experienced a steady growth. According to Park (1997), the U.S. annual production of frozen pollock surimi was 180-190,000 metric tons in the past three years.

Commercial production of surimi involves extensive use of water in various processing procedures. Apart from the conventional use of water in handling raw materials (handling, heading, gutting, and washing operations), large volumes of water are used to remove sarcoplasmic proteins and other unnecessary compounds in the fish flesh and to concentrate myofibrillar proteins by means of repeated washing and dewatering until a tasteless and odorless product is obtained. Quality of surimi is highly dependent on the washing operations.

As a consequence of extensive washing, a large volume of waste water is generated from the downstream dewatering operations. Not only the soluble proteins are removed from the fish mince, but also some insoluble myofibrillar proteins, are also lost in the water. According to Pacheco-Aguilar et al. (1989), 40-50% of the minced fish solids are lost in the washing and dewatering processes.

Depending on the location of the processing plants, there are different ways of

disposing of the waste water. At-sea surimi processing vessels discharge waste water directly to the open sea where organic wastes are readily dispersed. Although there is little concern of pollution caused by the disposal of surimi waste water on the high seas, there is an interest in reclaiming reusable water from the waste streams.

Disposing of waste water is more of a challenge for shore-based surimi processors. Since the waste water is high in the biological oxygen demand (BOD), chemical oxygen demand (COD), and total solids (TS), waste water disposal is strictly controlled by environmental regulatory authorities. For plants along the coast, limited amounts of waste water may be directly discharged with permission from the environmental regulatory authorities to bays or local rivers. Besides unpleasant odors generated from decaying organic materials in the waste water, concerns of negative environmental impacts caused by high concentrationsof organic substances has increased in the past few years. Although not toxic, the organic materials in the waste water may be utilized by aerobic microorganisms in the water, leading to oxygen depletion, which may in return threaten native aquatic organisms.

For plants located in the cities and towns where a direct discharge of waste water into the river is not allowed, waste water has to go through treatment procedures in the local waste water treatment plants. Costs of industrial waste water treatment are high, and can run upwards of $30,000 per month (CH2M Hill, 1993).

Unlike the waste water from other industries that generate toxic wastes, the waste water from surimi processing plants contains soluble and insoluble proteins that make up about 50% of the solids in the washed fish mince (Mohr at al., 1989). There may be

potential benefits from recovering proteins in the waste water. Soluble solids, including enzymes and polypeptides may retain activity and have a potential use if preferentially recovered. Moreover, the suspended solids, mainly myofibrillar proteins, if recovered, retain gel functionality and can be added back in surimi to increase the yield (Lin et al., 1995).

1.2 Research objectives

The objectives of this thesis are:

1. to understand how water is consumed and how waste water is generated in shore-based surimi processing plants;

2. to identify characteristics of waste water generated in surimi processing plants.

3. to develop technologies, particularly membrane filtration, to recover functional proteins from the waste water, and to reduce amount of solids in the waste water.

4. to investigate mechanisms of membrane fouling that greatly hamper the efficiency of microfiltration, and,

5. to analyze the membrane filtration process by numerical simulation.

2. LITERATURE REVIEW

2.1 Waste water from surimi processing industry

2.1.1 Surimi manufacturing process

The history of surimi can be dated to A.D. 1000 when the Japanese started using fresh fish mince to make Kamaboko, a Japanese fish sausage (Okada, 1992). Modern large scale industrial production was not possible until 1959 when the technique for cryoprotection of surimi was discovered (Matsumoto, 1978). Since then, the world surimi manufacturing industry has experienced a tremendous growth. The Japanese surimi operation expanded from small scale shore-based production to larger scale at-sea operations in the Bering Sea where fishing fleets processed freshly caught Alaska pollock into frozen surimi. To utilize the abundant resource of Alaska pollock in the U. S., both at-sea and shore-based surimi operations were established in Alaska. In 1995, 2.85 billion lbs of Alaska pollock were harvested with a total production of 177.9 thousand mt of pollock surimi (Johnson, 1996). With the discovery of protease inhibitors, underutilized fish species such as Pacific whiting were found suitable for making surimi. Since 1992, four processing plants have been set up in Oregon to manufacture Pacific whiting into frozen surimi. The annual U. S. harvest and processing of Pacific whiting has increased from 20,000 mt in 1990 to more than 200,000 mt in 1994 with the majority of the harvest used for surimi production (Radtke, 1995).

Surimi processing can be divided into two major stages involving several unit operations that process raw materials to frozen surimi (Fig. 1). The first stage includes unit operations (heading, gutting, deboning, and mincing) that prepare fish mince for the second stage washing. Streams of water are injected to the heading, gutting, and deboning machines to remove fish fluid and muscles that stick to the machines, and to provide lubrication for smooth operation. After fish are comminuted into 3-4 mm in diameter, fish mince is pumped to the second stage.

In the second stage, fish mince is repeatedly washed with chilled water. Washing and dewatering represent two critical operations to produce high quality surimi. The major objective of washing and dewatering is to remove soluble sarcoplasmic proteins, lipids, fish blood, and other water soluble matter in the flesh as well as to concentrate myofibrillar proteins. Depending on the freshness of raw fish and the desired surimi quality, water/mince ratio and the number of washing cycles may differ. For at-sea surimi operations where fresh fish are readily available and water is limited, only one washing cycle is used, while washing may be repeated 3-5 times for shore-based production (Lee, 1984; 1986; Lin, 1996).

In commercial operations, continuous washing is achieved using several washing tanks working in sequence (Fig. 2). Each washing is actually a batch operation, in which fish mince is mixed with a certain amount of chilled water and washed under a mild mechanical agitation. After washing, mince slurry may be dewatered using a combination of a rotary screen dehydrator, and a high speed dehydrator, which is essentially a single screw extruder with a perforated barrel. Washed mince is then pumped to a refiner to

Stage 1

Raw fish

Heading

Gutting

Deboning/mincing

Fish mince

Fresh water

Waste water

Stage 2

Fish mince

Fresh water

Washing

Dewatering

x 3-5 cycles

Refining

Screw press

Cryoprotectant

Mixing

Freezing
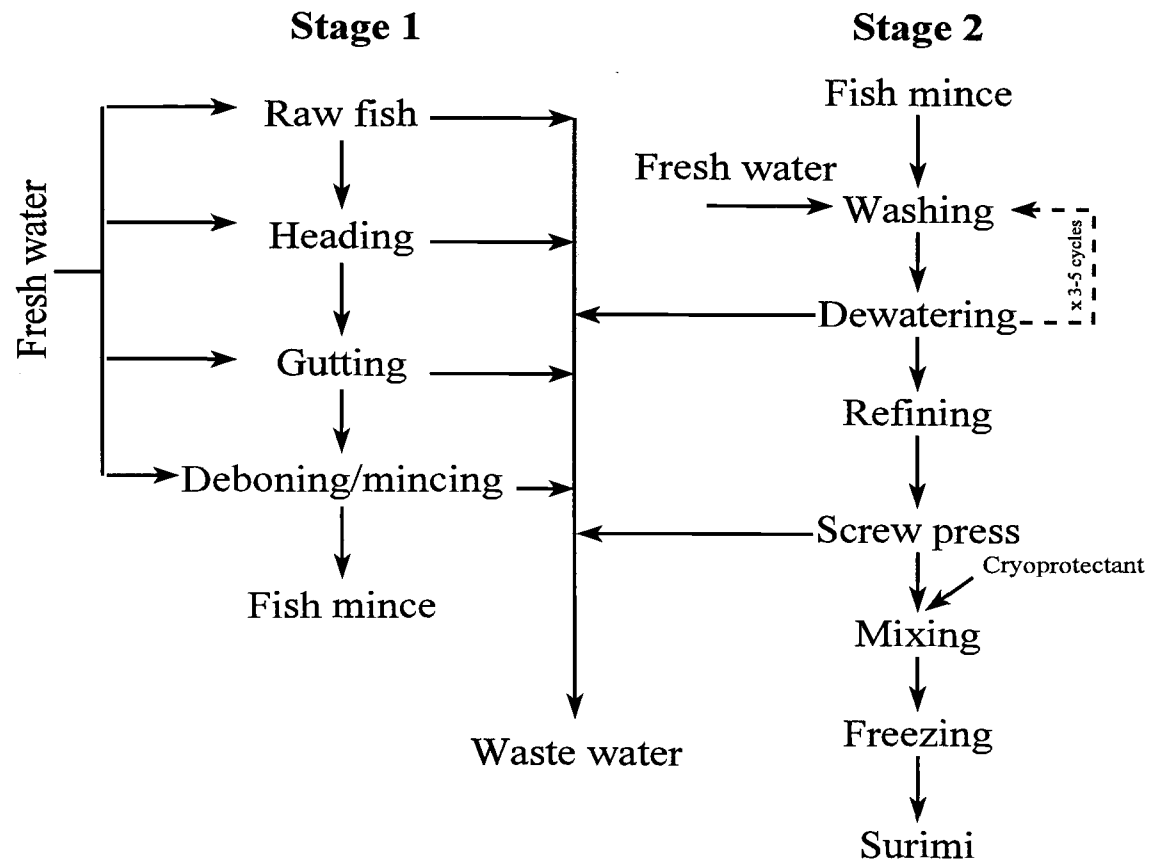
Surimi

Fig. 1 Surimi processing consists of two major stages in a typical shore-based processing plant.

9

First washing cycle

Second washing cycle

High speed dehydrator

High speed dehydrator

Rotary screen dehydrator

Rotary screen dehydrator
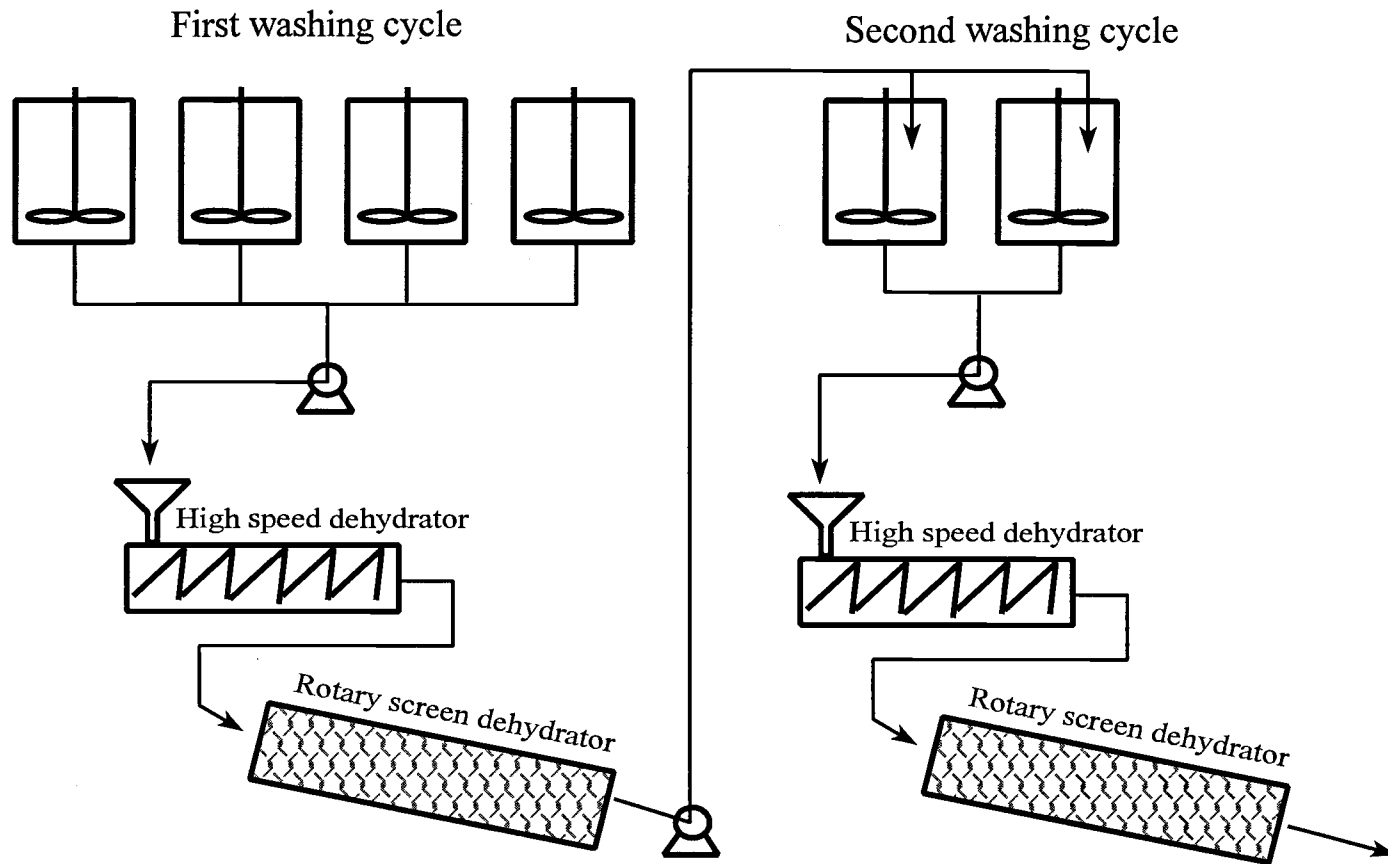
Fig. 2 Washing and dewatering operations in surimi manufacturing

remove connective tissues, and squeezed in a screw press to remove excess water. After mixing with cryoprotectants, surimi is frozen in a plate freezer.

2.1.2 Waste water generation

Surimi manufacturing consumes large volumes of fresh water in its washing procedures and consequently generates huge amounts of waste water high in BOD_5, COD, and TS. For shore-based surimi production, the overall water/meat ratio may be between 12-24 (Lin,1996). The majority of solid constituents in the waste water are soluble proteins together with fine meat particles that are lost in the wash water. During washing, soluble proteins and fine particulate material not retained by rotary screens, which account for approximately 40-50% of unwashed fish mince, are removed (Lee, 1984; Pacheco-Aguilar et al., 1989). For a typical multiple-use fish processing plant, the waste levels (BOD_5 and TSS) during processing seasons (April through September) can be 10 times as high as non-surimi seasons (Fig. 3).

Disposing of waste water poses a real challenge for shore-based surimi processors. In Oregon, if plants are located in the cities, waste water must go through publicly owned treatment works (POTWs) to reduce BOD and TS before it can be released into the local rivers. Charges for each waste water treatment facility are based on the levels of pollutants, and the total volume of waste water treated (Table 1). The plant represented in Fig. 3, which generated 50,000 gallons per day of waste water, averaged costs as high as $30,000 per month (Anonymous, 1994; CH2M Hill, 1993).
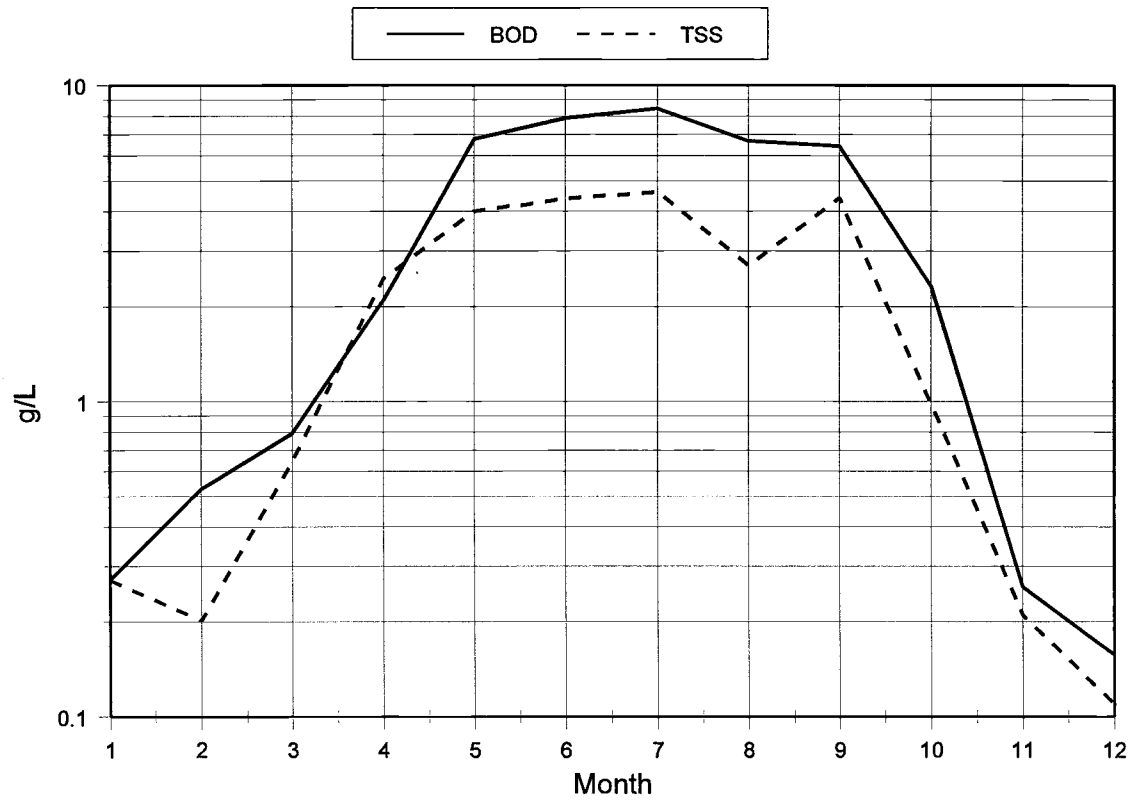
Fig. 3   Waste water effluents from a multi-purpose seafood processing plant (Anonymous, 1994)

Table 1. Demand charges for industrial waste water treatment in the City of Albany, Oregon

Pollutants	Charges
Flow	$0.30/pound
BOD	$0.32/pound
TSS*	$0.257/pound

* Total suspended solids

Limited direct discharge of waste water into local rivers and bays is allowable with permission of environmental regulatory authorities. Since waste water is high in organic loads, direct discharge can cause potential negative environmental impacts, threatening aquatic organisms in the water. The waste water effluent has to rapidly mix with the river current and the pollutants are quickly diluted to a level not harmful to the aquatic life. If direct discharge is not permitted, waste water has to be hauled away by trucks for further treatment. Waste water disposal seafood processing has been monitored and regulated by the environmental regulatory agencies since the 1960's (USEPA, 1967). Concerns of water shortage, stringent environmental regulations, and the rising costs of water disposal have caused increasing anxieties among surimi manufacturers.

2.2 Technologies for waste water treatment and product recovery

Generally, the objective of waste water treatment is to clean it up by removing organic or inorganic solids. If the effluent contains valuable solids that are worth recovering, waste water treatment is actually a product recovery process. Waste water can be treated by chemical, biological, and physical methods. Chemical methods involve the application of chemical agents to coagulate soluble and insoluble materials from the waste water. Biological methods utilize natural occurring microorganisms to digest the organic materials. Upon separation of the microbiological cells from the treated waste water, the organic load in the effluent is significantly reduced. Physical methods use screens, sand bed filters and, more recently, membrane filters, and other mechanical actions to remove the solids. Usually, a combination of these methods may be used to achieve effective

removal of waste materials in the waste water. The effectiveness of solids removal, costs of chemicals, and costs of equipment and maintenance are major factors to consider when selecting a waste water treatment facility.

2.2.1 Chemical methods

Adjusting the pH of the waste water to the isoelectric point of the proteins is the simplest approach for pretreating waste water. As the pH approaches the isoelectric point, due to the lack of the electrostatic repulsion between the protein particles, they tend to aggregate, grow in size and, finally, precipitate. The sedimented proteins can be easily separated from the waste water (Cheftel et al., 1985).

Soluble ferric and aluminum salts, and their polymeric forms (such as polyaluminum hydrochlorides), are the most commonly used inorganic coagulants (Lind, 1995). High charge density synthetic polymers (polyelectrolytes), such as polyacrylamide, polyDADMAC (dimethyl diallyl diammomiumchloride), and EPIXDMA (epichorohydrin/dimethyl amine), are widely used in place of aluminum- and iron-based coagulants (Kasper and Reichenberger, 1983; Lind, 1995). Although these polymeric coagulants are highly efficient (~10 ppm), less expensive, and suitable for a wider range of pollutants they are, basically, polymeric chains containing large amounts of amine groups (Fig. 4) that are potentially toxic to human and animals and are not biodegradable. Acrylamide, the monomer of polyacrylmide, is a highly neurotoxic chemical. Applying polyacrymide to foods is prohibited. No synthetic chemical coagulants have been
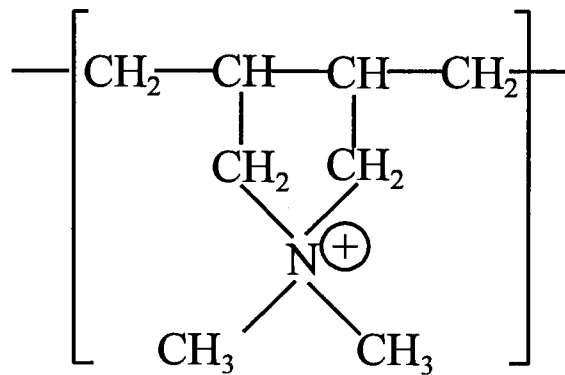
PolyDADMAC
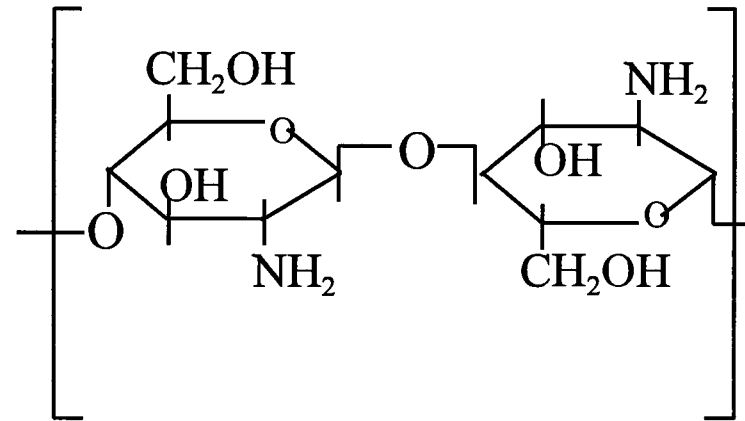
Chitosan

Fig. 4 Chemical structures of synthetic and natural polymeric coagulants

approved for food applications. Coagulated proteins may not be suitable for human or animal consumption, and can only be used for landfill.

Similar to synthetic polyelectrolytes, chitosan, a by-product of seafood processing, is a naturally occuring polysaccharide containing positively charged amine groups (Fig. 4). Since it carries positive changes at acidic conditions, it can attract and destabilize negatively charged pollutants in the water. Depending on the nature of the waste water, effectiveness of chitosan in protein recovery may differ (Table 2). Chitosan is partially deacetylated chitin, which is a natural polymer found in the shells of shellfish. Since chitosan is biodegradable and non-toxic in nature, it is an ideal candidate for recovering protein from the waste water (Bough et al., 1975; Knorr, 1991). However, in comparison to other synthetic coagulants, a large scale application of chitosan for waste water treatment is cost prohibitive. In recent years, the increased worldwide demand of chitosan for cosmetic and pharmaceutical applications has led to soaring prices (>$20/lb) for chitosan (Ludlow, 1997).

Harrison et al. (1992) conducted a series of tests to treat waste water from blue crab processing facilities. Concentrated sulfuric acid was used to adjust the pH of the waste water samples to 2.0, 3.0, 4.0, 5.0, and 6.0, respectively. It was found that a range between 3.0 to 4.0 seemed to be the optimum pH for solids removal. Reductions in COD, BOD_5, TSS, and protein ranged 12%-37%, 6-30%, 76-93%, and 0-24%, respectively. Final effluents after acidification still showed high BOD_5 (2.03-22.4 g/L) and TSS (0.05-1.05 g/L), suggesting that acidification alone might not be effective in solids removal.

Table 2 Effectiveness of Chitosan in protein recovery (Knorr, 1991)

Protein source	Chitosan concentration (mg/L)	pH	Crude protein content of coagulated solids (% dry solids)
Cheese processing	2.5-15	6.0	78
Fruitcake processing	2	4.5	13-22
Meat processing	5-30	6.0-7.3	41
	15-40	7.4	32-51
Poultry processing	6-30	6.4-6.7	34-68
Crawfish processing	150	6.0	27
Mussel processing	40	4.5	38
Shrimp processing	60-360	5.5-6.0	65

Watanabe (1974) used both inorganic and organic to coagulate proteins from marine processing waste water containing fish blood. Waste water was first heated to 70°C, then coagulated with 200 mg/L $Al_2(SO_4)_3$, and 10 mg/L of a polymeric coagulant. After filtration, 65-70% and 75-80% reduction in BOD and COD, respectively, were achieved.

Rusten et al. (1990) studied the efficiency of using $FeCl_3$ and $Al_2(SO_4)_3$ to remove organic matters in dairy and slaughterhouse waste water. It was found that pH affects the coagulation efficiency, with optimum pH dependent upon the chemical agent and dosage. After proper adjustment of pH, up to 90% of COD can be reduced by the addition of 0.10-0.15 mg/L $FeCl_3 \cdot 6H_2O$/mg COD or 0.20 mg/L $Al_2(SO_4)_3 \cdot 18H_2O$/mg COD.

Johnson and Gallanger (1984) compared the efficiency of ferric sulfate and chitosan in removing organic substances from the waste water of seafood processing plants. Effluents of crab, shrimp, and salmon processing were tested with different levels of ferric salts and chitosan. Up to 99% removal of TSS was observed, with chitosan being more effective. They concluded that, although effective, treatment of seafood waste water with both coagulants was not economical for seafood processors.

In the surimi industry, polyacrylamide is used in conjunction with other technologies such as the dissolved air flotation in wastewater treatment (Ismond, 1997). Application of polyacrylamide to the waste water causes proteins to flocculate and float to the surface, improving the efficiency of the dissolved air flotation system. However, the proteins recovered with the addition of polyacrylamide are not suitable for human or animal consumption.

2.2.2 Biological methods

The solids from the food industry waste water are mostly organic solids, such as protein, peptides, amino acids, sugar and other carbohydrates, animal and vegetable fats, that can be readily degraded by microorganisms. Biological treatment is the most successful method for treating large volumes of domestic and industrial waste water. The basic principle of a biological treatment is to grow cells of microorganisms, usually bacteria, in aerobic or anaerobic conditions. In both systems, soluble organic materials are converted to clusters of biological cells that are settlable and easily separated from the waste water by sedimentation or other conventional separation methods (Fresenius et al., 1989). Although very effective in reducing organic loads in the waste water, all the potentially useful nutritive components such as proteins are completely lost.

2.2.2.1 Aerobic process

The activated sludge method is the most commonly used aerobic method in waste water treatment (Fig. 5). In Japan, surimi waste water is treated with this method after a primary treatment (Okada, 1992). With sufficient supply of oxygen to the nutrient rich waste water, organic carbohydrates (C) and proteins (N) are rapidly consumed by bacteria and other microorganisms and are converted into CO_2 and water soluble inorganics (NH_4^+). The biomass, called "activated sludge", accumulates in the form of flakes containing a rich flora of aerobic bacteria, some fungi, and some bacteria-eating protozoa. After treatment, the majority of the sludge is dewatered and can be used as agricultural fertilizer. Some of the sludge, containing active bacteria, is recycled back to the treatment

Waste water

Primary
treatment
tank

O_2

Large particles

NH_4^+

NO_3^+

Nitrification
(trickling filter)

Denitrification tank

Biomass

N_2

CO_2

Cl_2

Biomass

Activated sludge tank

Sludge

Treated waste water
(to river)
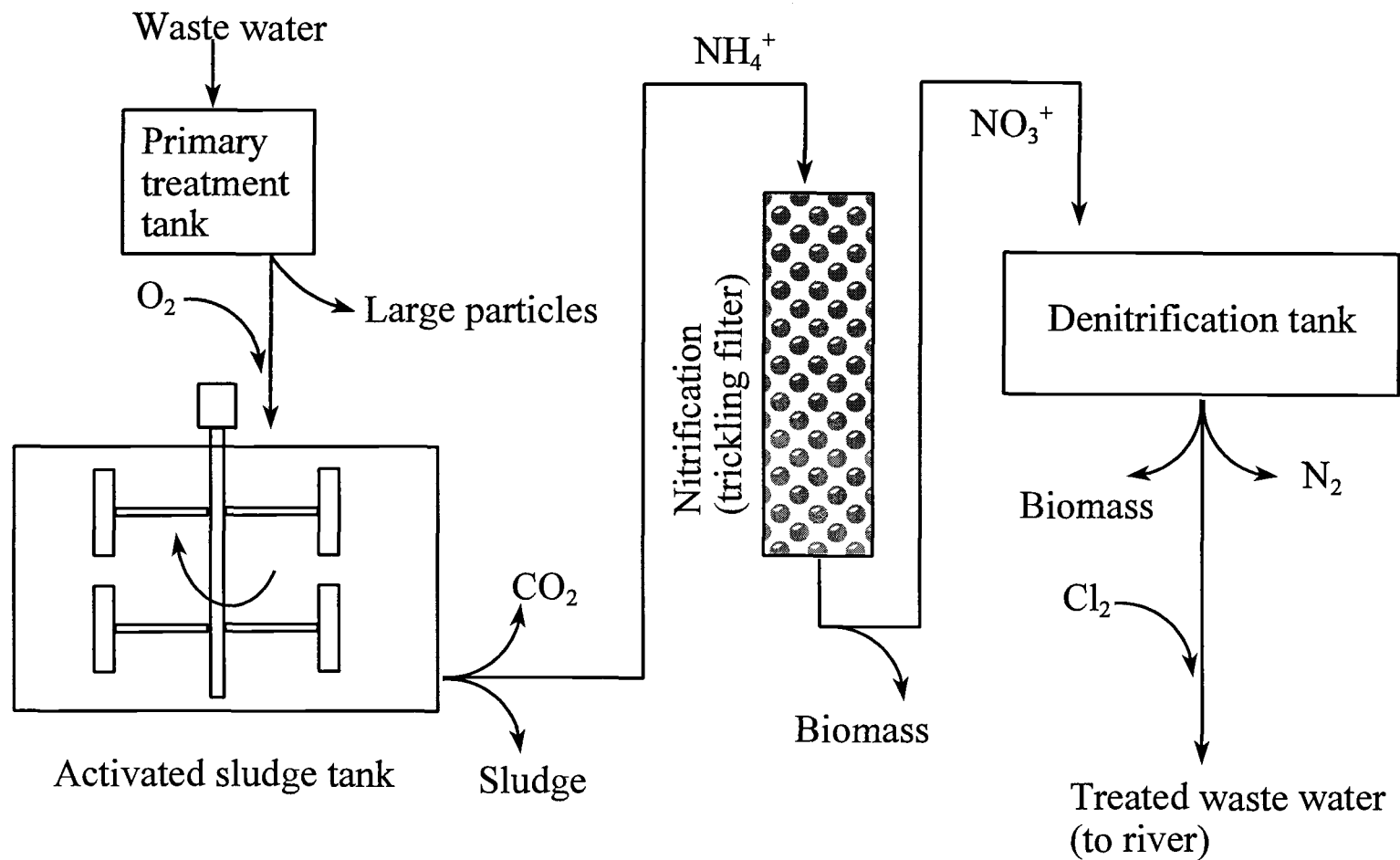
Fig. 5 Activated sludge treatment of waste water in a major waste water treatment plant

19

tank and used as a bacteria source. In a waste water treatment plant, usually another aerobic process is followed to grow lower aerobic priority bacteria. This process takes place in a trickling filter and is called a nitrification process in which NH_4^+ formed during the activated sludge treatment tank is converted to NO_3^+. The latter can be further converted into N^2 in an anaerobic process. After the complete treatment, organic matter and harmful inorganic substances in the waste water are removed. After disinfection, the treated waste water can be directly discharged to rivers (Fresenius et al., 1989).

In a case study by Mikkelson and Lowery (1992), a six-phase sequencing batch reactor (SBR) system (Fig. 6) was designed to continuously treat high strength waste water from a meat processing plant. The system was capable of handling 150,000 gallons of waste water per day. The BOD_5, TSS, and NH_3-N in the waste water were reduced from 1,000 mg/L, 200 mg/L, and 7 mg/L, respectively, to 10 mg/L, 10 mg/L, and 2 mg/L, respectively.

2.2.2.2 Anaerobic process

Seafood industry waste water can be treated with anaerobic treatment methods, since it contains high concentrations of organic matter suitable for the growth of anaerobic bacteria. Compared to aerobic treatment processes, however, anaerobic treatment is a slower process due to the slow growth rate of methanogenic bacteria. But because the process does not require aeration, it is a more economical process for treatment of waste water with high solids content (COD > 4000 mg/L), and more suitable for treatment of small quantities of waste water (Fresenius et al., 1989). The volume of sludge formed
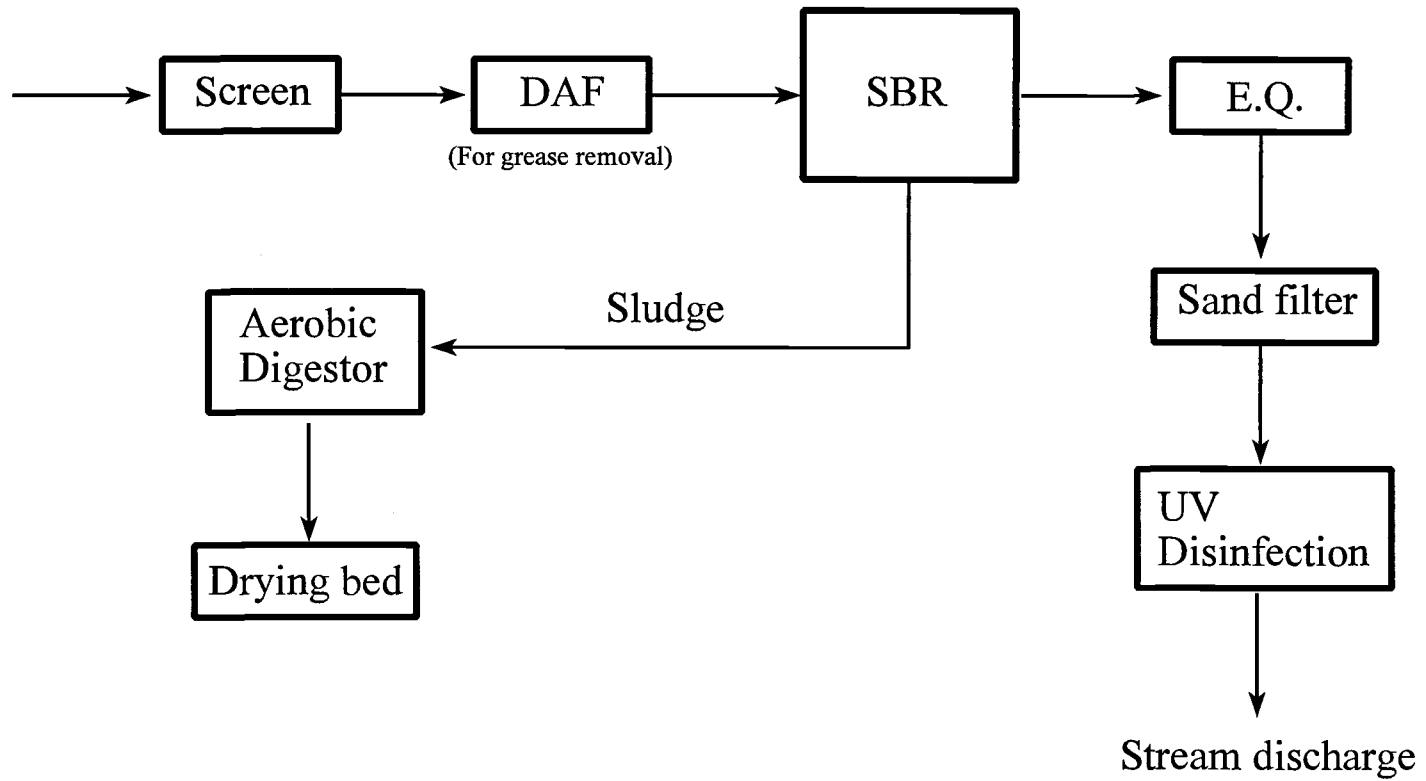
Fig. 6 A six-phase sequencing batch reactor for treatment of waste water from a meat processing plant

in an anaerobic process is smaller than that generated in an aerobic process, and the generated methane can be used as an energy source. However, the residence time for an anaerobic process is longer than that for an aerobic process (Fresenius et al., 1989).

A pilot study was conducted by Cocci et al. (1991) to treat clam processing waste water using an anaerobic treatment process (Fig. 7). After initial stabilization, COD, BOD and SS were reduced from 5874, 2342, and 976 mg/L, respectively, to 54.1, 21.6, and 9.0 mg/L, respectively. More than 80% of solids removal was achieved for all the pollutants. The authors concluded that the anaerobic process was well suited for treating clam processing waste water; no additional chemical supplement was needed, and the biogas produced was of high quality and could be used as an energy source.

2.2.3 Physical methods

Physical methods are usually used in primary treatment of waste water, and employ one or more physical principles to separate waste materials from the water phase. For the seafood processing waste water, fish heads, bones, and undersized fish in the waste water stream are examples of large matter that is separated by physical methods. In seafood processing plants, the simplest and the most widely used physical method is the use of screens to trap and prevent large materials from entering the waste stream.

2.2.3.1 Dissolved air flotation

For smaller materials, such as protein particles and particularly fats and oils, dissolved air flotation (DAF) can be used. In a DAF process, air bubbles are blown from
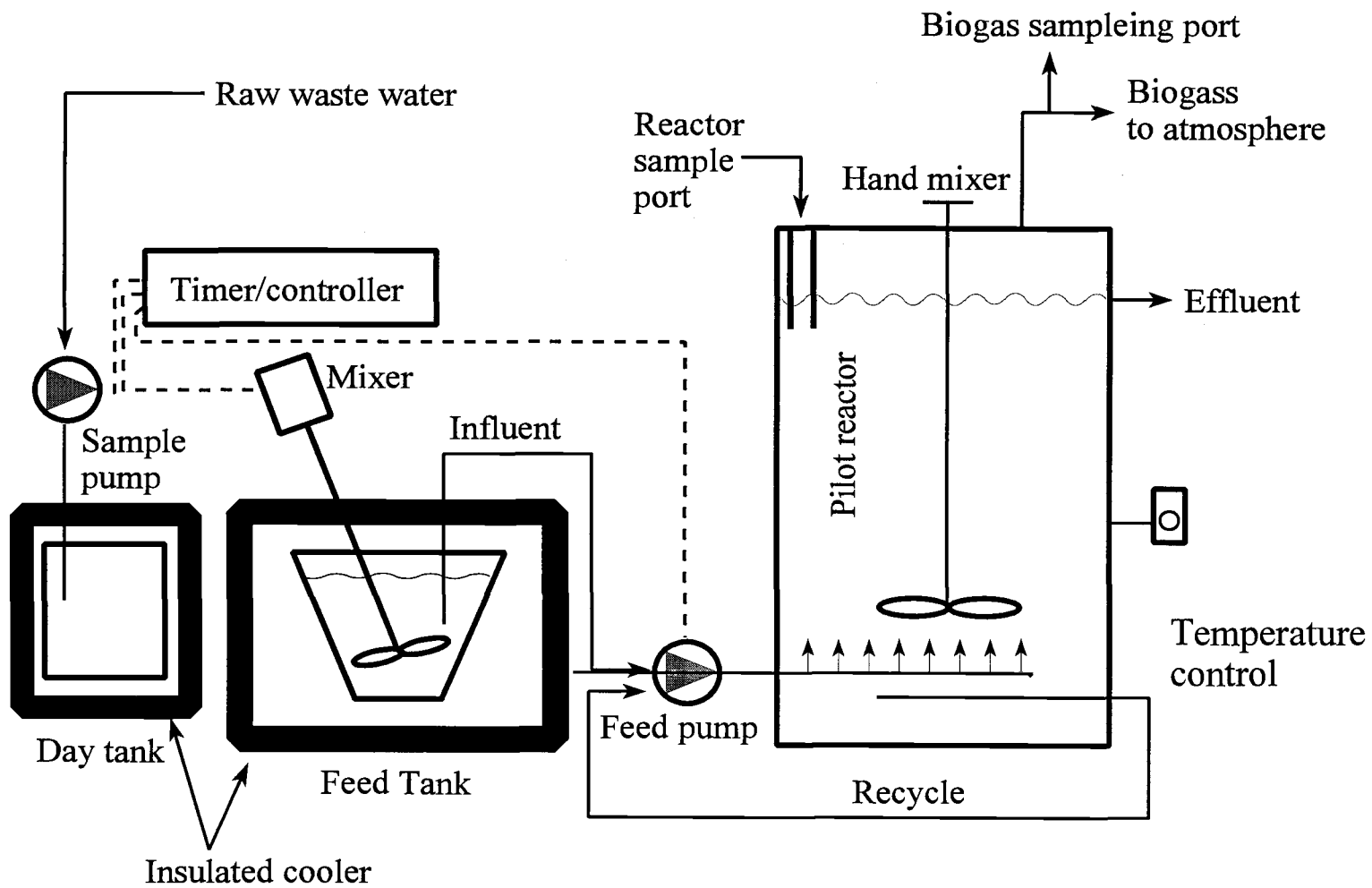
Fig. 7 An anaerobic process for treatment of waste water from a clam processing plant

the bottom of the waste water stream, causing the undissolved substances to float to the surface. As a result, a foamlike layer of solids floats upward and accumulates on the surface of the waste water stream, and can be easily skimmed off (Fresenius et al., 1989). To improve the efficiency of DAF, a foam generator is usually installed to introduce large amount of foams into the waste water stream. Depending on the types of solids in the waste water, the DAF process can be very effective, particularly for treating fat and oil containing waste water (Table 3).

Hopkins (1983) investigated the effectiveness of combined chemical coagulation and DAF operations in treatment of waste water from four poultry processing plants prior to discharge to the city waste water treatment facility. Chemical coagulating agents were applied before DAF operations. About 50-80% efficiencies of removal were observed for different solids. Since coagulation increased the sizes of protein particles, making them more difficult to float, and reduced the foaming ability of the protein, the efficiency of DAF might have been hampered.

DAF was adopted in a surimi processing plant located in Newport, Oregon. Polyacrylamide was added to the DAF unit, causing proteins in the waste water to flocculate. The protein flocci, having a lower density that water, floated to the surface of the waste water, thus reducing the consumption of compressed air (Ismond, 1997).

2.2.3.2 Heat coagulation

Heat coagulation represents another category of physical treatment that can recover proteins from the waste water for animal consumption. In a heat coagulation process, heat

Table 3 Effectiveness of DAF process on pollutant removal in the waste water (Fresenius et al., 1989)

Types of waste water	Raw water water			Clarified water			Purification effect		
	Undissolved substance	Ether soluble fat	BOD_5	Undissolved substance	Ether soluble fat	BOD_5	Undissolved substance	Ether soluble fat	BOD_5
	mg/L	mg/L	mg/L	mg/L	mg/L	mg/L	%	%	%
Edible oil production	230	460	2900	20	25	94	91.3	94.6	96.8
Cosmetics production	15000	5405	24500	1800	485	5880	88.0	91.0	76.0
Slaughter house	7428	3110	-	712	97	-	90.4	96.9	-
Meat processing	970	1706	1540	97	513	277	90.0	70.0	82.0
Poultry processing	1690	331	1075	275	74	86	83.7	77.6	92.0
Animal carcass utilization	5353	4614	-	780	775	-	95.4	83.2	-
Soy bean processing	1656	-	3000	42	-	800	97.5	-	73.4
Tomato processing	172	-	276	59	-	168	65.7	-	39.1

is supplied to elevate the temperature of waste water and this causes heat-sensitive proteins to coagulate and precipitate. The coagulated proteins can be easily removed from the waste water by conventional solid-liquid separation techniques; such as sedimentation, filtration, and centrifugation. In the dairy industry, thermal coagulation of whey protein is used as a pretreatment step to coagulate and recover whey protein (Pearce, 1992).

Generally, heat can be directly introduced to the waste water (direct heating) or transferred to the waste water through a heat exchanger (indirect heating). Direct steam injection is an example of direct heating where steam is directly injected and vigorously mixed with the waste water. The huge latent heat of steam can rapidly raise the temperature of the waste water, causing proteins to coagulate and precipitate. Since heat is in direct contact with the waste water, a relatively high energy efficiency can be achieved. However, condensation of the steam can cause an increase in the volume of waste water, often by 12% or more (Edwards and Kohler, 1981). Steam condensation not only increases the burden of the downstream dewatering operations, but also generally requires larger fluid handling equipment to cope with increased volumes.

When an indirect heating method is used, steam is supplied inside the heat exchanging tubes or plates of a heat exchanger, and heat is transferred from the steam through the wall of the heat exchanger to the waste water. As protein coagulation occurs, a considerable amount of proteins are deposited on the surface of the heating walls, causing the heat transfer resistance to increase (Sandu and Singh, 1991). Although scraped-surface heat exchangers can significantly reduce the coated foulants by a rotating shaft, these exchangers are generally very expensive and require higher operating and

maintenance costs.

Ohmic heating is a novel direct heating method, the application of which in the food industry is gaining momentum. When an alternating electric current is applied to the material to be heated, due to its electrical resistance, electric energy is directly converted to heat energy. Ohmic heating is believed to be a more energy efficient method, and has been developed in the food industry to aseptically process liquid foods containing particulate suspensions (Stirling, 1987; Biss et al., 1989; de Alwis and Fryer, 1990; Sastry and Palaniappan, 1992). Almost all research efforts have focused on using ohmic heating to sterilize foods. Huang et al. (1996) investigated ohmic heating in coagulation of frozen mince wash water. It was found that 33.0%, 59.3%, 33.3%, and 92.1% protein, COD, TS, and TSS, respectively, were removed from the wash water when the temperature reached 70°C.

Heat treatment to partially coagulate proteins may become necessary when preferentially extracting water soluble components such as heat stable enzymes from the waste water. Pacific whiting is a unique fish species that naturally contains active proteases, particularly cathepsin, in the fish muscle. These enzymes are found to be responsible for the degradation of functional myofibrillar proteins and gel weakening in surimi products (An et al., 1994a; An et al., 1994b; An et al., 1995; Seymour et al., 1994). During washing of the fish mince, some of the proteases are washed out of the fish muscles. Cathepsin L, one of the major proteases found in Pacific whiting, has a molecular weight of 28,800 Dalton, and shows a maximum activity at 55°C and pH 5.5. According to Benjakul et al. (1996), Cathepsin L was found in the surimi waste water

collected from a surimi processing plant. The high thermal stability of this enzyme makes it possible to selectively remove other fish proteins by heat coagulation, and thus partially purify the protease in the waste water. The removal of other proteins in the waste water makes it easier for the subsequent purification of the protease. The recovered protease would have much higher commercial value than fish proteins. According to Huang and Morrissey (1997a), a threefold increase in enzyme activity was observed in the ohmically treated wash water samples.

2.2.3.3 Electrocoagulation

Electrocoagulation is a combined physical and chemical process involving an alternating or direct current that passes through the waste water to initiate a coagulation process. Ions released from the electrodes can neutralize the charge-carrying particles in the waste water, causing them to destablize and coagulate. It is very effective in removing metal ions, and has also been demonstrated to remove BOD, TSS and oil and grease from the waste water. Application of electrocoagulation to treat three streams of waste water from a fish processing plant showed that more than 93% TSS and 35.5-76.9% COD could be removed (Dalrymple, 1994).

2.2.3.4 Centrifugation

Centrifugation is another conventional method widely used for solid-liquid separation (Perry et al., 1984). In principle, there are two general types of centrifuges, sedimentation centrifuges and centrifugal filters (Fig. 8). In a sedimentation centrifuge,
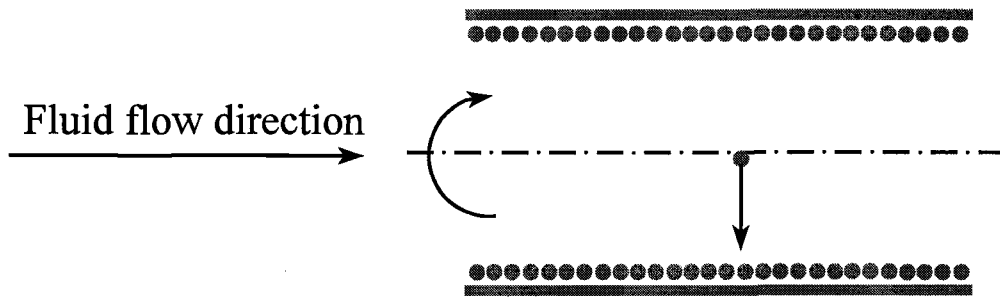
(A) Sendimentation centrifuge
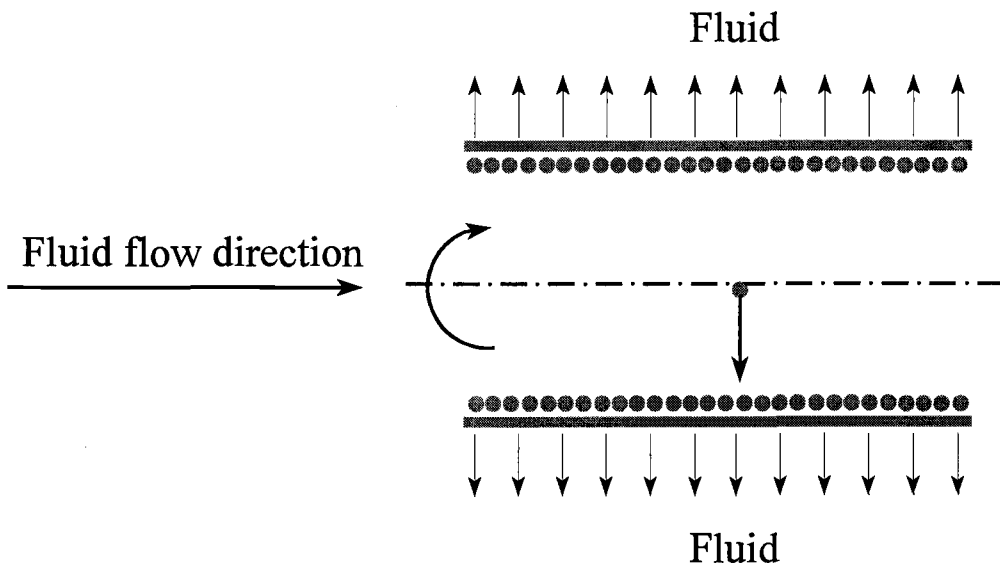
(B) Centrifugal filter

Fig. 8 Two types of centrifuges: sedimentation centrifuges and centrifugal filters

a fluid solution containing solid particles is moving under a centrifugal force applied perpendicular to the moving direction of the fluid. Due to the difference between the densities of the solid phase and liquid phase, solid particles move along the radius direction towards the wall of the centrifuge, and then accumulate on the wall, and thus liquid is separated from the solid phase. If the wall of the centrifuge is a perforated filter, allowing fluid to pass freely through the wall, then the solid phase will stop and accumulate on the surface of the filter. This type of filter is a centrifugal filter.

Swafford et al. (1985) reported the use of a decanter centrifuge (Fig. 9) manufactured by Alfa-Laval Co. to recover insoluble solids from rinsing and dewatering wastewater. Up to 80% insoluble solids could be recovered. The centrifugation produced a cake containing 10.5-18.1% dry solids with a variable composition. They proposed that the recovered solids might be blended with surimi to increase yield and profit, or used for developing new products. Decanter centrifuges have been adopted by the seafood industry to recover large particles from the waste streams. Typically, a range of 1700-3000x g centrifuge force is used for recovering protein particles from the surimi waste water streams (Ismond, 1997). In large volume Alaska pollock surimi plants, several centrifuges may be installed to recover suspended solids from the wash water (Peters, 1997).

Although centrifugation is a proven technology for liquid-solid separation, it has some inherent shortcomings (Biotol, 1992; Mir et al., 1992). The centrifuge requires high capital investment due to the complexity of the equipment and high maintenance costs due to in high speed moving parts. It consumes a relatively high amount of energy, and generates a slurry concentrate containing 5-20% dry solids. The separation capacity is

Fluid

Liquid
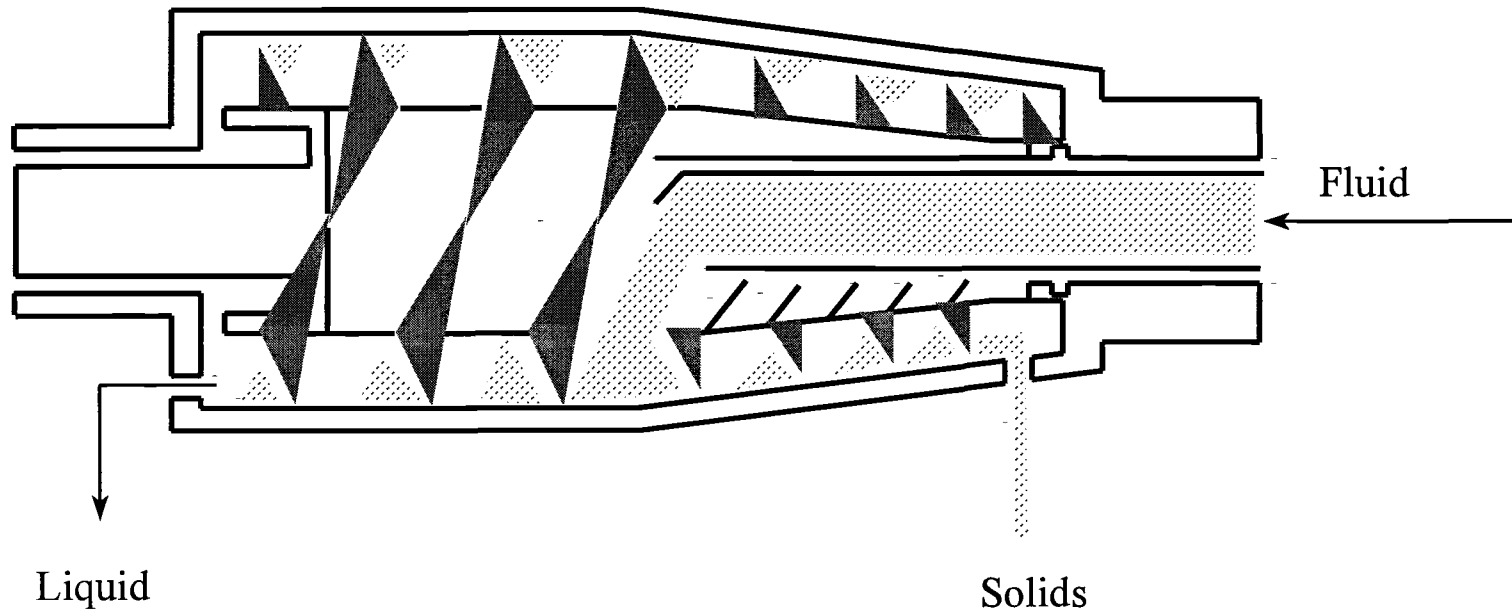
Solids

Fig. 9 A decanter centrifuge can be used to recover suspended solids from the waste water

highly dependent on the particle size and density, which results in an incomplete separation for the industrial centrifuges.

2.2.3.5 Membrane filtration

Pressure driven crossflow membrane filtration seems to be a natural alternative for recovering proteins with native functionality from the waste water. When waste water is pumped across the membrane, water and particles with sizes smaller than the membrane pores will pass through it, while particles with sizes larger than the membrane pores will be retained. With the removal of water and smaller particles, solids larger than the membrane pores will be concentrated.

Membrane filtration employs a positive pressure as a driving force to push the liquid phase through the membrane pores, without involving a phase change. It is particularly suitable for recovering and concentrating thermal sensitive components, such as protein, in the food and biotechnology industry. It has been widely used in the dairy industry to concentrate milk, to partially remove water from the milk prior to cheese making, and to recover whey protein and lactose from the waste steams of cheese making (Cheryan, 1986; Renner and Abd El-Salam, 1991). Using membrane filtration in concentration and fractionation of milk offers several advantages: 1) reduced overall energy consumption; 2) increased yield (10-30%) in cheese making; 3) reduced enzyme (rennet) usage; 4) reduced space requirement due to reduced milk volume; and 5) reduced environmental pollution due to whey protein recovery.

Recovering whey protein is a successful example of membrane filtration

(ultrafiltration, in particular) in the dairy industry (Cheryan, 1986). In cheese manufacturing, large volumes of cheese whey generated each day are a major problem. Depending on origination, 8-9 kg of whey can be generated from every 10 kg of milk (Dziezak, 1990). Due to high concentrations of organic substances in cheese whey (Table 4), very high concentrations of BOD (32-60 g/L) have been observed. According to Cheryan (1986), about 50% of the approximately 40 billion kg of whey worldwide is generated in the U.S. Since whey protein shows high gelling, emulsifying functionality, and potential nutritive values, ultrafiltration (UF) has been applied to concentrate whey protein by removing water and lactose from the cheese whey (Fig. 10). Permeates from the ultrafiltration of cheese whey can be further treated with reverse osmosis (RO) to recover lactose or converted to ethanol by fermentation.

RO is more suitable for recovering smaller molecular weight compounds such as sugars from the fruit and vegetable industry waste water (Mannapperuma et al. 1993). A mobile demonstration test unit was launched by the California Institute of Food and Agricultural Research (CIFAR) to test the applicability of RO in recovering sugars and reclaiming water from the waste stream of fruit and vegetable processing plants. Preliminary economic analyses show that benefit/cost ratio of 1.1 and 3.9, respectively, for a membrane filtration system for recovery of solids concentrates and recycling of water in peach pitter and tomato peeler operations (Mannapperuma et al., 1993).

In South Africa, treatment of red meat abattoir effluents with membrane filtration was studied by Cowan et al. (1992). Their research led to a small scale commercial application (25 m³/d) using full size modules. Polyethersulfone UF membranes with a

Table 4 Proximate composition of cheese whey (Cheryan, 1986)

Composition	Acid whey	Sweet whey
Total solids	6.60	6.90
Protein (N x 6.38)	0.76	0.85
Ash	0.61	0.53
Fat	0.09	0.36
Carbohydrate (mainly lactose)	5.12	5.14

Whey after
fines removal → [Balance tank] → ⊙ → [Fat separator] → [Balance tank] → ⊙ → [||||||||||||] → [||||] → 55°C
                                                                                    HTST Pasteurizer   Cooler

[Balance tank] ← [UF plant] ← ⊙ ← [Balance tank]
UF concentrate

UF permeate for utilization
by additional processing

Balance tank
(30 min - 1 hr)

⊙ → [Evaporator] → [Spray dryer] → [Power blender] → [Bagger] → Baggered protein powder

25-40% solids   96% solids
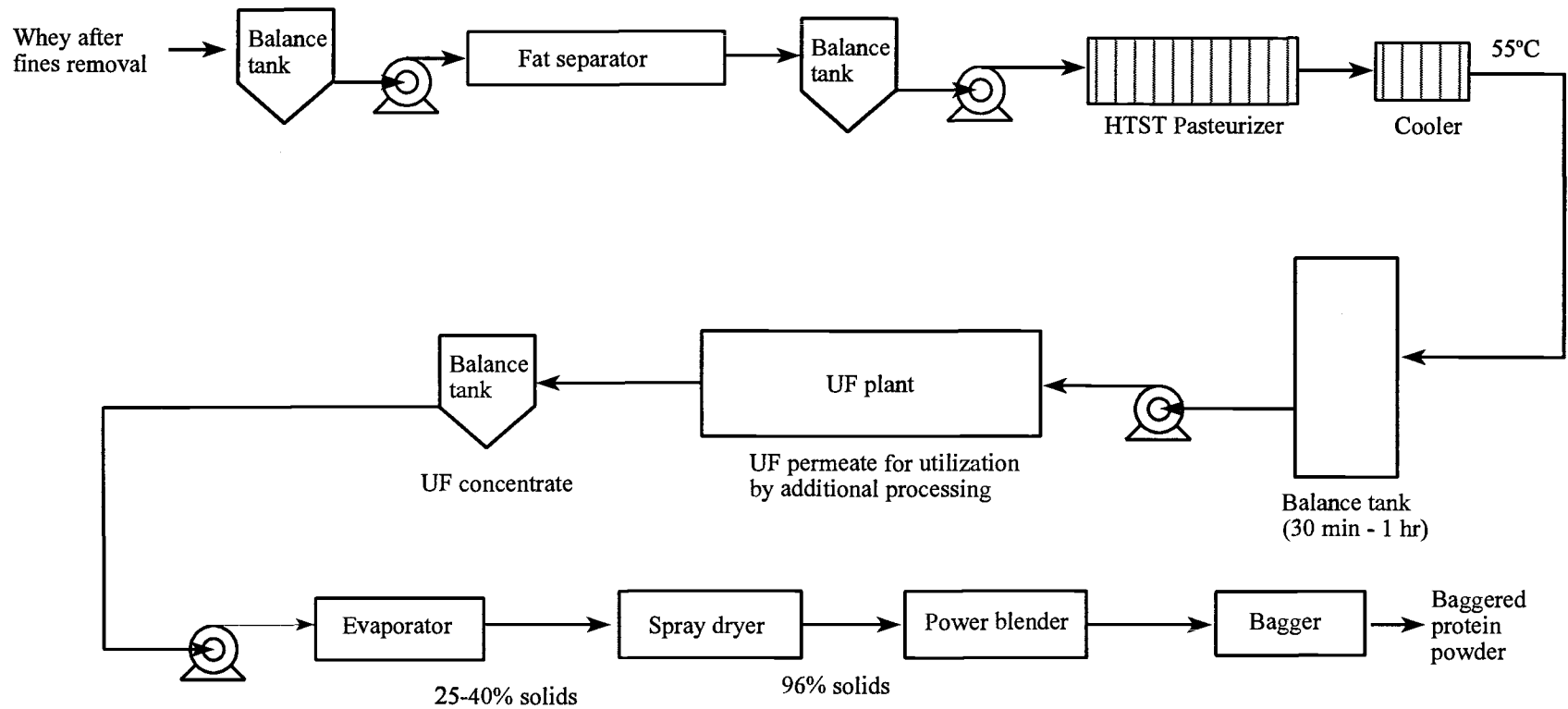
Fig. 10 Recovering whey protein from the waste water of cheese manufacturing (Cheryan, 1986)

molecular weight cutoff (MWCO) of 40,000 Dalton were used to directly treat effluents with preliminary screening (0.5 mm). For a mixed stream of abattoir wastes containing average COD, TS, conductivity, and soluble phosphate of 6 g/L, 3.5 g/L, 120 mS/m, and 40 mg/L, respectively, ultrafiltration removed 90% COD and 85% phosphate from the effluent, and provided a relatively non-fouling feed for reverse osmosis (cellulose acetate) used to generate reusable water for abattoir use (Table 5). Overall costs for the membrane filtration system compared favorably with the anaerobic treatment system.

The application of membrane filtration to recover solids from the waste water of seafood processing has been studied by Japanese scientists. Miyata (1984) used a bench scale ultrafiltration system to concentrate proteins from the wash water of red muscle fish. After centrifugation to remove coarse particles, the waste water was pumped to a tubular filter until a 10/1 volume reduction was achieved. Results (Table 6) showed that about 90% of protein in the feed could be concentrated, and the recovery was independent of the feed concentration. A more comprehensive study was conducted by Ninomiya et al. (1985) using ultrafiltration to recover waste soluble proteins in the waste water from surimi processing plants. Waste water of different fish species was used in their investigation. An ultrafiltration unit with a MWCO of 20,000 was used to concentrate the waste water samples containing 0.1-2% protein to 0.4-18% protein. A 90% recovery was achieved, with proteins having molecular weights higher than 10,000 retained by the membrane. Microporous membranes were also used to recover solids from the wash water of fish paste processing (Watanabe et al., 1986 & 1988; Shoji et al., 1988). Ceramic membranes with pore sizes ranging from 0.05 to 1.5 μm were used in their

Table 5 Effectiveness of UF and RO in treatment of red meat abattoir effluents (Cowan et al. 1992)

Feed stream	UF	RO
	Screened effluent after fat skimming	UF filtrate
Feed pressure (kPa)	400	2500
Feed temperature (°C)	20-28	25-30
Rejection %		
COD	90-93	94-96
PO_4	85	95
Conductivity	25	90-95
Flux (L/m^2h)	45 declining to about 20 in 2-3 days	20-22 with no short-term decline

Table 6 Changes of components in wash water of mackerel meat by ultrafiltration (Miyata, 1984)

Sample	Proteins (A) g/100 mL	Total solids (B) g/ 100 mL	Protein content (dry base) (A/B) x 100(%)	Electric conductivity μΩ/cm (25°C)	Specific gravity
Feed (crude wash)	0.50	0.98	51	4880	1.007
Permeate	0.038	0.53	7.2	4760	1.002
Concentrate	4.8	5.2	92	5480	1.018

research. Under high pressure (0.45-0.5 MPa) and low crossflow velocity, a dynamic membrane was formed within 20 min due to deposition of soluble proteins on the membrane surface and inner pores. Almost 100% recovery of protein with molecular weights > 10,000 Dalton was observed. The thickness of the protein layer deposited on the membrane surface was about 5 μm, much smaller than that of a ceramic membrane. This study is an unusual application of microfiltration membranes in recovering soluble proteins, since the artificially induced dynamic membrane was actually a result of membrane fouling, which should be avoided in most applications of membrane filtration.

French scientists also conducted research on application of membrane filtration to recover soluble proteins from the surimi wash water (Jaouen et al., 1989 & 1990; Jaouen and Quemeneur, 1992). Ultrafiltration membranes with MWCO ranging from 10 - 100 KD were used in their laboratory and pilot experiments. Surimi wash water reconstituted from freeze-dried sarcoplasmic proteins was used to select suitable ultrafiltration membranes, and fresh surimi wash water was used in the pilot studies. Results showed that more than 75% of effluent polluting loads (expressed in BOD_5 and COD) could be reduced with a 100% retention of protein. A clear filtrate, which contained dissolved amino acids and other lower molecular compounds, was obtained. Permeate fluxes started from 50 L/m^2h at the beginning of filtration and dropped to 10 L/m^2h in the end. Regenerated cellulose membranes performed better than polysulfone membranes due to their superior hydrophilicity. However, regenerated cellulose membranes are not a good choice for wastewater treatment since they cannot withstand the harsh chemical conditions during cleaning and sanitation operations.

American scientists started in the 1980s to apply the membrane filtration technology to seafood processing waste water treatment, and their efforts continue. Chao et al. (1980; 1983; 1984) applied ultrafiltration to recover the insoluble solids from high strength crab cooker waste water effluents (Table 7). Batch operations with retentate recycle were used to achieve a 10:1 volume reduction. Test results show that 60-68%, 60-71%, 17-40%, and 99% of COD, BOD_5, TS, and TSS, respectively, were removed from the waste stream. The permeates were still high in COD and BOD_5. They suggested that a membrane with a lower MWCO should be used, or that a secondary filtration unit with a lower MWCO (such as 5000 or 10000 Dalton) membrane should be used to further treat the permeates.

Ultrafiltration to recover proteins from Alaskan pollock surimi wash water was investigated by Peterson (1990). Plate-and-frame configuration was found superior to other configurations for filtration of the highly viscous product in an economically feasible manner. Gel strength of recovered protein concentrate was comparable to second grade surimi. Lin et al. (1995) used a microfiltration unit and a spiral-wound polysulfone (30 KD MWCO) membrane filtration unit to recover solids from surimi wash water. They found that proteins recovered by microfiltration showed very high gelling functionality and had a composition comparable with proteins in regular surimi. A 10% substitution with recovered proteins did not affect the quality of surimi. Solids recovered by ultrafiltration had considerable dark color and strong odor characteristics, therefore, were not suitable as a surimi ingredient. An 89-94% reduction in COD was achieved

Table 7. Effectiveness of ultrafiltration (MWCO 50,000) in recovering solids from blue crab steam cooker effluent (Chao et al. 1980)

Pollutants	Raw waste (mg/L)	Concentrate (mg/L)	Permeate (mg/L)
COD	20,000-25,000	67,000-74,000	8,000
BOD$_5$	10,000-14,000	50,000-60,000	4,000
TS	18,000-25,000	52,000-64,000	15,000
TSS	700-1,000	10,000-13,000	10
NH$_3$-N	200-250	240	20
pH	7.0-7.5		

after UF treatment of Surimi waste water. The UF permeates had a high degree of clarityand could be potentially recycled (Lin et al., 1995).

Membrane fouling dramatically reduces the efficiency and becomes a major disadvantage of the membrane filtration process. Usually a large surface area of membrane and frequent cleaning to remove the fouled layer is needed. Costs of membranes and systems may vary (Table 8). Polymeric membranes are less expensive than ceramic and metallic membranes, but they are not as chemical-resistant as ceramic and metallic membranes. Ceramic membrane filters can have higher fluxes and withstand strong chemical agents when cleaning, but they are more expensive (Mir et al. 1992).

2.3 Waste water treatment: reality and perspectives

Waste water treatment in the seafood industry is a very complicated issue raising concerns from environmental regulatory agencies, law makers, the general public, and seafood processors. The real focus of the issue is to reduce environmental pollution and also hold down the costs of the waste water treatment.

The Federal Water Pollution Control Act was introduced in 1972 amended in 1977 (also known as "Clean Water Act"), and in 1987 (known as "Water Quality Act") to regulate waste water disposal in the United States. The Marine Protection, Research and Sanctuaries Act (MPRSA) was passed in 1972 and amended in 1988 (known as "Ocean Dumping Ban Act of 1988"). The MPRSA covers discharge into the ocean past the three mile territorial sea boundary. The Clean Water Act governs discharges into nearshore waters, rivers, and estuaries; therefore, the Act currently covers any seafood processing

Table 8. Costs of microfiltration systems (Mir et al. 1992)

Materials	Cost of medium ($/ft^2)	Cost of installed system ($/ft^2)
Polymers	6-90	160-650
Ceramics	80-300	230-700
Metals	60-120	220-900

effluent discharged directly into these waterways. In 1974, the Safe Drinking Water Act was passed to prevent ground water contamination. In 1974, USEPA established limitation guidelines that required seafood processors to employ the Best Available Technology (BAT) to treat waste water (Forsht, 1974). These guidelines set the standards for waste water disposal, and are also referred to as BAT standards that should have been enforced by 1983. However, the BAT standards have been considered by industry as not achievable due to the high costs of waste water treatment. In 1978, the BAT standards were reviewed by USEPA and replaced with the "Best Conventional Pollutant Control Technology (BCT)" standards. The BCT standards are less strict and easier to implement in the industry. From the governmental standpoint, the success of waste water pollution control can only be achieved by strictly enforcing rules and regulations for pollution control and prevention. This may temporarily curtail the economic activities of small businesses, but it will help develop a more environmentally friendly industry.

The seafood industry must be willing to treat and reduce waste water, and cooperation with federal and local environmental regulatory agencies is necessary to develop short-term and long-term waste water reduction and treatment strategies. Technically, waste water from the seafood or other sectors of the food industry is not difficult to treat, but costs for the treatment can be high.

It is important for seafood processors to develop environmental awareness among their employees and to educate them not to waste fresh water (Ismond, 1994). It would be very helpful for companies to establish a water saving plan. This plan must include guidelines for fresh water usage and spent water recycling in the places where fresh water

is not needed. Any activities leading to water usage savings should be encouraged, and any activities leading to increased waste water generation discouraged. From the technical standpoint, to achieve a cost effective and successful waste water treatment, it is necessary to develop a prioritized plan. There are many sources in a company that generate waste water, and not all the points produce high levels of waste. There are usually only a few point sources that generate the waste water high in BOD, COD, TS, and TSS. Waste water from these points must be separated from the other waste water streams, and to do so requires a prioritized treatment. The majority of low strength waste water can be treated with less expensive technologies since not all the treatment methods cost the same.

It is necessary to clearly define goals for solids recovery, as they directly determine the technology to be employed and the costs for operation and maintenance. It is not hard to comprehend that a technology adopted to recover solids for human consumption is more expensive than for animal feeds or landfills. Therefore, a combination of different technologies for achieving different goals and meeting different criteria is needed for the most cost effective waste water treatment.

3. MEMBRANE FOULING: THEORY AND HYPOTHESIS

3.1 Membranes: the Basics

Development and application of modern artificial membranes have been closely related to the phenomenon of osmosis discovered in 1748 by the French scientist Nollet. A classical experiment can be used to demonstrate the phenomenon of osmosis (Fig. 11), and the principle of reverse osmosis. In an apparatus shown in Fig. 11-A, two L-shape tubes are separated by a membrane that is permeable to water but not to solutes. The solution in the left tube has a higher concentration and therefore possesses a higher osmotic pressure than the one in the right tube. Due to the difference in osmotic pressure, water in the right tube will migrate to the left tube. As a result, the solution volume in the left tube will increase until an equilibrium is reached when the osmotic pressure in both tubes equals (Fig. 11-B). If an external pressure is applied to the left tube to overcome the difference in the osmotic pressures, water in the left tube will be forced to move to the right tube. Consequently, the level of the solution in the right tube rises (Fig. 11-C). This process is called reverse osmosis.

At the early stage of membrane development, scientists and engineers showed a tremendous interest in the potential applications of membranes. The artificial kidney was one of the most significant developments that brought hope to many end-stage kidney patients. During World War II, Kolff and Berk (1944) applied the principle of dialysis and developed a method that used cellulose film as a membrane to reduce the concentration of metabolic end products in the blood of a kidney patient. Although
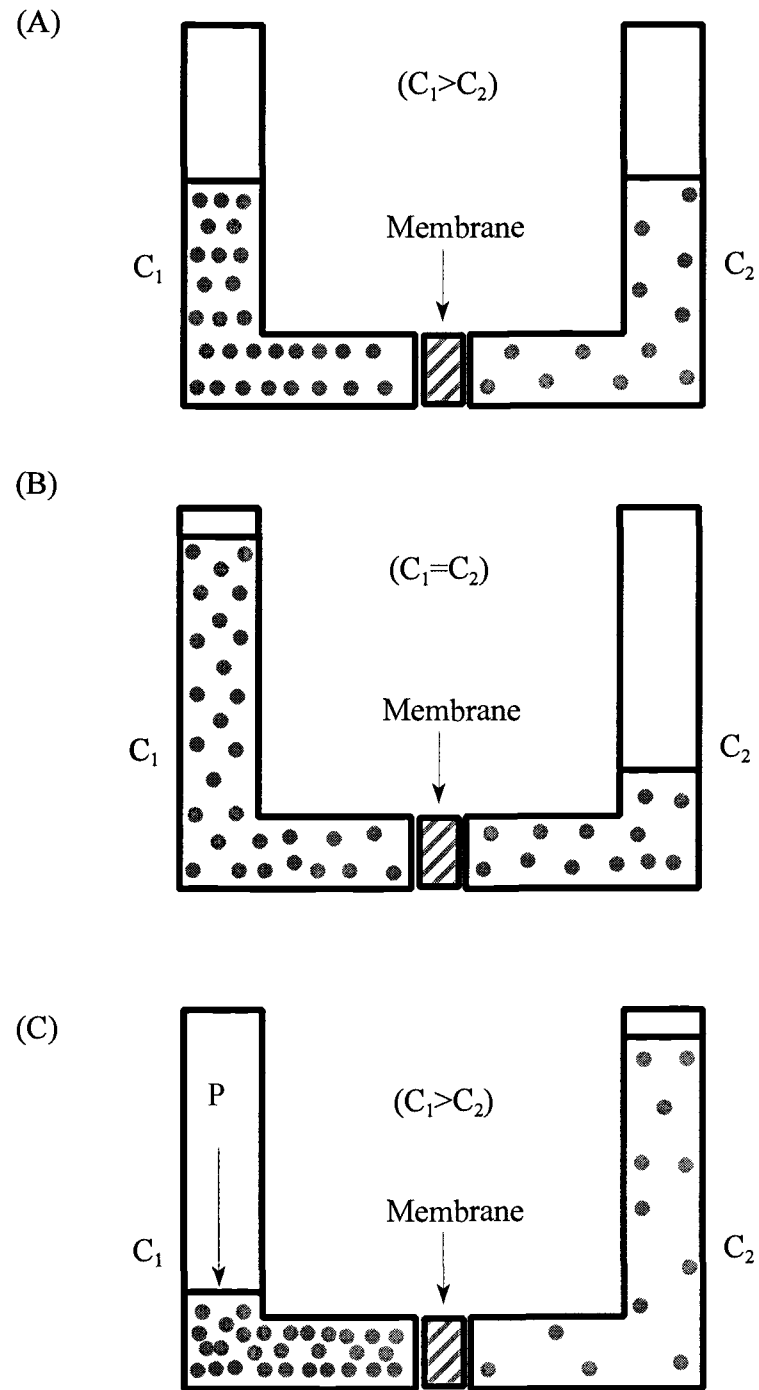
Fig. 11 Phenomenon of osmosis and reverse osmosis

primitive by today's standards, their experiment led to the development of a new therapy for thousands of end-stage kidney patients worldwide (Drukker et al. 1983).

Another force driving the development of modern membranes is to perfect a process to extract fresh water from seawater. This research was of critical importance to national defense during the cold war when submarines had to cruise under the sea for long periods without fresh water supplies. In 1953, C. E. Reid, Professor, University of Florida, initiated studies of seawater desalination by reverse osmosis (Madsen, 1977; Longsdale, 1983). The real breakthrough, however, took place in the late 1950s at the University of California, Los Angeles where the first high flux asymmetric cellulose acetate membrane was developed by Loeb and Sourirajan. Funds from the U.S. Department of Interior Office of Saline Water supported the research. Since then, new membrane materials and devices have been developed and commercialized. Membranes with larger pore sizes for ultrafiltration and microfiltration were also developed.

A membrane is actually a thin sheet of artificial or natural polymeric material with pores distributed in it. Under a certain pressure, species smaller than the pores can pass through, while large particles are rejected by the membrane. Pore sizes and pore size distribution determine the type and performance of a membrane. Reverse osmosis membranes have pore sizes smaller than 2 nm, usually operating under a very high pressure (15-80 bar), and they are particularly suitable for rejecting small species such as ions. Ultrafiltration membranes have pore sizes between 1-100 nm, operating under a medium range of pressure (1-10 bar). They are suitable for rejecting macromolecules such as soluble proteins with molecular weights between 300-500,000 Daltons. Based on

the ability to reject solutes, ultrafiltration membranes are categorized by their nominal molecular weight cutoff, or MWCO, which is usually defined as the smallest molecular weight at which molecules will be rejected by the membrane. Microfiltration membranes are even larger in pore sizes (0.05-10 μm). Since these membranes have very porous pores, they are particularly suitable for retaining large particles, such as viruses, bacteria, and other biological cells. Reverse osmosis, ultrafiltration and microfiltration are all pressure driven processes, but differ in the ability to reject particles in the solutions (Table 9).

Saudi Arabia seems to have benefited the most from the membrane filtration technology (particularly reverse osmosis). Many desalination plants have been installed there, including the world's largest plant (57,000 m³/day) in Saudi Arabia (Muhriji et al., 1989; Wojcik, 1983). The semiconductor industry is a major user of membrane filtration technology to generate "particle free" or ultrapure water for semiconductor and integrated circuit processing. The pharmaceutical industry is another big user of membrane filtration technology in process for concentration, fractionation, clarification, and sterilization of parenteral drugs (Geol et al., 1992; Mir et al., 1992a).

3.2 Membrane filtration systems: modules and configurations

3.2.1 Dead-end filtration or crossflow filtration

There are two types of membrane filtration: dead-end filtration and crossflow filtration. In a dead-end filtration process, fluid flows perpendicular to the membrane

Table 9 Differences in reverse osmosis, ultrafiltration , and microfiltration (combined from Mulder, 1990)

	Reverse osmosis	Ultrafiltration	Microfiltration
Membrane structure	asymmetric or composite	asymmetric porous	(a)symmetric porous
Thickness	sublayer $\approx$ 150 μm; top layer $\approx$ 1 μm	150 μm	10-150 μm
Pore size	0.05-10 μm	1-100 nm	<2 nm
Driving force	pressure: brackish 15-25 bar seawater 40-80 bar	pressure: 1-10 bar	pressure: < 2 bar
Separating principle	solution-difusion	sieving	sieving
Membrane materials	cellulose acetate, aromatic polymide, poly(ether urea)	polymer (polysulfone, polyacrylonitrile) ceramic (zirconium oxide, aluminum oxide)	polymer (polysulfone) ceremic
Main applications	- desalination of seawater - production of ultrapure water for electroinc industry - concentration of food juice and milk	- concentration of milk and whey protein - pharmaceutical industry (concentration of enzymes, antibiotics, pyrogens) - electropaint recovery	- analytical applications - sterilization (food, pharmaceuticals) - ultrapure water (semiconductor) - cell harvesting and membrane bioreactor - plasmapheresis

surface. Due to a rapid accumulation of solutes on the membrane surface, the permeate flux declines dramatically (Fig. 12-A). This filtration type is widely used in laboratories for filtering small volume liquids. It is also used in the pharmaceutical industry for sterile filtration (Geol et al., 1992).

Crossflow filtration is a major, revolutionary concept in the development of membrane filtration technology. In crossflow filtration, fluid flows in a direction tangential to the membrane surface (Fig. 12-B). In addition to the pressure applied normally to the membrane surface, a shear force is exerted tangentially to the membrane surface, removing the solutes accumulated on that surface. A steady state filtration can develop after the shearing force is in equilibrium with the forces that lead to the accumulation of the solutes on the membrane surface. The permeate flux in crossflow filtration is much higher than that of dead-end filtration. Crossflow filtration is predominately used in reverse osmosis, ultrafiltration, and microfiltration.

3.2.2 Modules

Other than inorganic membranes made of ceramic or stainless steel, most membranes are thin sheets of organic polymers, and are mechanically fragile. For laboratory purposes, membranes are sold in disks, rectangular sheets, or rolls. For larger scale operations, membranes are built into customized housings, called modules. Membrane module designs should be 1) mechanically strong to protect the membrane and housing; 2) hydrodynamically fit to prevent concentration polarization and membrane fouling; and 3) inexpensive to fabricate and replace (Bhattacharyya et al., 1992). After

(A)

Fluid flow, pressure

Permeate

Cake thickness

Permeate flux

Time

(B)

Pressure

Fluid flow, shear force

Permeate

Permeate flux

Cake thickness

Time
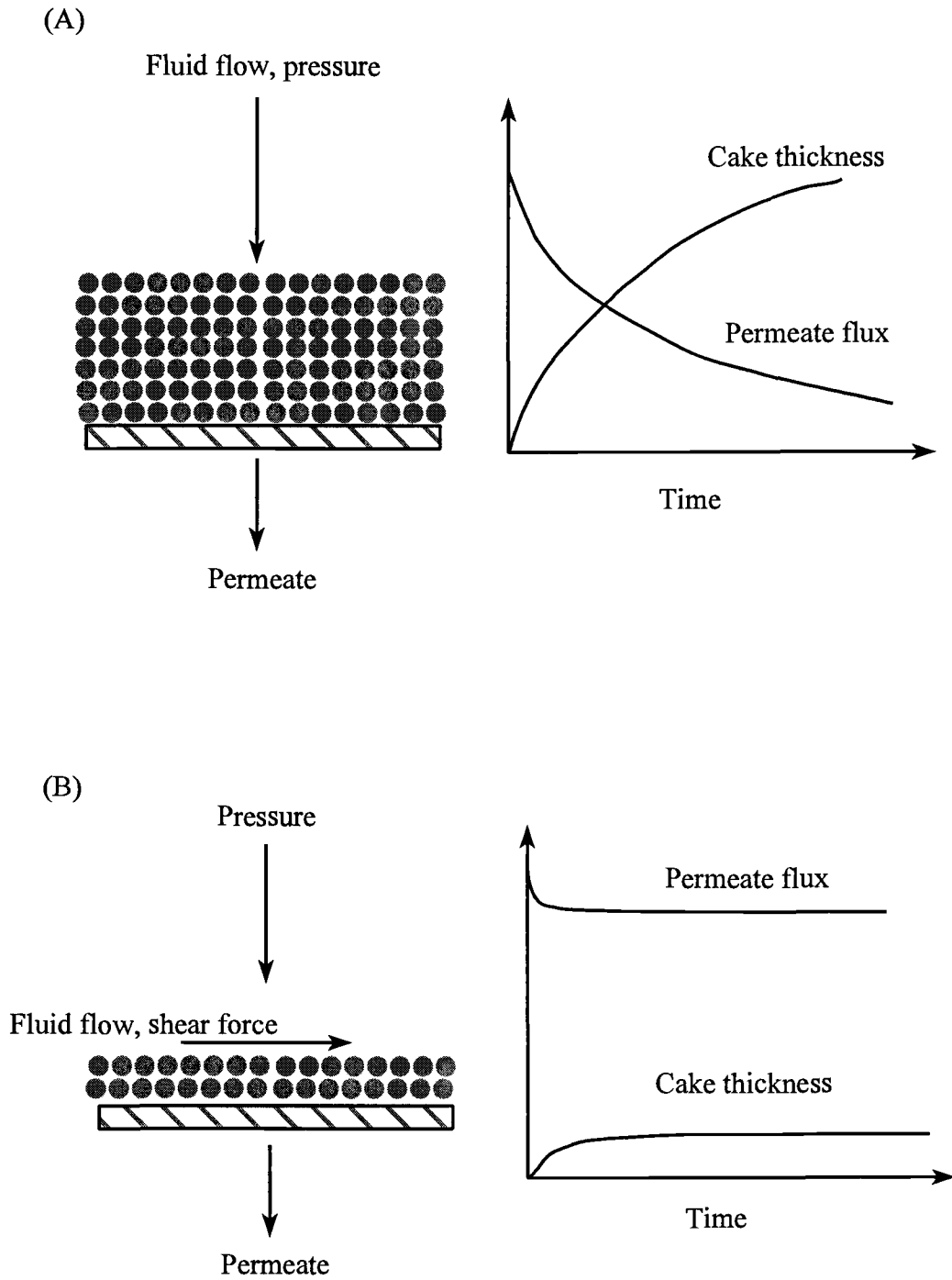
Fig. 12 Dead-end filtration and crossflow filtration

years of development, plate-and-frame, tubular, spiral wound, and hollow fiber modules are four major membrane modules commercially available.

Plate-and-frame modules (Fig. 13-A) were some of the first modules tested and commercialized. In a plate-and-frame unit, fluid flows into one end of a thin rectangular channel and leaves at the other end as a retentate. The permeate flows through the wall (membrane) of the channel. The packing density of plate-and-frame units is between 100-400 m^2/m^3 (Rautenbach and Albrecht, 1989).

Tubular design (Fig. 13-B) is another popular module. In a tubular unit, a narrow sheet of membrane is rolled into a tube (diameter > 10 mm) and supported by an external stainless steel, ceramic, or plastic tube (Mulder, 1990). Usually 4-18 tubes are packed together in a housing. Feed flows into the tube and the liquid permeates through the wall of the membrane. Due to the large tube diameter, turbulent flows can be pumped into the membrane tubes. It is a design with the least fouling or concentration polarization problem. Packing density is usually less than 300 m^2/m^3.

Hollow fiber design (Fig. 13-C) is the most popular design for reverse osmosis. A bundle of small membrane tubes having an internal diameter 40-100 μm and an external diameter of 80-200 μm is molded to a membrane housing. A feed can flow into the fiber tubes or from outside the tubes. This design has the highest packing density (<30,000 m^2/m^3). A hollow fiber module is most suitable for clean feed streams, since it is a structure most likely to foul.

The spiral wound design is the most widely used module. In this type of module, two sheets of membrane, sandwiched with a permeate channel spacer and a feed flow
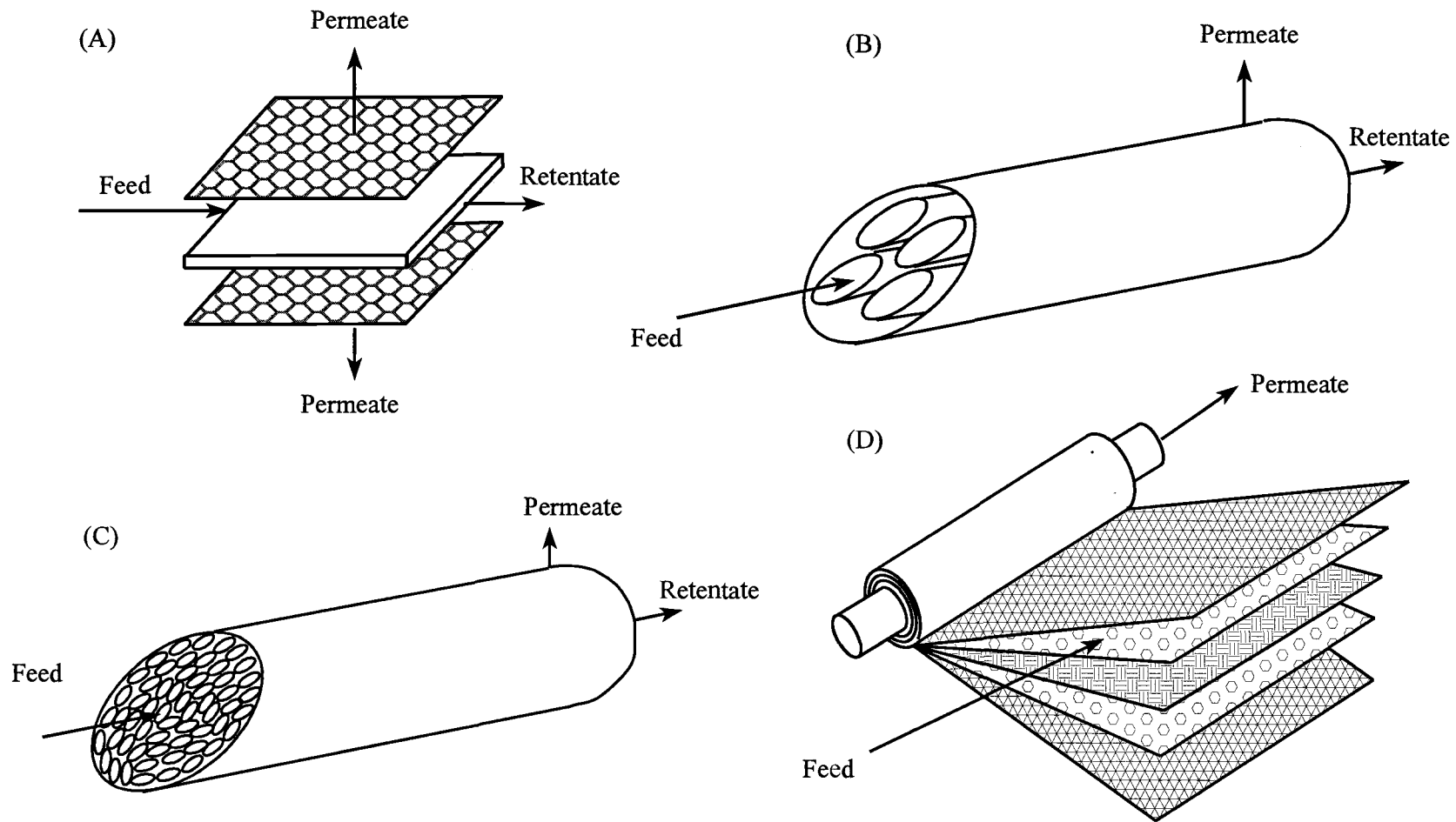
Fig. 13 Four commercially available membrane modules

channel spacer are glued and rolled together around a center tube where the permeate collects (Fig. 13-D). This design has a moderately high packing density (300-1000 m^2/m^3), and is suitable for relatively clean feeds with a turbidity <1 NTU. Cleaning a spiral wound membrane filter is difficult, however.

3.2.3 Membrane configurations

During membrane filtration, membrane modules may be installed in different configurations. For small fluid quantity operations, batch concentration with retentate recirculation is most commonly used (Fig. 14-A). Using this configuration, the feed concentration increases with the removal of the permeate, which increases the tendency of membrane fouling. The process is an unsteady state operation.

The feed-and-bleed configuration (Fig. 14-B) is used to concentrate solids in the feed in a steady state operation. Most of the retentate is recycled back to the feed solution, while a small portion of the retentate is bled off as a product. Because of retentate recirculation, feed flows at a high velocity to the filter, reducing the tendency of fouling.

In large scale membrane filtration operations, one stage is usually not sufficient to obtain a desired retentate concentration or permeate quantity. Many modules can be connected in a serial or parallel manner with multiple arrays of membrane modules that are arranged to handle a large volume of fluids (Fig. 15). This type of operation is called a cascade operation. Depending on characteristics of the feed and desired final concentration of the retentate, a combination of module arrangement can be used.

A. Batch operation

Retentate
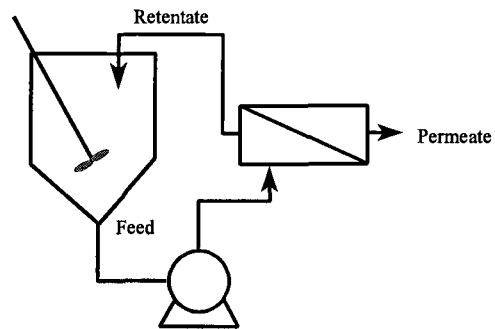
Permeate

Feed

B. Feed-and-breed operation

Retentate

Retentate breed

Permeate

Feed
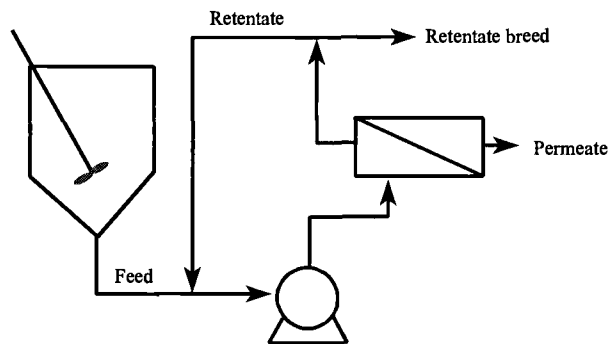
Fig. 14 Membrane filtration configurations
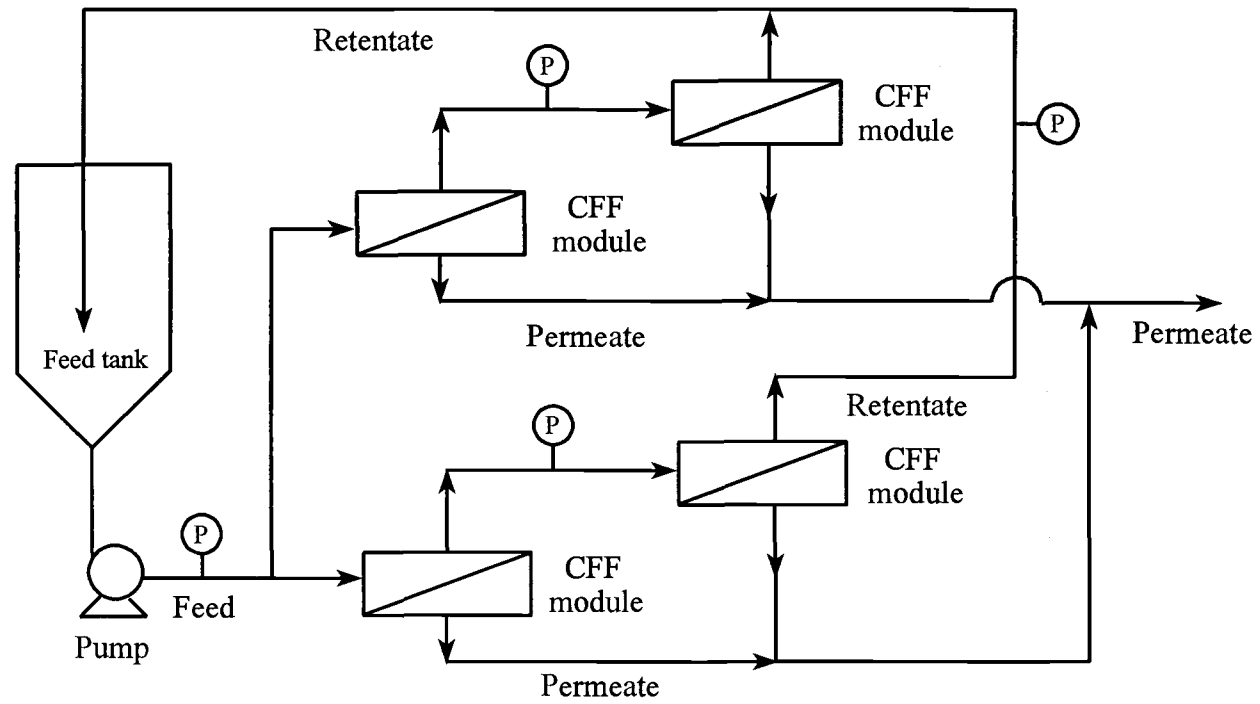
Fig. 15   Schematic diagram of a two-stage series/parallel batch crossflow filtration system (Mir et al., 1992)

3.3 Permeate flux decline: concentration polarization and membrane fouling

3.3.1 Concentration polarization

Membrane filtration would have gained more applications without the problems of concentration polarization and membrane fouling. When starting with pure water, the permeate flux is very high. When solutes are present in a feed solution, a dramatic permeate flux decline results. In early years of membrane filtration, membranes were used to remove salts and some macromolecules from water. Permeate flux decline was found to be related to the buildup of the solutes with a high concentration near the membrane surface. A high osmotic pressure due to the concentration buildup near the membrane surface reduces the overall driving force (Eq. 1). Within a certain range, the permeate flux increases with the pressure. At very high pressures, J^1 becomes independent of ΔP, which may attribute to the increased solution concentration, or consolidation of the membrane. In some severe cases, solids may form an insoluble layer deposited on the membrane surface. At that point, membrane fouling may have occurred.

$$J = \frac{\Delta P - \Delta \pi}{\mu \ R_m} \tag{1}$$

The permeate flux decline caused by concentration polarization is considered temporary, and can be adjusted or removed by changing the feed concentration. If there exist no other fouling mechanisms that lead to flux decline, rinsing the membrane unit with pure water can totally restore the permeability of the membrane.

---

[1] List of symbols and their definitions is located in Chapter 7.

3.3.2 Membrane fouling

Prolonged filtration of biological molecules may lead to formation of a gel-like layer that can dramatically reduce the permeate flux. For soluble protein molecules, the gel or gel-like layer on the membrane surface is considered an extension of the concentration polarization layer in which the solubility of the solutes reaches the critical limit (Nilson, 1990). These solutes form a layer of deposits through physicochemical associations with the membrane surface, and thus irreversibly modifies the membrane characteristics in terms of both permeate flux and rejection capability. This phenomenon is called membrane fouling.

Different mechanisms of interactions between solutes and membranes have been conceptualized. Belfort et al. (1994) stated that several phenomena are responsible for membrane fouling and they summarized that fouling may be a 5-stage process. During the very early phase of membrane filtration, the membrane surface is immediately exposed to the macromolecular solutes in the feed. Adsorption of the macromolecular solutes on the membrane may occur quickly within the membrane structure and on its surface. The second stage involves the development of a monolayer adjacent to the membrane surface. During this stage, the suspended solids slowly deposit on the membrane surface until the whole surface is completely covered. The interaction between the solutes and the membrane controls the rate of monolayer development. The third stage continues with the buildup of multi-sublayers resulting from the interactions between the solutes. The filtration resistance increases significantly. Increasing the pressure may temporarily increase the permeate flux, and it also leads to a compression in the deposited layers,

which in turn reduces the flux. When the multilayer growth reaches its maximum, densification of the sublayers may occur. The permeate flux is affected by the rearrangement of the particles on the membrane surface. This is the fourth stage of fouling. If the filtration is a batch process, removal of permeate from the feed leads to increased concentration and viscosity. The bulk solution may become a non-Newtonian fluid, thus precipitously decreasing the permeate flux (Belfort et al. 1994).

There is a distinct difference between concentration polarization and membrane fouling. Concentration polarization involves a concentration gradient near the membrane surface. It may be affected by the hydrodynamic conditions in the membrane filtration system. The membrane structure and characteristics (pore size and porosity, i.e., permeability) are not affected by the concentration buildup on the membrane surface (Marshall et al., 1993). Membrane fouling, on the other hand, is the consequence of interaction between the feed solution and the membrane, leading to modified pore structure and surface characteristics of the membrane.

Multilayer protein adsorption and deposition may play an important role in the development of membrane fouling (Ingham et al., 1980). A protein layer of 0.5-1.0 μm deposited on the membrane surface has been reported by Lee and Merson (1975) and Cheryan and Merin (1980). Compared with the monolayer protein deposition (1 mg/m^2), up to 1 g/m^2 of protein deposition can be found in fouled membranes (Nilson, 1990). Protein deposition on the membrane surface is highly pH dependent. According to Suki et al. (1984), maximum bovine serum albumin (BSA) deposition was observed at pH around the isoelectric point (pI) of BSA. In another study, however, the protein

deposition was found to decrease with an increase in pH. Matthiasson (1983) used ^{14}C-BSA solution to investigate the mechanism of membrane fouling at various pH using different membranes. He found that at pH below pI the positively charged BSA molecules may enhance the interaction with the negatively charged membrane surface. At alkaline pH conditions, both protein molecules and membranes (cellulose acetate and polysulfone) are negatively charged. An electrostatic repulsion exists between the membrane surface and protein molecules, leading to reduced protein deposition.

3.4 Mathematical modeling

3.4.1 Empirical and semi-empirical models

3.4.1.1 Thin film model

The thin film model first proposed by Brian (1966), is still the most successful theory in membrane science. Although developed for reverse osmosis, the thin film model is also applied to ultrafiltration and microfiltration (Blatt et al., 1970; Colton et al., 1975; van den Berg and Smolders 1988; Zydney and Colton, 1986). The thin film model was developed based on the concentration polarization theory. It is assumed that there is a solute concentration gradient developed near the membrane surface (Fig. 16). The solute is transported to the membrane surface by the permeate flux, leading to a concentration buildup on the membrane surface. Existence of the concentration gradient
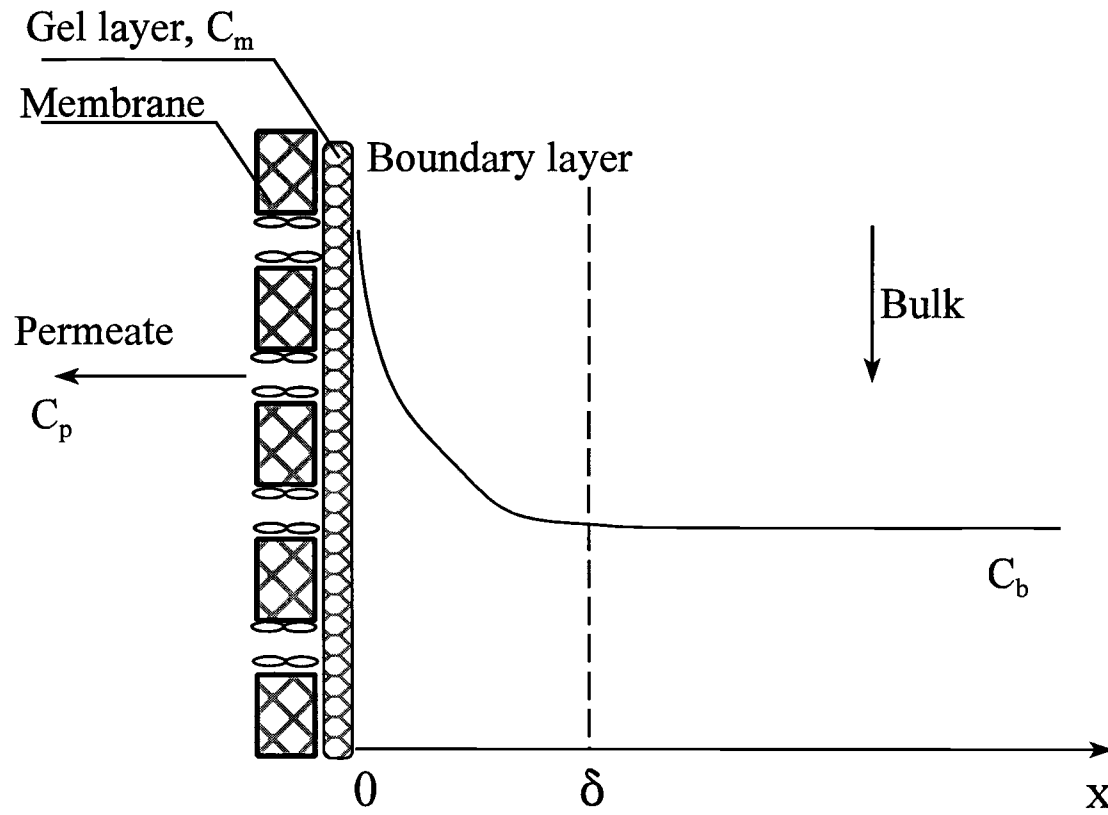
Fig. 16 Concentration profile in the thin film theory

causes the solute to transport back to the feed stream. At a steady state, a very thin layer of concentration gradient develops. Within the boundary, the solute mass transport is governed by:

$$JC - D \frac{dC}{dx} = JC_p. \qquad (2)$$

The boundary conditions for Eq. 2. are:

x=0, C= C_m

x=δ, C=C_b

After integration of Eq. 2, the permeate flux J can be expressed as a function of feed concentration C_b, the permeate concentration C_p, and the solute concentration C_m on the membrane surface (Eq. 3). The ratio of diffusion coefficient D and the thickness δ of the boundary layer is the mass transfer coefficient k. The thin film model can be rewritten as (Eq. 4).

$$Ln \left(\frac{C_m - C_p}{C_b - C_p} \right) = \frac{J\delta}{D} = \frac{J}{k} \qquad (3)$$

$$J = k \, Ln(C_m - C_p) - k \, Ln(C_b - C_p) \qquad (4)$$

Defining the apparent rejection coefficient as r_a, and the true rejection coefficient as r_t,

$$r_a = 1 - \frac{C_p}{C_b}$$

$$r_t = 1 - \frac{C_p}{C_m}$$
(5)

the thin film model can be further written as:

$$J = kLn\left(\frac{r_t}{1-r_t}\right) - kLn\left(\frac{r_a}{1-r_a}\right).$$
(6)

From Eq. 4 or Eq. 6, the mass transfer coefficient k and the solute concentration C_m on the membrane surface can be experimentally determined. If J is plotted against $Ln(C_b-C_p)$ or $Ln(r_a/(1-r_a))$, a linear relationship should be observed.

Under the assumption of concentration polarization theory, the property of the membrane is not altered during membrane filtration. The performance is affected by the hydrodynamics of the membrane filtration system, and is related to Sherwood, Reynolds and Schmidt numbers (Mulder, 1990).

$$Sh = aRe^b Sc^c$$

$$\text{Sherwood number} = Sh = = \frac{kH}{D}$$

$$\text{Reynolds number} = Re = = \frac{Hu}{\nu}$$
(7)

$$\text{Schmidt number} = Sc = = \frac{\nu}{D}$$

The coefficients (a, b, and c) for Eq. 7 are different for the membrane filtration (RO, UF, and MF), and the fluid flow types. For a turbulent flow (Gekas and Hallstrom, 1987), the mass transfer can be expressed as

$$Sh = \frac{kH}{D} = 0.023 \, Re^{0.8} \, Sc^{0.33}. \tag{8}$$

For a laminar flow (Porter, 1972), a different relationship can be used (Eq. 9).

$$Sh = \frac{kH}{D} = 1.62 \, (Re \, Sc \, d_h/L)^{0.33} \tag{9}$$

Eqs. 4 and 6 are also valid for microfiltration of feeds containing large particle size suspensions, but the particle diffusion is not significant due to large particle size. According to Eckstein et al. (1977) and Zydney and Colton (1986), the effective particle diffusion coefficient is a function of the particle size and shear rate:

$$D = 0.03 \, d_p^2 \gamma. \tag{10}$$

The permeate flux in microfiltration can be expressed as

$$J = 0.078 \left(\frac{d_p^4}{L}\right)^{\frac{1}{3}} \gamma_w \, Ln\left(\frac{C_m - C_p}{C_b - C_p}\right). \tag{11}$$

3.4.1.2 Resistance-in-series model

Resistance-in-series model is based on the traditional filtration theory (van den Berg and Smolders, 1988). In this model, the total filtration resistance is composed of two parts: the resistance of the clean membrane and the resistance of the cake layer deposited on the membrane surface. The permeate flux is proportional to the applied pressure, and can be described by the Darcy's Law (Eq. 12) (Belfort et al., 1996). This model assumes that there is no interaction between the feed solution and the membrane, and that the internal structure of the membrane is not modified by the permeate. In a dead-end filtration process, the cake continues to grow as permeate passes through the membrane. If all the solutes and particles are rejected and retained by the membrane, the cake layer resistance is proportional to the thickness of the cake layer (Eq. 13). Substituting Eq. 13 to Eq. 12, a new model can be derived (Eq. 14). Eq. 14 is commonly known as the Ruth's law (Suki et al., 1984; Nakao et al., 1986), and is widely used to model dead-end filtration processes. If t/V is plotted against the accumulated permeate volume, a straight curve should be observed.

$$ J = \frac{1}{A_m} \frac{dV}{dt} = \frac{\Delta P}{\mu (R_m + R_c)} \tag{12} $$

$$ R_c = R_{sc} L_c = \frac{R_{sc} C_b V}{C_m A_m} \tag{13} $$

$$\frac{t}{V} = \frac{R_m \mu}{\Delta P A_m} + \left[\frac{R_{sc} C_b \mu}{2 A_m^2 \Delta P} \right] V \qquad (14)$$

During the early stage of crossflow, the development of the cake layer on the membrane surface also follows Ruth's law (Iritani et al., 1991; Tanaka et al., 1993; Murase et al., 1995). As crossflow filtration progresses and reaches a steady state, the interaction between the deposited layer and the feed solution is stabilized. Then t/V in Eq. 14 becomes independent of the filtrate volume.

3.4.1.3 Pore blocking model

When filtering soluble proteins or suspended protein particles through a membrane with pore sizes significantly larger than the proteins, some proteins may enter the membrane matrix and interact with the pore walls of the membrane and accumulate in the inner pores (Marshall et al., 1991; Bowen, 1993; Kawakatsu et al., 1993). The flow path of membrane pores may be reduced due to the adsorbed layer of proteins on the pore walls. The pore blocking model is based on an assumption that the amount of protein deposited on the pore walls is proportional to the permeate passing through the pores (Blanpian et al., 1993; Bowen and Gan, 1991; Bowen and Gan, 1992; Bowen and Hall, 1995).

In development of the pore blocking model, a membrane is assumed to have a uniform thickness and uniformly distributed parallel cylindrical pores. The initial pore

has a diameter of d_o, and a height of h (Fig. 17). Assuming the protein molecules or particles form a uniform coating on the inner pores and the porosity of the coating solids is negligible, then the pore volume decreases proportionally to the total permeate volume:

$$-\frac{\pi}{2} Nh\,d(d_p) = \frac{m_s}{\rho_s} dV$$
$$\text{at } t = 0, \ d_p = d_o, \ V = 0,$$
$$\text{at } t = t, \ d_p = d_p, \ V = V \tag{15}$$

In Eq. 15, m_s is the amount of solids deposited on the membrane inner walls per unit volume of the permeate. By integrating both sides of Eq. 15, as shown in Eq. 16, the total permeate volume can be expressed as a function of pore diameters (Eq. 17).

$$V = \frac{\pi Nh\rho}{4m_s} \left(d_o^2 - d_p^2\right) \tag{16}$$

$$\int_{d_o}^{d} -\frac{\pi}{2} Nn\,d(d) = \int_{0}^{V} \frac{m_s}{\rho_s} dV \tag{17}$$

Top view of membrane surface

At t = 0

At t = t

d_o

d_o

d_t

h

h

An initial clean pore

A pore with protein deposited on the wall after time t.
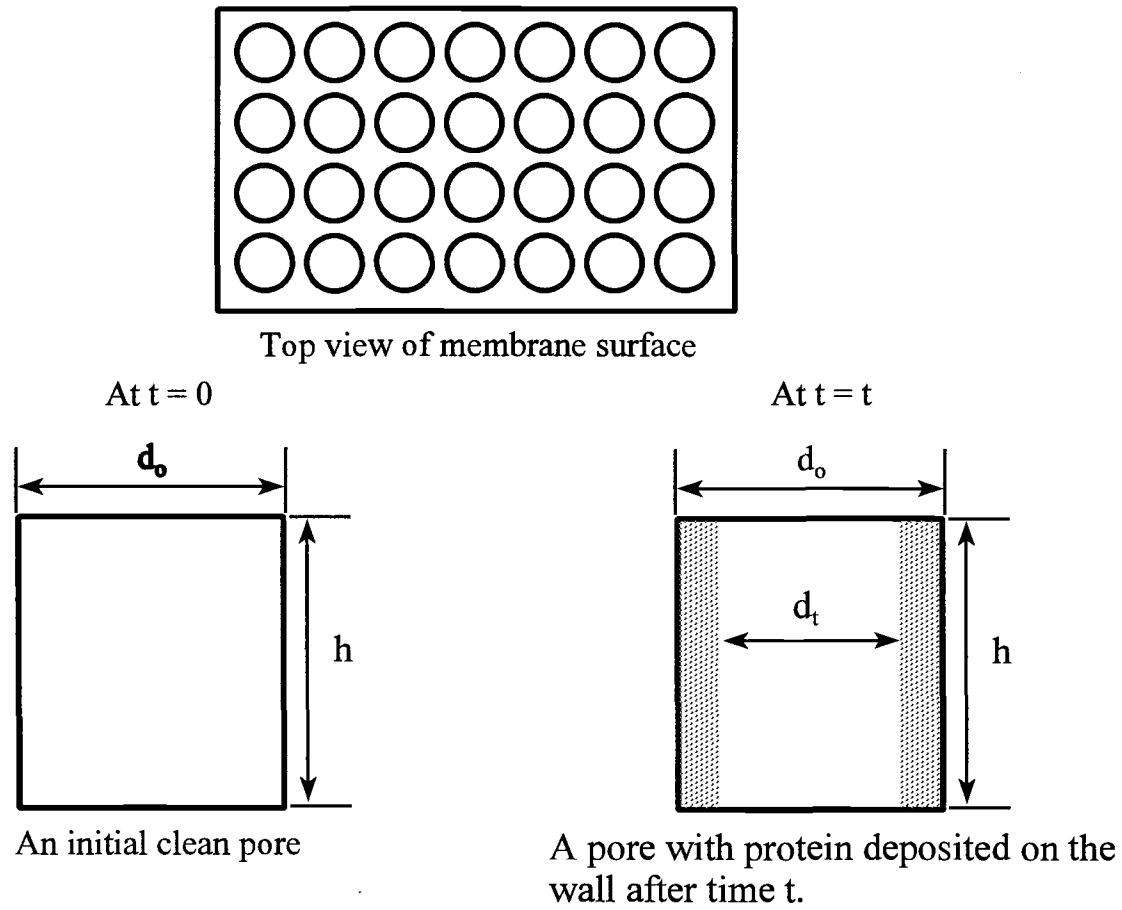
Fig. 17   Schematic diagram of pore blocking model

For membrane filtration under a constant pressure ΔP without a cake layer deposited on the surface, the permeate flux is governed by the Hagen-Poisseuille law (Eq. 18):

$$J = \frac{1}{A_m} \frac{dV}{dt} = \frac{\epsilon \, d^4 \, \Delta P}{128 \, \mu \, \tau \, h} N \qquad (18)$$

Combining Eq. (17) and Eq. 18, then

$$dV = J_o A_m \left(1 - \frac{d_o^2 - d_p^2}{d_o^2} \right)^2 dt$$

$$= J_o A_m \left(1 - \frac{4 m_s}{\pi N h \rho d_o^2} V \right)^2 dt . \qquad (19)$$

Denoting the initial pore volume as

$$V_{po} = \frac{\pi \, d_o^2 h}{4} N . \qquad (20)$$

Integrating Eq. 19, the pore blocking model can be obtained (Eq. 21).

$$\frac{1}{V} = \frac{1}{J_o A_m}\frac{1}{t} + \frac{m_s}{V_{po}\rho} = \frac{K}{t} + B_1 \qquad (21)$$

If plotting 1/V against 1/t, a straight line can be observed if the filtration process is governed by the pore blocking law. The slope in Eq. 21 is proportional to $1/J_o$, and can be used to estimate the membrane area.

3.4.1.4 Hypothesis

Eq. 14 is derived from the traditional dead-end filtration process with an assumption that all the solid particles are completely rejected and retained by the membrane surface. During microfiltration of a protein solution containing particles with different particle sizes, particles larger than the membrane pores will be rejected by the membrane, and smaller particles will penetrate into the inner pores. According to Suki et al. (1984), the linear relationship t/V and V was observed only in the initial stage of crossflow filtration, while non-linear relationship was observed in most filtration processes, suggesting that a different cake formation mechanism may be responsible for the non-linear relationship between t/V and V.

During the initial stage of microfiltration, the initial permeate flux is much higher than the steady state flux and declines in a very short period. The high initial permeate flux can bring more particles into the pores and deposit these within the pores, causing the pathway to narrow rapidly.

In microfiltration of surimi wash water, where fouling may occur both in the inner pores and on the membrane surface (Fig. 18), the membrane resistance in Eq. 14 is not that of the clean membrane, but that of the membrane with fouled internal pores. Since the composition of the surimi wash water is so complex, the rejection of solids cannot be 100%. Both pore narrowing and cake formation may develop depending on the stage of the filtration process. Assume that the pore blocking is the dominating resistance during the initial stage, and that cake resistance begins to develop at time t-t_c, where t_c is the reference time point at which fluid flow begins to stabilize. Assuming that the total filtration resistance R is a nonlinear function of the total volume of permeate (V), it can be expressed as:

$$R = \frac{1}{\alpha \beta} (V - V_c)^{\frac{1}{\alpha} - 1}, \tag{22}$$

where α is a function of solids concentration, and β is a constant to be empirically determined. Obviously, the total resistance R is composed both of the resistance of a membrane with fouled pores, and of the boundary layer near and the cake layer deposited on the surface.

Substituting Eq. 22 into Eq. 12 and by integration, it can be obtained that

$$V - V_c = \left(\frac{\Delta P \, \alpha \, \beta}{\mu} \right)^{\alpha} (t - t_c)^{\alpha}. \tag{23}$$

(A)

Flow direction

Bulk feed

Deposited layer

Membrane

Permeate

(B)

Flow direction

Bulk feed

Deposited layer

Membrane

Permeate
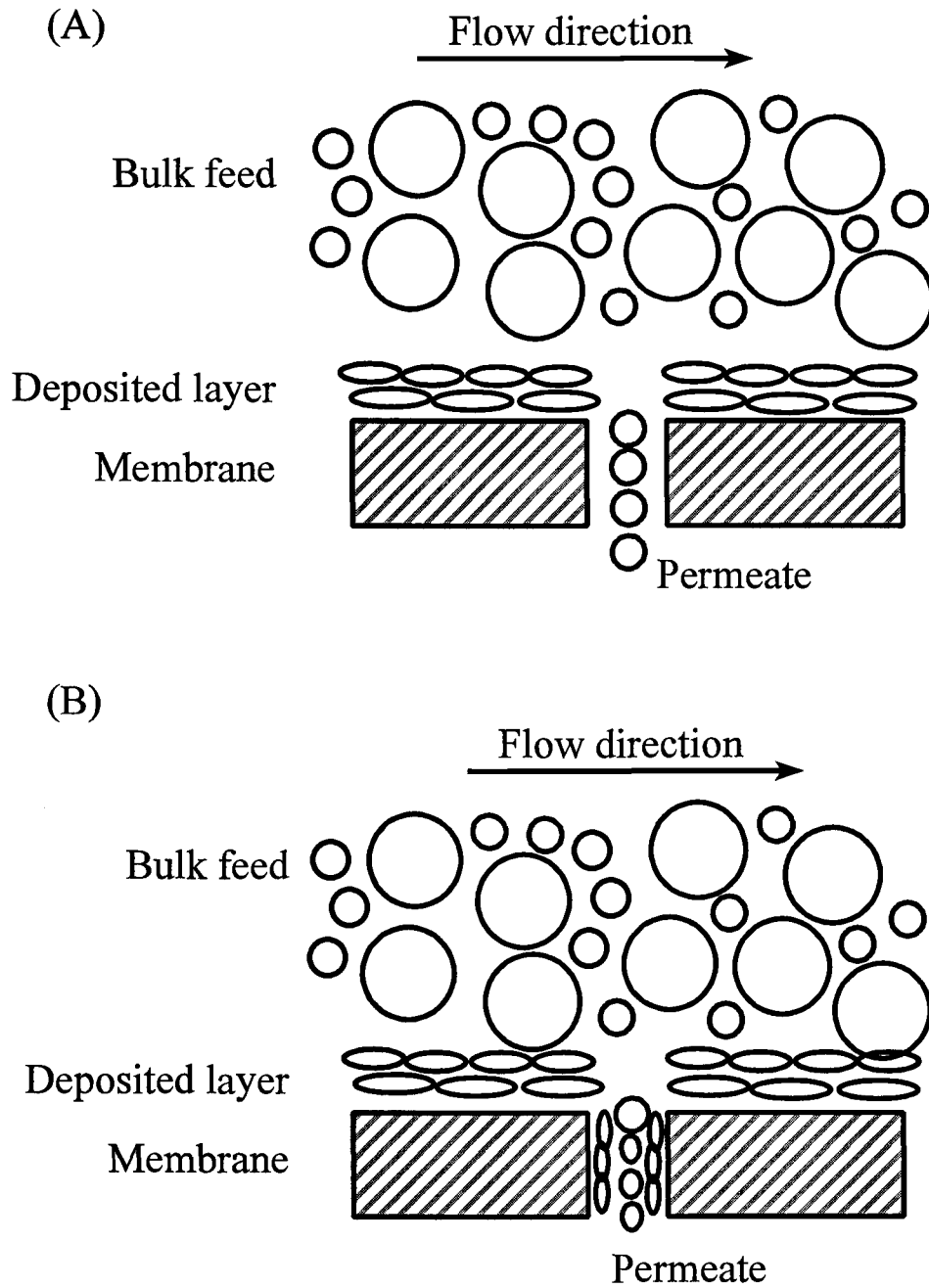
Fig. 18   Fouling may occur on the surface and in the matrix of membrane

Taking logarithms on both sides of Eq. 23 transforms it into a linear relationship

between Ln $(V-V_c)$ and Ln $(t-t_c)$:

$$\text{Ln}\left(V-V_c\right) = \alpha\,\text{Ln}\left(\frac{\Delta P\,A\,\beta}{\mu}\right) + \alpha\,\text{Ln}\left(t-t_c\right) = \xi + \alpha\,\text{Ln}\left(t-t_c\right) \tag{24}$$

3.4.2 Fundamental models

3.4.2.1 Velocity profiles in the membrane flow channel

Consider a feed solution containing protein molecules that is pumped into a plate-and-frame membrane filter (Fig. 19). The filter flow channel is composed of two parallel walls, with one being a membrane and the other an impermeable wall. The feed is flowing tangentially across the flow channel with a height of H and length of L. A coordinate system is chosen with the origin located at the entrance point of the impermeable wall. The z axis is perpendicular to the channel wall toward the membrane surface. If 1) the filtration is at a steady state; 2) the fluid is incompressible; 3) the flow is laminar; 4) the velocity (flux) of the permeate leaving the membrane wall is independent of position, then the fluid flow within two parallel walls is governed by Navier-Stokes equations. These equations are expressed as (Berman, 1953):

$$u\frac{\partial v}{\partial x} + \frac{v}{H}\frac{\partial v}{\partial \lambda} = -\frac{1}{\rho}\frac{\partial p}{\partial x} + \nu\left(\frac{\partial^2 v}{\partial x^2} + \frac{1}{H^2}\frac{\partial^2 v}{\partial \lambda^2}\right) \tag{25}$$
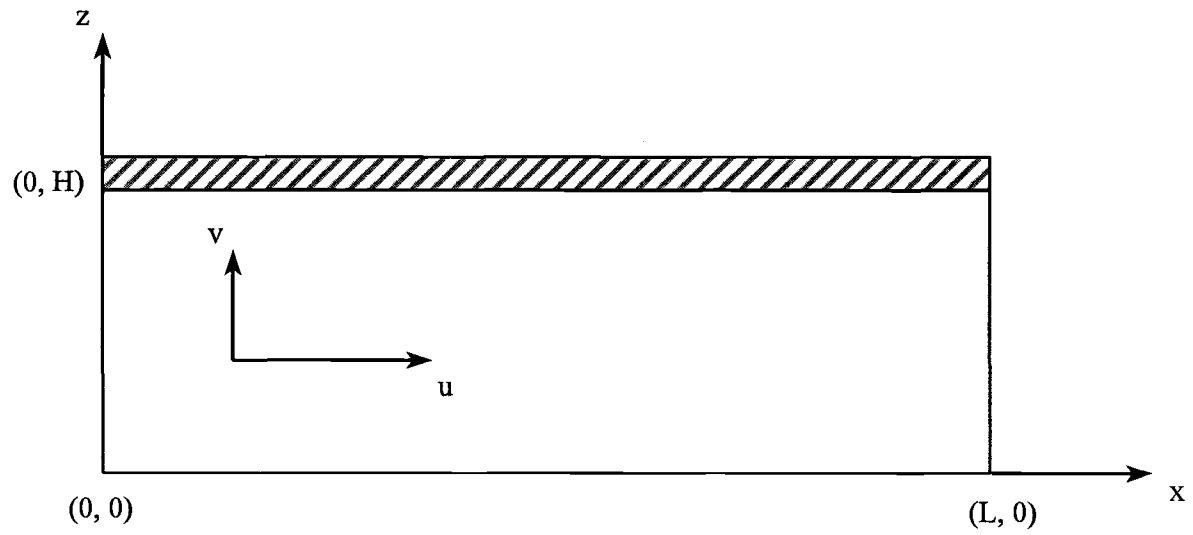
Fig. 19 Ultrafiltration flow channel with one membrane wall

$$u\frac{\partial u}{\partial x} + \frac{v}{H}\frac{\partial u}{\partial \lambda} = -\frac{1}{\rho}\frac{\partial p}{\partial x} + v\left(\frac{\partial^2 u}{\partial x^2} + \frac{1}{H^2}\frac{\partial^2 u}{\partial \lambda^2}\right) \qquad (26)$$

$$\frac{\partial u}{\partial x} + \frac{1}{H}\frac{\partial v}{\partial \lambda} = 0 \qquad (27)$$

$$\lambda = \frac{z}{H} \qquad (28)$$

The boundary conditions for the Navier-Stokes equations are (Kleinstreuer and Paller, 1983; Ganguly and Bhattacharya, 1994):

$$\begin{aligned} u(x, \pm 1) &= 0 \\ \left(\frac{\partial u}{\partial \lambda}\right)_{\lambda = 0} &= 0 \\ v(x, 0) &= 0 \\ v(x, 1) &= J. \end{aligned} \qquad (29)$$

For a laminar flow, the fluid enters the membrane channel having a parabolic velocity profile, with an average velocity $\bar{u}_0$. According to Berman (1953) and Kleinestreuer and Paller (1983), a stream function $\psi(x, z)$ exists such that the continuity equation could be satisfied (Eq. 30).

$$u(x,\lambda) = \frac{1}{H}\frac{\partial\psi}{\partial\lambda}$$

$$v(x,\lambda) = -\frac{\partial\psi}{\partial x}$$

(30)

For a constant permeate flux J, the stream function $\psi(x, z)$ can be found:

$$\psi(x,\lambda) = (H\bar{u}(0) - Jx)\, f(\lambda).$$

(31)

The velocity components in the x and z direction u and v can be expressed a function of x and λ:

$$u(x,\lambda) = \left(\bar{u}(0) - \frac{Jx}{H}\right)f(\lambda)$$

(32)

$$v(\lambda) = J\, f(\lambda)$$

(33)

Substituting Eqs. (32) and (33) into Eqs. (25) and (26), then the momentum transfer equations can be expressed as:

$$-\frac{1}{\rho}\frac{\partial p}{\partial x} = \left(\bar{u}(0) - \frac{Jx}{H}\right)\left(-\frac{J}{H}(f^2 - ff'') - \frac{\nu}{H^2}f'''\right)$$

(34)

$$-\frac{1}{h\rho}\frac{\partial p}{\partial\lambda} = \frac{v}{H}\frac{\partial v}{\partial\lambda} - \frac{v}{H^2}\frac{\partial^2 v}{\partial\lambda^2} \qquad (35)$$

Since $\partial p/\partial\lambda$ in Eq. (35) is only a function of λ, and is independent of x, it is possible to differentiate Eq. (34) and Eq. (35) with respect to λ and x, respectively, such that

$$\frac{\partial^2 p}{\partial x\partial\lambda} = 0. \qquad (36)$$

After differentiation with respect to λ, Eq. (34) becomes

$$\left(\overline{u}(0) - \frac{Jx}{H}\right)\frac{d}{d\lambda}\left(\frac{J}{H}(f^2 - ff'') + \frac{v}{H^2}f'''\right) = 0. \qquad (37)$$

If Eq. 37 has to be satisfied for all x, then

$$\frac{d}{d\lambda}\left(\frac{J}{H}(f'^2 - ff'') + \frac{v}{H^2}f'''\right) = 0. \qquad (38)$$

Defining the Reynolds number in the z direction as

$$Re_z = \frac{JH}{v}. \qquad (39)$$

Integrating Eq. 38, a new equation involving $f(\lambda)$ only can be obtained (Eq. 40):

$$Re_z(f'^2 - ff'') + f''' = k, \tag{40}$$

where k is the integration constant.

The boundary conditions for the newly derived Eq. 40 are:

$$\begin{aligned} &\text{at } \lambda = 0, \; f' = f = 0; \\ &\text{ar } \lambda = 1, \; f' = 0 \text{ and } f = 1 \end{aligned} \tag{41}$$

Since the permeate flux during membrane filtration is very small, Re_z is also very small and is in the range of 0.005 ~ 0.05 (Kleinstreuer and Paller, 1983; Bouchard et al., 1994), then the first term in Eq. 40 become negligible and

$$f''' \approx k. \tag{42}$$

A perturbation solution to Eq. 40 is possible (Berman, 1953; Singh and Laurence, 1979; Kleinstreuer and Paller, 1983; Bouchard et al., 1994) using Re_z as a perturbation parameter, by expanding $f(\lambda)$ and k as a power series (Eqs. 43 and 44).

$$f(\lambda) = f_o(\lambda) + f_1(\lambda)Re_z + f_2(\lambda)^2_{Re_z} + \dots + f_n(\lambda)Re_z^n + \dots \tag{43}$$

$$k = k_o + k_1 Re_z + k_2 Re_z^2 + \dots k_n Re_z^n + \dots \tag{44}$$

Substituting Eqs. 43 and 44 into Eq. 40 using the first order perturbation and,

applying the boundary conditions, u and v can be expressed as a function of x and λ (Kleinstreuer and Paller, 1983).

$$u(x,\lambda) = \left[\bar{u}(x_i) - \frac{x}{H}J(x)\right]\left[6\lambda - 6\lambda^2 + \frac{Re_z}{70}(-28\lambda^6 + 84\lambda^5 - 105\lambda^4 + 81\lambda^2 - 32\lambda)\right] \quad (45)$$

$$v(x,\lambda) = J(x_i)\left[3\lambda^2 - 2\lambda^3 + \frac{Re_z}{70}(-4\lambda^7 + 14\lambda^6 - 21\lambda^5 + 27\lambda^3 - 16\lambda^2)\right] \quad (46)$$

The term $J(x_i)$ in Eqs. (45) and (46) is the average permeate flux in the i-th segment on the discretized membrane surface.

3.4.2.2 Mass transfer in the membrane flow channel

If the feed solution contains only a single small specie such as BSA with a very low concentration, then concentration polarization is the main resistance causing the flux decline. As the feed flows across the membrane surface under a positive pressure, the solute in the feed solution is convected to the membrane surface by the permeate, causing the concentration to build up in the vicinity of the membrane surface. The high solute concentration near the membrane causes the solute to diffuse back to the main stream. Neglecting the diffusion in the x direction, the steady state convection-diffusion mass

transfer process is governed by

$$u\frac{\partial C}{\partial x} + \frac{v}{H}\frac{\partial C}{\partial \lambda} = \frac{D}{H^2}\frac{\partial^2 C}{\partial \lambda^2}.$$ (47)

The boundary conditions for Eq. 47 are:

$$
\begin{aligned}
&\text{at } x = 0, \ C = C_o \\
&\text{at } \lambda = 0, \ \frac{\partial C}{\partial \lambda} = 0 \\
&\text{at } \lambda = 1, \ \frac{\partial C}{\partial \lambda} = \frac{J_w}{D} C
\end{aligned}
$$ (48)

The term J_w is the permeate flux on the membrane wall, and can be determined by Eq. 1. The osmotic pressure of a small chemical species is usually a polynomial function of solution (Cheryan, 1986):

$$\Delta \pi = a_1 C + a_2 C^2 + a_3 C^3 + ...$$ (49)

3.5 Numerical simulation by finite element methods

Analytical solutions to the convection-diffusion mass transfer equation (Eq. 47) are very difficult to obtain, and have not been published. For partial differential equations such as Eq. 47, numerical simulation may be the method of choice. Different researchers

have attempted to solve Eq. 47 numerically by a finite difference method to predict the concentration profile within the flow channel (Brian, 1965; Singh and Laurence, 1979; Kleinstrauer and Paller, 1984; Lebrun et al., 1989; Bouchard et al., 1994; Ganguly and Bhattacharya, 1994). Solutions of the mass transfer equation by finite element methods have not been cited in the literature.

Solving partial differential equations numerically by finite difference methods involves subdividing the problem domain into a finite number of grids to achieve a finite number of solution points, choosing a calculation algorithm, applying the boundary values, and then calculating the values in the next grid points based on the previous points (Fig. 20). The number of grids and points determines the accuracy of the approximation. Using the implicit method, Eq. 47 can be transformed into a numerical computation form:

$$u_{i,j1}\left[\frac{C_{i,j1}-C_{i,j}}{\Delta x}\right] - v_{i,j1}\left[\frac{C_{i1,j1}-C_{i1,j1}}{2\Delta z}\right] = D\left[\frac{C_{i1,j1}-2C_{i,j1}+C_{i1,j1}}{\Delta z^2}\right] \quad (50)$$

The finite element method is a numerical simulation technique that can produce near-optimal approximate solutions to initial-boundary value engineering problems (Baker and Pepper, 1991). This approximation method employs subdivision of the problem domain into a finite number of small regions called finite elements. Applying a weak statement or a weighted-residual that minimizes the approximate errors combined with the boundary conditions, a set of algebraic equations can be developed on each finite element, and then collected to form a global matrix statement. The matrix can be solved using any linear algebra technique to obtain the variable values in the problem domain (Baker and
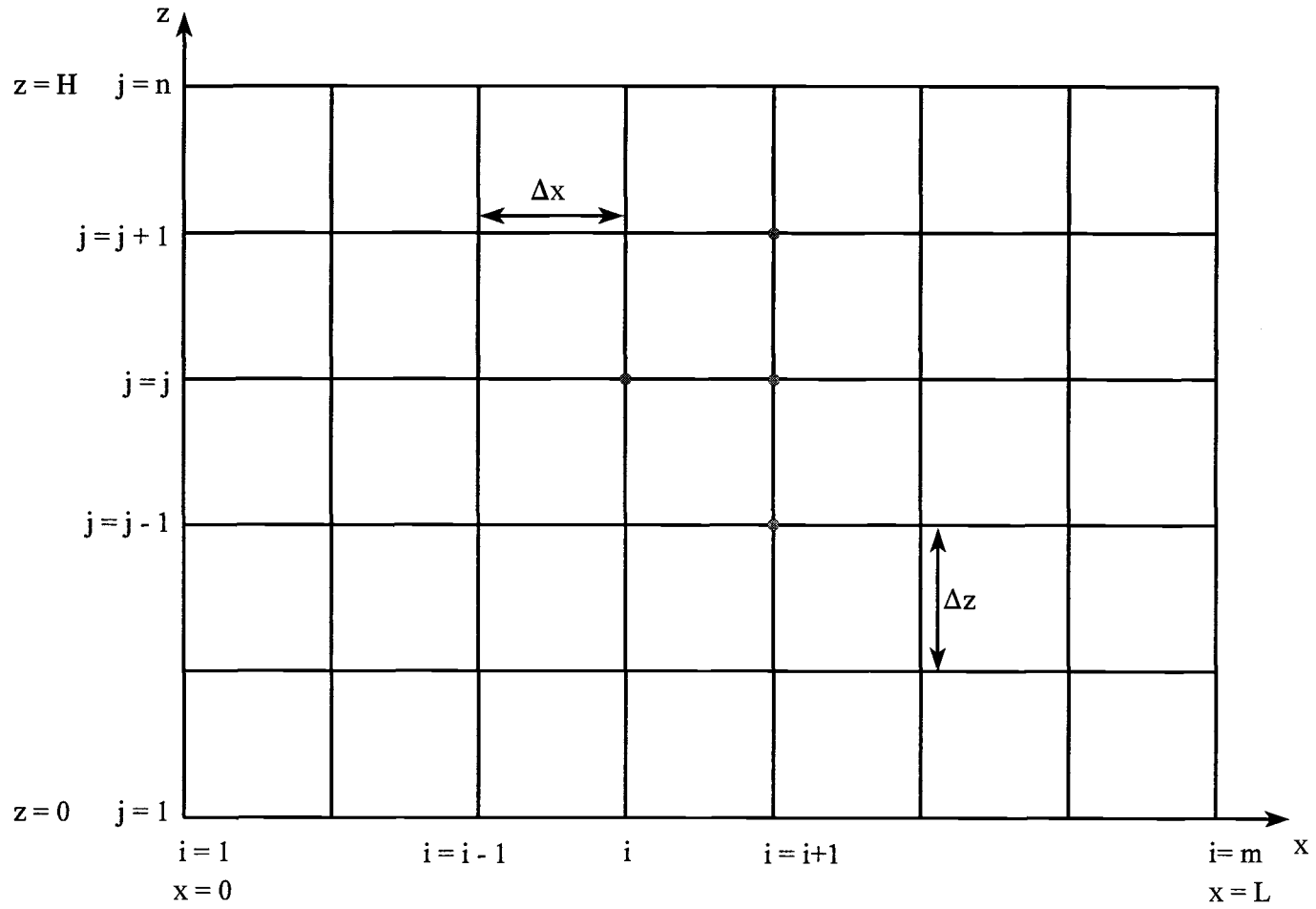
Fig. 20 Implicit finite difference grid (Bouchard et al., 1994)

Pepper, 1991). The finite element method is very useful in handling problems with Dirichlet, Neumann, and Robin boundary conditions.

The key step in the finite element analysis is to employ a Galerkin weak statement. For an x-z 2-dimensional problem, a finite number Taylor (or power) series of known trial function of x and z can be used to approximate the variables:

$$C^n(x,z) = \sum_{i=1}^{n} a_i \phi_i(x,z) \tag{51}$$

To derive a Galerkin weak statement for the mass transfer equation governing the membrane filtration process, Eq. 47 can be rewritten as:

$$L(C) = u \frac{\partial C}{\partial x} + \frac{v}{H} \frac{\partial C}{\partial \lambda} - \frac{D}{H^2} \frac{\partial^2 C}{\partial \lambda^2}. \tag{52}$$

To achieve a minimized approximation error, the weighted residual must vanish, that is:

$$\int_{\Omega} \phi(x,z) \, L(C^n) d\tau = \int_{\Omega} \phi(x,z) \, L(C^n) dx\,dz \equiv 0 \quad \text{for} \quad 1 \le i \le n \tag{53}$$

The Galerkin weak statement for Eq. 47 becomes:

The finite element analysis uses a non-overlapping sum of finite element basis

$$WS = \int_{\Omega} \phi_i \left(u \frac{\partial C^n}{\partial x} + \frac{v}{H} \frac{\partial C^n}{\partial \lambda} - \frac{D}{H^2} \frac{\partial^2 C^n}{\partial \lambda^2} \right) d\tau$$

$$= \int_{\Omega} \phi(x,z) \, L(C^n) d\tau \tag{54}$$

$$= \int_{\Omega} \nabla \phi_i \, L(C^n) d\tau - \int_{\partial \Omega} \phi_i \, L(C^n) \mathbf{n} ds$$

$\{N_k(\zeta_i)\}$ to replace $\phi_i(x, z)$ in the discretized elements Ω^h in the domain Ω and its boundary $\partial\Omega$ (Eq. 55).

$$\phi^h(x,z) = C^h(x,z) = \bigcup_e C_e(x,z)$$
$$C_e(x,z) = \{N_k \, (\zeta_i)\}^T \{C\}_e \tag{55}$$

Then the finite element discrete approximation to the Galerkin weak statement becomes:

$$WS^h = \sum_e \int_{\Omega_e} \nabla\{N_k\} \, \nabla\{N_k\}^T d\tau \, \{C\}_e$$
$$- \int_{\partial\Omega} \{N_k\} \, L(C)_e \mathbf{n} ds \tag{56}$$

In a triangular finite element shown in Fig. 21, defining the local natural coordinate system ζ_i spanning Ω_e as (Baker and Pepper, 1991):

$$\zeta_1 = \frac{(X_2 Z_3 - X_3 Z_2)_e + (Z_2 - Z_3)_e x + (X_3 - X_2)_e y}{2 A_e}$$

$$\zeta_2 = \frac{(X_3 Z_1 - X_1 Z_3)_e + (Z_3 - Z_1)_e x + (X_1 - X_3)_e y}{2 A_e} \tag{57}$$

$$\zeta_3 = \frac{(X_1 Z_2 - X_2 Z_1)_e + (Z_1 - Z_2)_e x + (X_2 - X_1)_e y}{2 A_e}$$
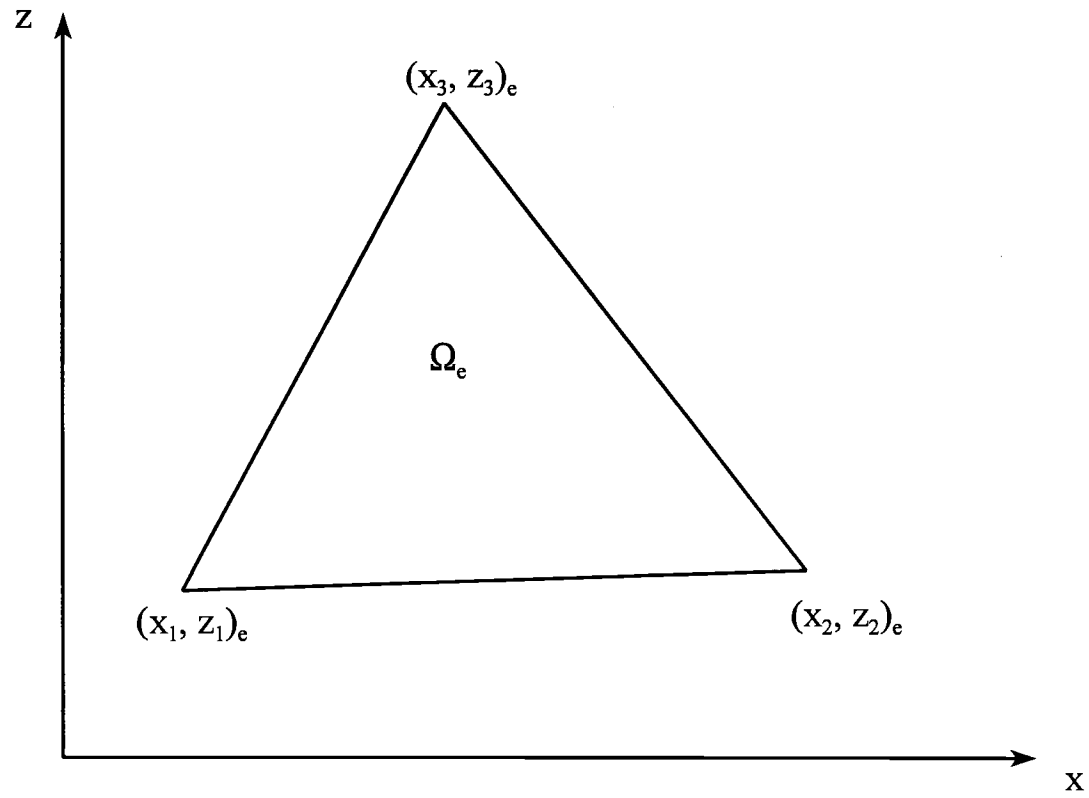
Fig. 21 A generic two-dimentional triangular element Ω_e

Then the generic quadratic basis for the two dimensional finite element analysis

is

$$\{N_2(\zeta_i)\} = \begin{Bmatrix} \zeta_1(2\zeta_1 - 1) \\ \zeta_2(2\zeta_2 - 1) \\ \zeta_3(2\zeta_3 - 1) \\ 4\zeta_1\zeta_2 \\ 4\zeta_2\zeta_3 \\ 4\zeta_3\zeta_1 \end{Bmatrix} \tag{58}$$

and

$$\nabla\{N_2\} = i \; \frac{\partial\{N_2\}}{\partial\zeta_i} \frac{\partial\zeta_i}{\partial x} + j \; \frac{\partial\{N_2\}}{\partial\zeta_i} \frac{\partial\zeta_i}{\partial z} \tag{59}$$

The Galerkin weak statement generates a set of matrices that can be solved by any computational technique to obtain approximated values of $\{C\}_e$, the concentration distribution over the system domain.

4. MATERIALS AND METHODS

4.1 Characterization of waste water generation in the surimi industry

One plant was selected for this study in the summer of 1994, which was a peak season for Pacific whiting (*Merluccius productus*) surimi manufacturing. The plant was located in a coastal city of Oregon, on the Columbia River. It directly discharged the waste water into the river without any pretreatment.

To completely understand the waste water generated by this plant, three steps were taken. The first step was to understand and identify all the unit operations in the surimi processing line, and to develop a process flow diagram. The second step was to conduct a water and waste water audit, and to collect waste water samples at selected sampling points. The third step was to analyze and characterize the waste water generated in the processing plant.

4.1.1 Process flow diagram development

The surimi processing line was examined to understand the functions of each unit operation and the relationship between different unit operations. Water supply lines and locations of waste water generation were identified. A flow diagram of surimi processing was then developed.

A system approach was adopted. Based on the preliminary observation, it was found that the whole processing line was treated as a major system with two subsystems (Fig. 22 and Fig. 23). The first subsystem processed raw fish into minced fish, which

Material in
Fish

Material out
Solid wastes

Processing plant

Product

Water

Waste water
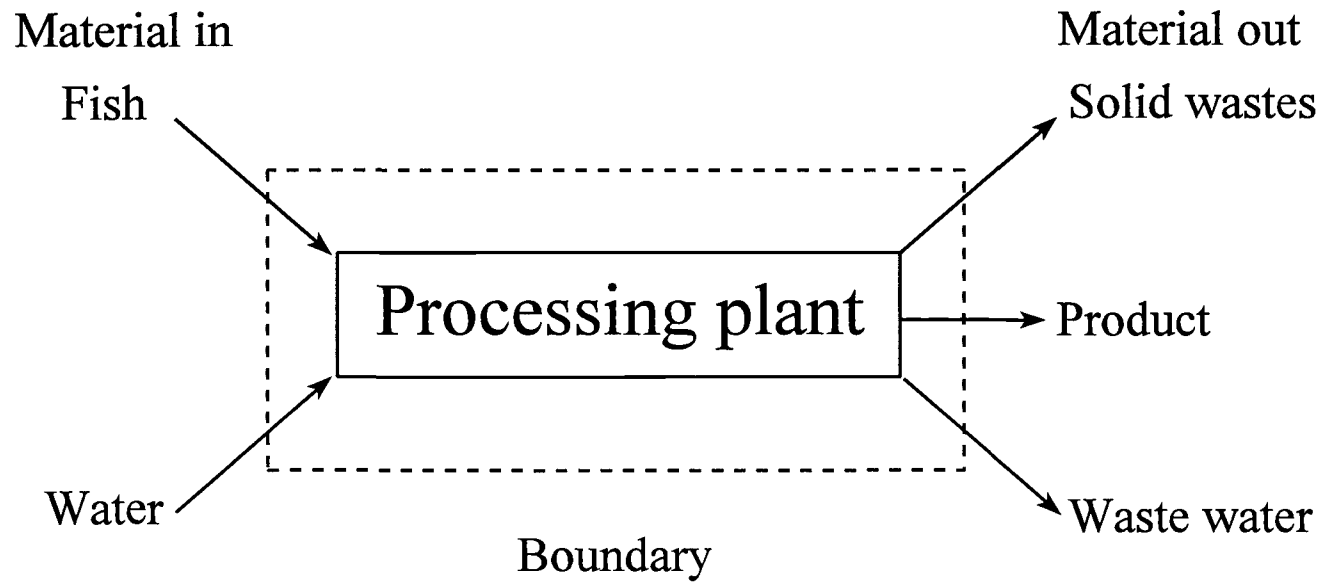
Boundary

Fig. 22 The plant could be treated as a big system with interactions with the environment utside the boundary
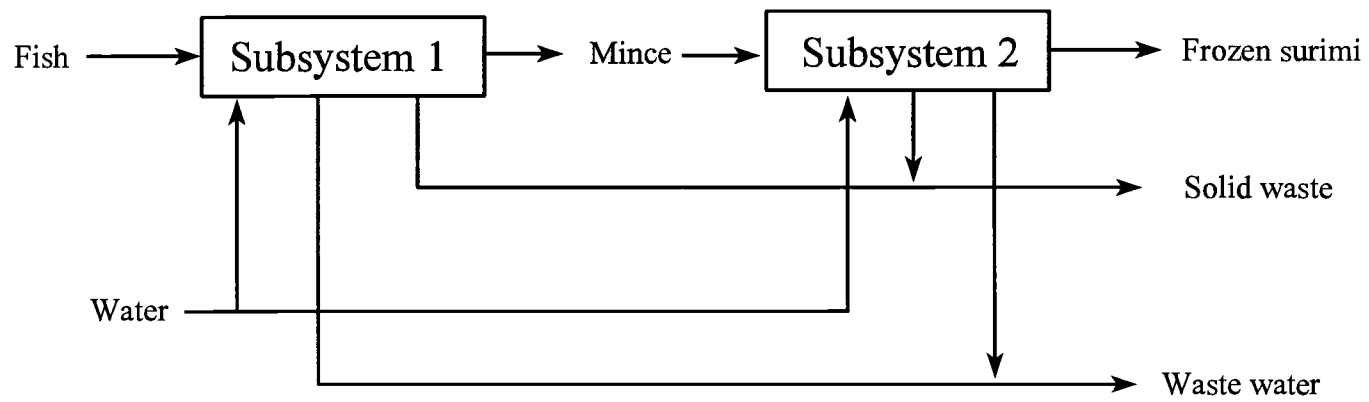
Fig. 23 The big system may be divided into two subsystems that interact with each other through an intermediate product, fish mince

was then a raw material for the second subsystem. Two subsystems interacted with each other through the intermediate product, fish mince. Each subsystem was composed of different unit operations (Fig. 24).

4.1.2 Audit of water consumption and waste water generation

After the flow diagram was developed and sources of waste water were identified, a 3-day water and waste water audit was conducted using the methods modified from Mate (1992) and Mannapperuma et al. (1993). Daily measurements of water and waste water flow rates from each unit operation were conducted, and a 3-day average was used to represent the water and waste water flow rates.

1. Water audit

Water consumption in the processing lines was determined by measuring the water flow rate in the pipes using a microprocessor-based ultrasonic water flow rate meter (Fig. 25) manufactured by Polysonics Co. (TYME-FLYTE portable ultrasonic flowmeter, Model TF-P, Polysonics, Washington, D.C.). This device consisted of two ultrasonic signal transducers that were mounted on the external wall of the pipes at a distance determined by the pipe size. The time required for an ultrasonic signal to travel between the two transducers was measured electronically. The difference in time between signals traveling upstream and downstream is proportional to the liquid flow velocity. With a known internal diameter of the pipe, the flow rate could be calculated. This device was a non-invasive water flow rate meter and could be used to measure the water flow rate
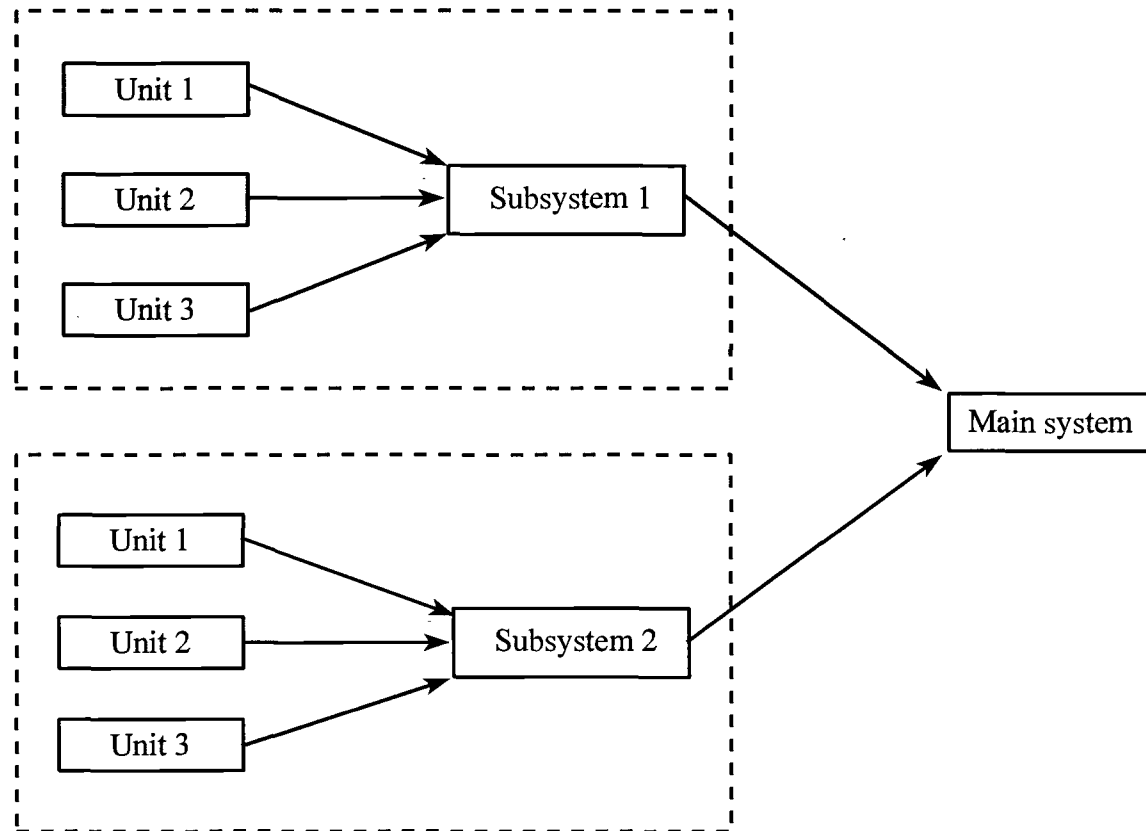
Fig. 24 Each subsystem can contain different numbers of units operations

Water pipe

Water flow direction →

Ultrasonic signal

Upstream signal
transducer

Downstream signal
transducer

Microprocessor-based ultrasonic flow meter
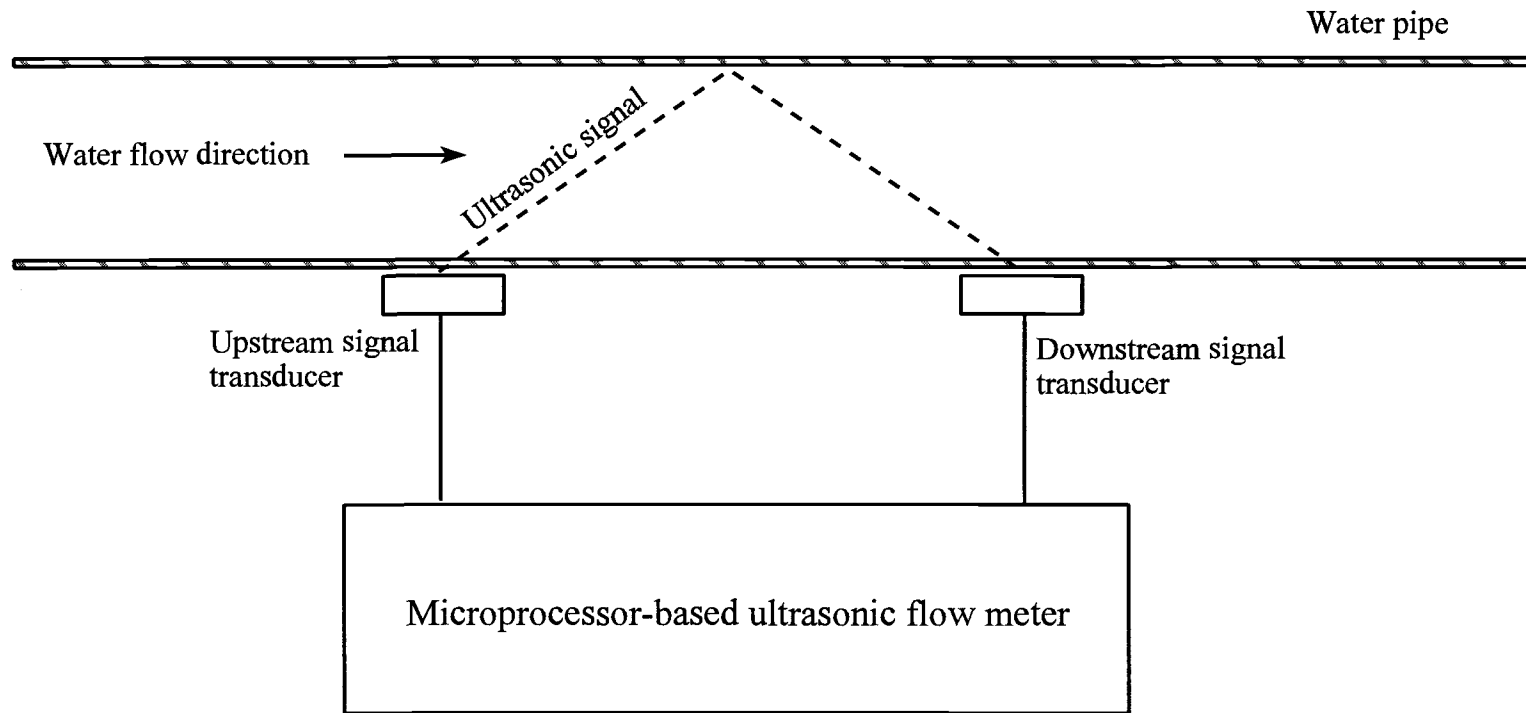
Fig. 25 Schematic diagram of a ultrasonic flow meter

in the existing processing lines without interrupting normal operations. When measuring water flow rate, three determinations were taken at each sampling point.

Some unit operations in surimi processing require a continuous supply of water to ensure a smooth operation. These operations were almost all located in the raw material treatment stages (Subsystem 1). Fresh water was supplied to prevent fish body fluids and fish muscles from sticking to the machines. In washing of fish mince, sequential batch operation was used. As a characteristic of batch-type operation, water was not continuously supplied to the washing tanks, but was automatically fed to the tanks according to the operation sequence determined by the process logic controller (PLC).

In Subsystem 2, batch operations (such as surimi washing) were repeated periodically. If the time needed to complete a washing cycle was t, and during which period only a fraction of the time, t_a, was used to pump fresh water into a washing tanks, as graphically shown in Fig. 26 the total amount of fresh water pumped to the washing tank can be calculated with Eq. 60.

$$V_{H2O} = Q_{H2O,a} \times t_a \tag{60}$$

where V_{H2O} = total volume of water used in a washing cycle, L;

$Q_{H2O,a}$ = flow rate of water when being pumped to the washing tank, L/min.

If water is continuously supplied to a machine (rinsing), Eq. 60 can also be used, in which t_a is equal to t. To analyze the water consumption in a washing batch, it is more desirable to use an averaged water flow rate to express an overall water flow rate over the

Washing

$$\longleftrightarrow \quad t \quad \longleftrightarrow$$

| Water in | Fish mince in | Stirring/washing | Discharging |

t_a

Dewatering

$$\longleftrightarrow \quad t \quad \longrightarrow$$

| Idling | Dewatering |

t_a
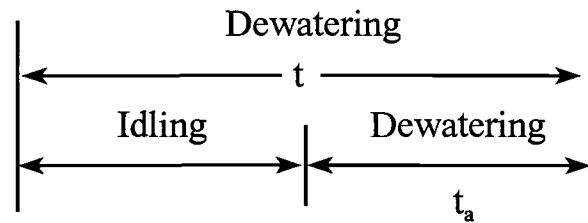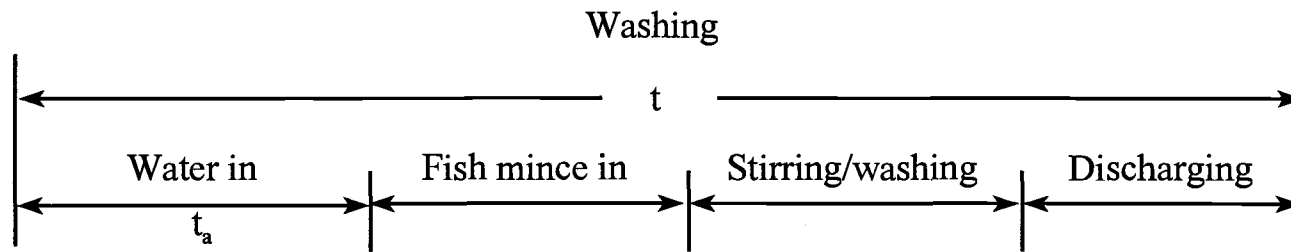
Fig. 26 Time distribution in on-off control of batch operation in Subsystem 2

time period of t. So the averaged water flow rate in a batch, Q_{H2O}, is expressed as (Eq. 61):

$$Q_{H2O, AVG} = \frac{V_{H2O}}{t} \qquad (61)$$

The total water consumption in a subsystem is the sum of each individual operation (component), as expressed in Eq. 62.

$$Q_{H2O, Subsystem, i} = \sum Q_{H2O, AVG, j} \qquad (62)$$

where subscript *i* represents a subsystem, and *j* represents a component in that subsystem containing a total number of *n* components.

2. Waste water audit

Waste water flow rates were calculated from the volume of the waste water collected in plastic buckets, divided by the time measured by a stopwatch. For some operations, such as the heading operation where waste water was scattered all around the heading machine, more than one bucket was used to collect the waste water within a specified time period. At each sampling point, measurements were replicated for three times. The volume of waste water was measured, and the flow rate could be calculated by Eq. 63:

$$Q_{WH2O,\,AVG} = \frac{V_{WH2O}}{t_m} \qquad (63)$$

where V_{WH2O} was the volume of waste water collected, and t_m is the time needed to collect the waste water.

In batch-type operations such as the dewatering process where waste water was intermittently released, equations similar to Eq. 60, Eq. 61, and Eq. 62 were used to calculate average flow rates of waste water from a unit operation (Eqs. 64 and 65).

$$Q_{WH2O,\,AVG} = \frac{Q_{WH2O} \times t_a}{t} \qquad (64)$$

$$Q_{WH2O,\,Subsystem,\,i} = \sum Q_{WH2O,\,AVG,\,j} \qquad (65)$$

where subscript *WH2O* represents waste water. In a continuous operation t_a was equal to t.

4.1.3 Chemical analysis

Approximately 1 L of waste water samples was collected at each sampling point. Samples were kept in a refrigerated container and immediately transferred to a deep freezer (-40 °C) (Fresenius et al., 1989). Prior to conducting chemical analyses, samples were thawed overnight in a refrigerator (3-5 °C).

Chemical analyses were conducted to determine total solids (TS), chemical oxygen

demand (COD), protein, and 5-day biological oxygen demand (BOD_5). TS and BOD_5 were measured using the Standard Methods (Greenberg et al., 1980). COD was measured using the method developed by Hach Chemical Co. (Gibbs, 1979).

4.2 Treatment of surimi wash water by ohmic heating

4.2.1 Ohmic heating device

A batch-type ohmic heating device (Fig. 27) developed by Huang et al. (1996) was used in this study. A 500 mL beaker containing a 250 g sample was enclosed in a styrofoam box, and placed on top a magnetic stirrer (Model SP18425, Barnstead/Thermolyne, Dubuque, IA). The sample was gently stirred with the magnetic stirring bar to ensure uniform heating. The electric voltage was set at 90 V throughout the test. Heating temperatures were controlled by a temperature controller (Type E5CS-R1KJX-520, Omron Manufacturing, the Netherlands B.V.). The sample temperature was measured with a Type C thermocouple every 5 s and recorded in a datalogger (Model CR10, Campbell Scientific, Inc., Logon, UT). To measure the current passing through the samples, an AC current transducer (Model OM8-2182AFA0, OMEGA Engineering, Stamford, CT) was used to linearly convert the AC current signals into DC voltages measurable by the datalogger.

Temperature controller

70 C

SSR

A

3

110 VAC

CR10 Datalogger

1
2
4
5
6

1. Type C thermocouple
2. Type J thermocouple
3. Transformer

4. SS electrode
5. Styrofoam box
6. 500 mL beaker
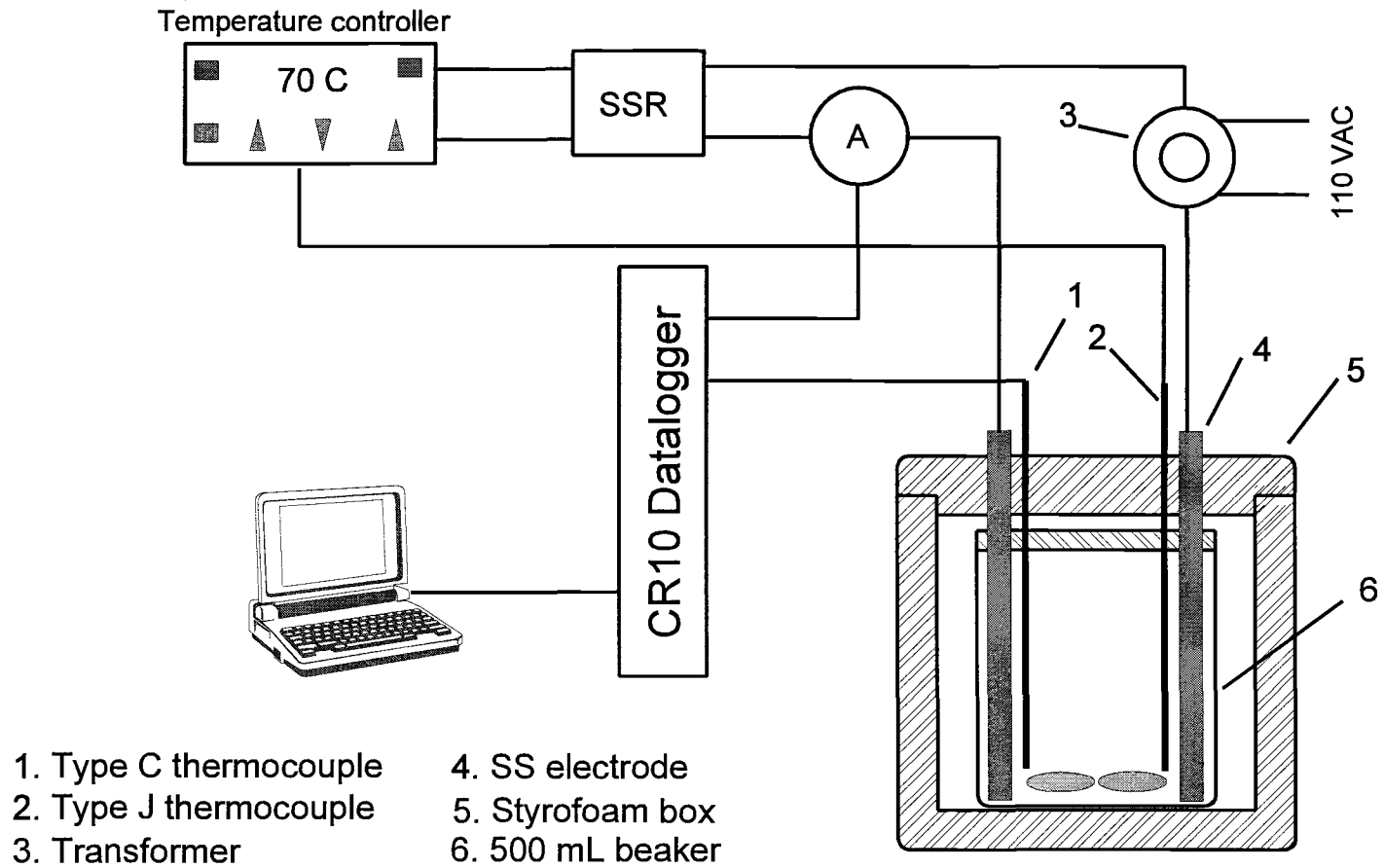
Fig. 27 Ohmic heating device for treatment of surimi waste water

4.2.2. Calibration of the device and determination of electrical conductivity

To measure the electrical conductivity of surimi wash water, the device was calibrated with a standard solution with a known electrical conductivity (Palaniappan and Sastry, 1991a; 1991b). Solutions (250 g) of 0.17 M sodium chloride (NaCl) were quickly heated to 25 °C in the ohmic heating device at 90 Vac, and kept constant at this temperature. The electrical voltage was quickly reduced to 5 Vac after the temperature reached 25 °C. The current passing through the solution at 25 °C was measured and recorded. The effective device coefficient, which is determined by the geometry of the ohmic heating device, can be calculated from Eq. 66 (Palaniappan and Sastry, 1991a; 1991b):

$$K_c = \frac{\sigma}{\left(\dfrac{I}{V_e} \right)} \qquad (66)$$

where K_c is the effective device coefficient, defined as:

$$K_c = \frac{L_e}{A_e} \qquad (67)$$

4.2.3 Sample preparation

Pacific whiting fish (500-600g) less than 24 hr postharvest were obtained from a local surimi processing company. Fish were headed, gutted, filleted, and comminuted into fish mince. Fish mince was mixed with chilled distilled water (fish/water = 1:3) and washed for 3 min under a gentle mixing condition. After washing, the mixture was filtered consecutively through two stainless steel strainers (hole diameters 2 mm and 1 mm, respectively) to remove fish mince. The wash water was stored in a cold room (5 °C) and subjected to ohmic heating the same day.

4.2.4 Coagulation of fish proteins by ohmic heating

Wash water samples (250 g) were heated to 30, 40, 50, 60, 70, and 80°C, respectively, using the method described by Huang et al. (1996). After heating, samples were quickly cooled to below 5°C in an ice bath to retard the enzymatic degradation. Samples were centrifuged at 1700 x g for 10 min. Supernatants were collected for chemical analyses. All tests were run in triplicate.

4.2.5 Chemical analysis

Total solids (TS), total suspended solids (TSS), protein concentration, and chemical oxygen demand (COD) were analyzed. TS and TSS were measured using Standard methods (Greenberg at al., 1980). After the samples were solubilized in 5% sodium dodecylsulfate (SDS) solution (Lin et al., 1995), protein content was determined by the method of Lowry et al. (1951) with bovine serum albumin (BSA) as the standard.

COD was assayed using the method developed by Hach Chemical Co. (Gibbs, 1979). Sodium dodecylsulfate polyacrylamide gel electrophoresis (SDS-PAGE) was employed using the method modified from Laemmli (1970) to evaluate the effect of heating on protein coagulation. Samples (100 μg) were mixed with a treatment buffer containing β-ME at 1:1 (v/v) and loaded to the gel. SDS-PAGE was conducted at room temperature using 20 mA current overnight. The gel was stained with 0.125% Coomassie brilliant blue R-250 and then destained.

4.2.6 Enzyme assay

Protease activity was assayed using the method described in An et al. (1994b) using casein as substrate. Wash water samples (200 μL) with and without ohmic heating were mixed with 500 μg of casein and 1000 μL of McIlvaine's buffer (pH 5.5) containing 1 mM β-mercaptoethanol (β-ME), and incubated at 55°C for 1 hr. The reaction was terminated by adding 500 μL ice-cold 50% (w/v) trichloride acid (TCA) solution. Blanks were prepared by adding TCA solutions to the samples prior to incubation. TCA-coagulated proteins (unhydrolyzed) were allowed to precipitate for 15 min at 4 °C, and centrifuged at 5000 x g for 10 min. Supernatants (800 μL) mixed with 200 μL 5 N NAOH solution were assayed for tyrosine(Tyr) concentration using the Lowry's method (Lowry et al., 1951). Specific activities of proteases were expressed as nmol Tyr/min per mg of protein.

4.3. Microfiltration of surimi wash water

4.3.1 Membrane filtration unit

A stainless steel plate-and-frame crossflow membrane filtration unit was fabricated and installed (Fig. 28). The unit had a channel height of 7.934×10^{-3} m (5/16 inches) and a filtration area of 0.03 m^2 (6 x 8 inches). An air-driven double diaphragm pump (Model BK-5, All-Flo Pump Co., Mentor, OH) was used to pump the feed into the filtration unit. To achieve a pulseless flow during filtration, a flow stabilizer (Model Sentry II, Blacoh Fluid Controls, Moreno Valley, CA) was mounted at the exit of the diaphragm pump. A rotameter (Model FL7304, OMEGA Engineering, Inc., Stamford, CT) was installed to measure the flow rate of the feed. Two pressure sensors (Model PX236-100G V, OMEGA Engineering, Inc., Stamford, CT) were installed in the inlet and outlet of the filter to measure and monitor the applied pressures. The permeate was collected in a pre-weighed plastic bucket and the weight was continuously measured by a loadcell (Model LCL-010, OMEGA Engineering, Inc., Stamford, CT). The sample and ambient temperatures were measured by Type T thermocouples. A datalogger (Model CR10X, Campbell Scientific, Inc., Logan, UT) was used to collect the real time data of pressures, permeate weight, and temperatures. The datalogger was programmed to collect the data at variable sampling rates (every 5 s for the first 30 min, every 1 min for the next 1 h, and every 5 min for the rest of filtration process). The filtration data were transmitted to a notebook computer through the I/O port of the datalogger, and the process was monitored by the PC.

Fig. 28 A plate-and-frame crossflow membrane filtration unit with a data acquisition system.

1. Pressure sensor
2. Top plate
3. Spacer and gaskets
4. Membrane
5. Support plate
6. Bottom plate

4.3.2 Preparation of samples

Fresh Pacific whiting (< 24 h post harvest) were obtained from a local surimi processing plant in Warrenton, Oregon. Fish were manually headed, gutted, and comminuted into fish mince in a Hobart meat grinder (Model K5SS, Hobart Co., Troy, OH). Fish mince was mixed with chilled ($\approx$ 3°C) distilled water (w/v = 1/3) and washed for 3 min under a gentle mixing condition at ambient temperature. Wash water was strained through 2 stainless steel strainers (hole diameters 2 mm and 1 mm, respectively). Approximately 12 L of wash water was obtained and used in each test. Wash water was mixed with 20 ppm silicone antifoam (Antifoam 1510-US, Dow Corning, Midland, MI) to prevent foam formation during pumping. To evaluate the effect of solid concentration on pore blocking and cake formation, solutions with different concentration were prepared.

4.3.3 Membranes

Polysulfone (Supor 20 and Supor 45, with pore sizes 0.2 and 0.45 µm, respectively) and polyethersulfone (HT 20 and HT 45, with pore sizes 0.2 and 0.45 µm, respectively) membranes were purchased from Gelman Sciences Inc. (Ann Arbor, MI).

4.3.4 Characterization of membranes

Two parameters, specific flux and membrane resistance, were used to macroscopically characterize the membranes. To characterize membranes, deionized water (>16 MΩ) was pumped into the membrane unit. Volumes of the permeate through the

membrane were measured for calculation of the flux (L/m^2s). Specific flux J^* ($L/m^2s\,Pa$) was defined as the pure water flux through the membrane per unit area (m^2) per unit pressure (Pa). Membrane resistance R_m can be calculated from Eq. 12 when pure water was used in filtration. The viscosity of water was chosen as 0.001 Pa·s.

4.3.5 Filtration process

Surimi wash water was pumped from the feed tank to the filtration unit at 19 L/min (5 GPM) under an average transmembrane pressure of 34.5 KPa (5 psi). The retentate was recycled back to the feed tank. To simulate a continuous filtration process (constant feed concentration), the total permeate weight was controlled at less than 5% of the total feed weight so that the increase in the feed concentration could be neglected (Redkar and Davis, 1993). The filtration temperature was controlled at 12 - 15°C throughout the tests. Samples of feed, permeate, and concentrate were collected for chemical analyses.

4.3.6 Chemical analysis

Samples of feed, permeate, and concentrate were collected for chemical analyses of TS, TSS, protein, and total ash. TS, TSS, and ash were measured according to the Standard Methods (Greenberg et al., 1980). Total organic solids (TOS) was calculated from the difference between TS and ash. Biuret method was used to detect protein concentrations in the samples with solubilized caseinate as the standard. The protein content of caseinate was calibrated using the Kjedahl method (AOAC 1995) using a

conversion factor of 6.38.

To understand the components in the wash water samples that passed through the membrane pore, sodium dodecylsulfate polyacrylamide gel electrophoresis (SDS-PAGE) was performed using the method modified from Laemmli (1970). A Bio-Rad vertical electrophoresis unit (20 x 20 x 0.08 cm) was used. Samples of 100 µg were loaded to 10% polyacrylamide gels. From the band patterns of the gels, it was possible to understand the molecular weight ranges of protein components in the wash water samples passing through the membrane pores.

4.4. Finite element analysis of concentration polarization during ultrafiltration of bovine serum albumin

4.4.1 Membrane filtration unit

A small scale stainless steel (SS 304) radial crossflow plate-and-frame membrane filtration unit was designed and fabricated. It was composed of two separate parts, a top section (Fig. 29) and a bottom section (Fig. 30). A stainless steel screen (200 mesh) disk was placed in the bottom section to provide a mechanical support to the membrane. Polysulfone ultrafiltration membrane disks (MWCO=30,000 Dalton), obtained from Millipore Corp. (Biomax-30, lot No. P5HM0882) was positioned on top of the stainless steel screen. The membrane was 47 mm in diameter with an effective filtration area of 11.4 cm^2 after installation in the filter housing. A new membrane was used for each test.
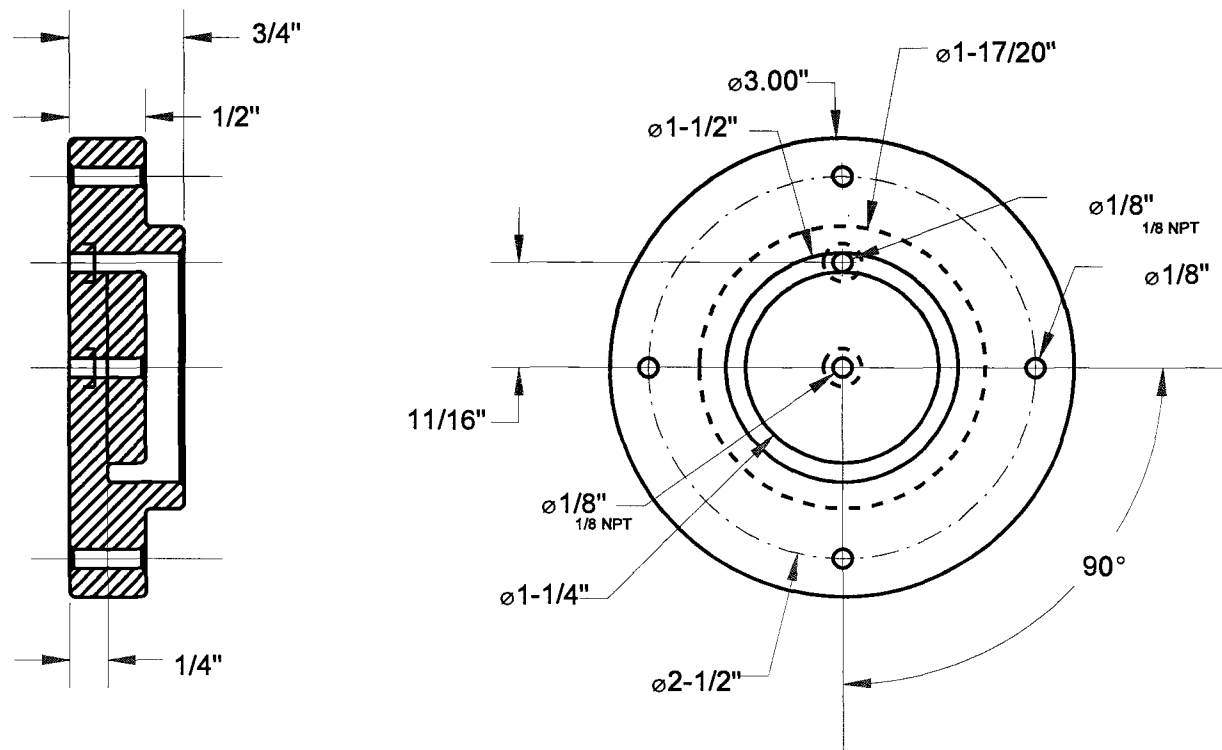
Fig. 29 Top section of a radial crossflow filter
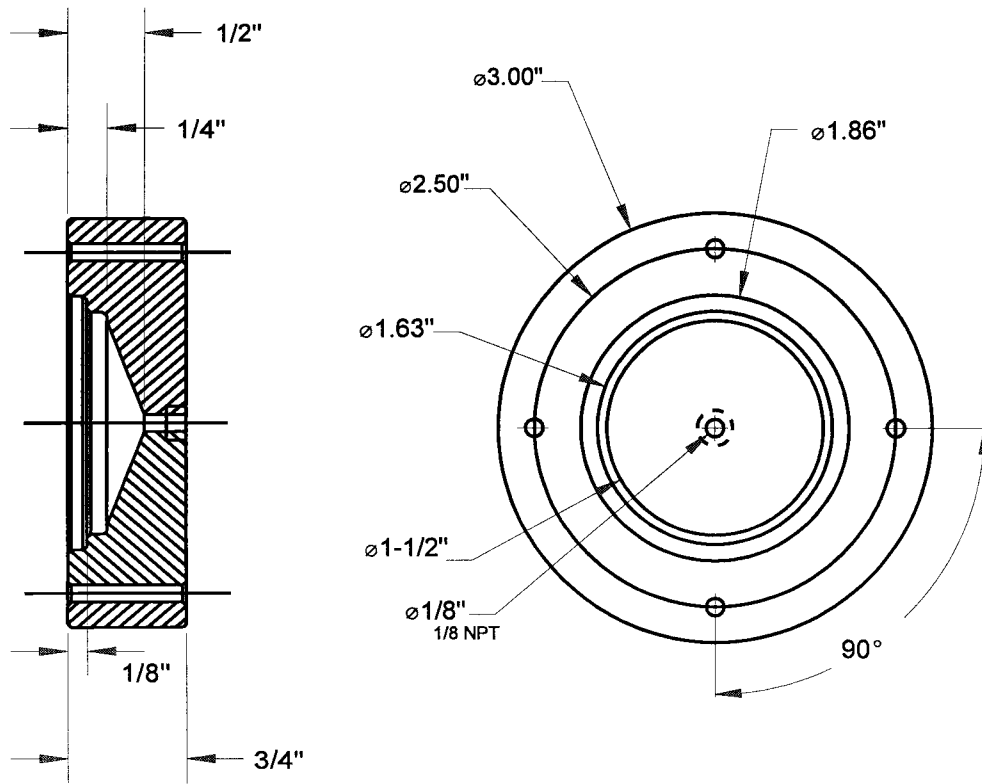
Fig. 30 Bottom section of a radial crossflow filter

A gear pump was used to pump and pressurize the feed solution into the filter unit. The feed was pumped into the center port of the top section and flowed radially across the filter, and exited the filter in the exit port shown in Fig. 31. The inlet and outlet pressures were measured by two pressure sensors (Model PX236-100G V, OMEGA Engineering, Inc, Stamford, CT). The transmembrane pressures were adjusted by a valve installed in the outlet of the membrane filter. The permeate was collected in a small plastic bottle, and weighed by a loadcell (Model CLC-454G, OMEGA Engineering, Inc, Stamford, CT). A datalogger (Model CR10X, Campbell Scientific, Inc., Logan, UT) was used to collect the real time data of pressures, permeate weight, and temperatures. The datalogger was programmed to collect the data at every 5 s throughout the filtration process. The filtration data were transmitted to a notebook computer through the I/O port of the datalogger, and the process was monitored by the PC.
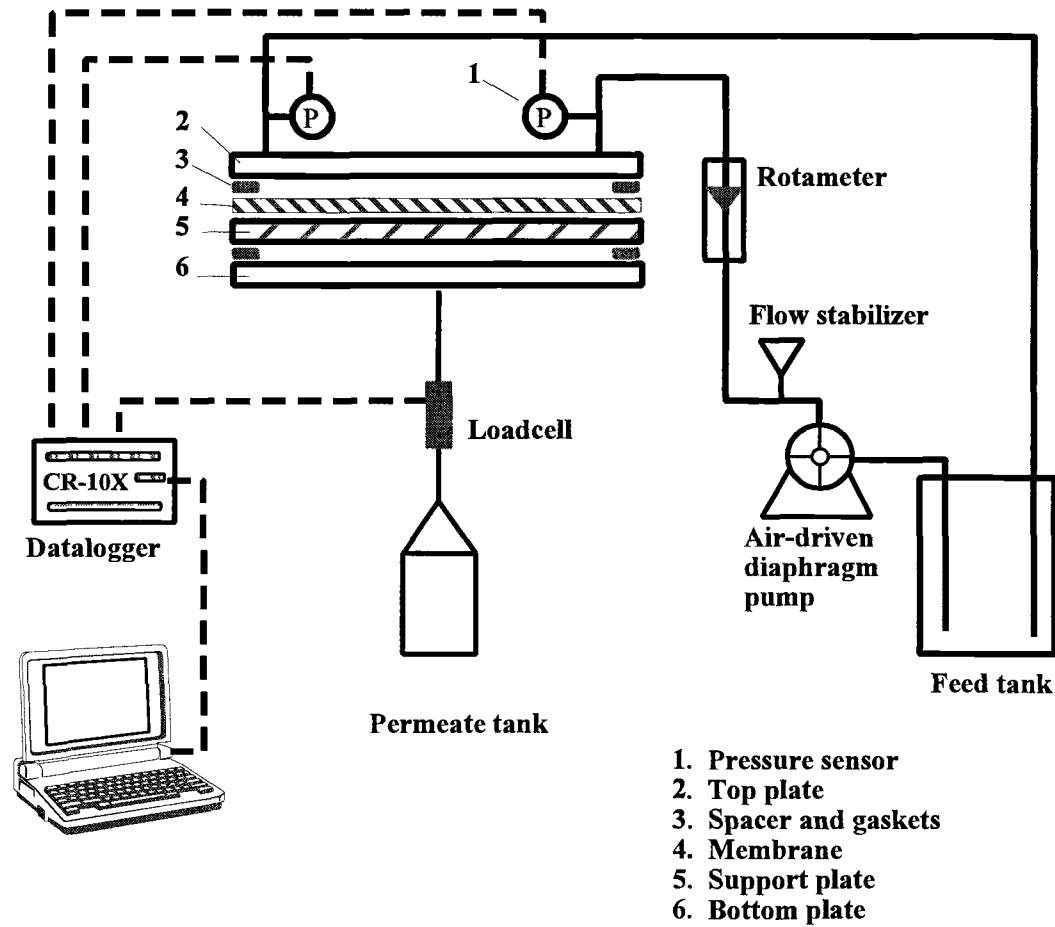
BSA (68,000 Dalton, Sigma A7906, Fraction V Powder) solutions were prepared by dissolving 0.25 g dry powder in 1 L of pH 6.0 0.05M McIlvaine's buffer and 0.15M sodium chloride solution. Freshly prepared BSA solution was used in the tests.

4.4.2 Finite element analysis of concentration polarization during ultrafiltration

Since BSA molecules are larger than the MWCO membrane, complete rejection was observed and experimentally verified. If the BSA molecules are regarded as rigid spheres, the mass transfer is governed by Eq. 47. With known boundary conditions and diffusion coefficient, the convection-diffusion mass transfer equation can be solved numerically.
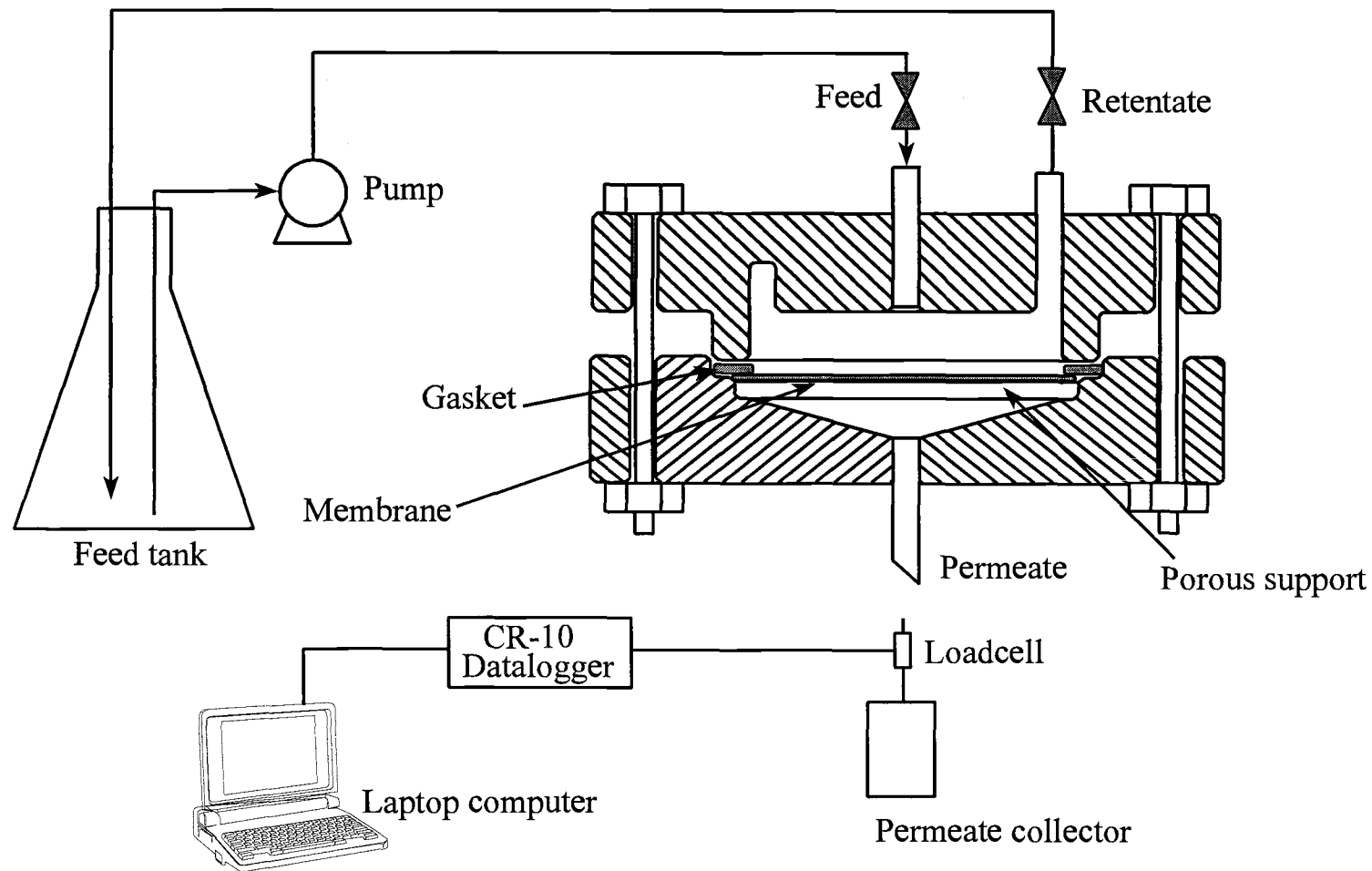
Fig. 31 A radial crossflow ultrafiltration unit with a computer-assited data collection system

Since the filtration unit is a radial crossflow device, the x coordinate in Eqs. 25-27 must be replaced by the radius r (Ganguly and Bhattacharya, 1994). Eq. 47 becomes

$$u\frac{\partial C}{\partial r} + \frac{v}{H}\frac{\partial C}{\partial \lambda} = \frac{D}{H^2}\frac{\partial^2 C}{\partial \lambda^2}. \tag{68}$$

The boundary conditions for Eq. 68 are:

$$
\begin{aligned}
&\text{at } r = 0, \; C = C_o \\
&\text{at } \lambda = 0, \; \frac{\partial C}{\partial \lambda} = 0 \\
&\text{at } \lambda = 1, \; \frac{\partial C}{\partial \lambda} = \frac{J_w}{D} C.
\end{aligned}
\tag{69}
$$

In the radial crossflow membrane, the fluid flow velocity changes as a function of radius, i.e.,

$$u(r) = \frac{Q_o}{2\pi r H}. \tag{70}$$

In a discretized domain, the velocity profiles of Eqs. 45 and 46 can be rewritten as:

$$u(r,\lambda) = \left(\bar{u}(r_i) - \frac{r}{H}J(r_i)\right)\left(6\lambda - 6\lambda^2 + \frac{Re_z}{70}(-28\lambda^6 + 84\lambda^5 - 105\lambda^4 + 81\lambda^2 - 32\lambda)\right)$$

(71)

$$v(r,\lambda) = J(r_i)\left(3\lambda^2 - 2\lambda^3 + \frac{Re_z}{70}(-4\lambda^7 + 14\lambda^6 - 21\lambda^5 + 27\lambda^3 - 16\lambda^2)\right)$$

(72)

4.4.3 Finite element analysis

A Windows 95® based finite element analysis package called Pdease2D™ developed by Macsyma, Inc. (Arlington, MA) was chosen for simulation of concentration polarization during ultrafiltration. Pdease2D™ is a general purpose two dimensional finite element analysis program for obtaining numerical solutions to steady or non steady state boundary value, time-dependent boundary value, initial value, and eigenvalue problems. It uses the Galerkin statement with quadratic basis to convert continuous partial differential equation into discrete nodal equations. It features automatic mesh generation and adaptive grid refinement, and can handle linear and nonlinear problems. It can generate a series of output graphics after numerical computation.

In finite element analysis, normalized coordinates were used to transform the membrane flow channel into a dimensionless square region with each side having a length of one. In the region near the membrane surface, more meshes were placed using a

command called "feature" in Pdease2D™. The average effective diffusion coefficient D

of BSA molecule was assumed constant, and was chosen as 3.5 x 10^{-10} m/s (Kleinstreuer

and Paller, 1983). The osmotic pressure as a function of BSA concentration was obtained

from Viker et al. (1981). Simulations were completed in Cyrix P-200 computer within

30 min.

5. RESULTS AND DISCUSSION

5.1. Characterization of waste water generation in the surimi industry

5.1.1 Process flow diagram

The audit of water and waste water was conducted in a shore-based surimi processing plant. Therefore, the results of this study are pertinent to the shore-based surimi operations only. Fig. 32 is a detailed flow diagram of the surimi processing line. The surimi processing line was treated as a system with two interacting subsystems Fig. 33 and Fig. 34. Each subsystem was composed of unit operations that were closely related to each other.

5.1.1.1 Subsystem 1 - raw material treatment

Raw fish were caught off the coast of Oregon and transported to the plant for processing. Fish were conveyed from the fishing boat in the receiving dock through a pipe via sea water and stored in four 50,000-pound storage tanks. Most of the sea water was returned to the sea. Fish in the storage tanks were immersed in the sea water that provided lubrication and was a conveying agent when fish were released to the feeding tank located in the bottom of the storage tanks.

A conveyor belt was used to transport the fish from the feeding tank to the heading machine. Each fish was properly aligned on the conveyor belt by the operators for the heading operation. In the heading machine, fish heads were separated from the
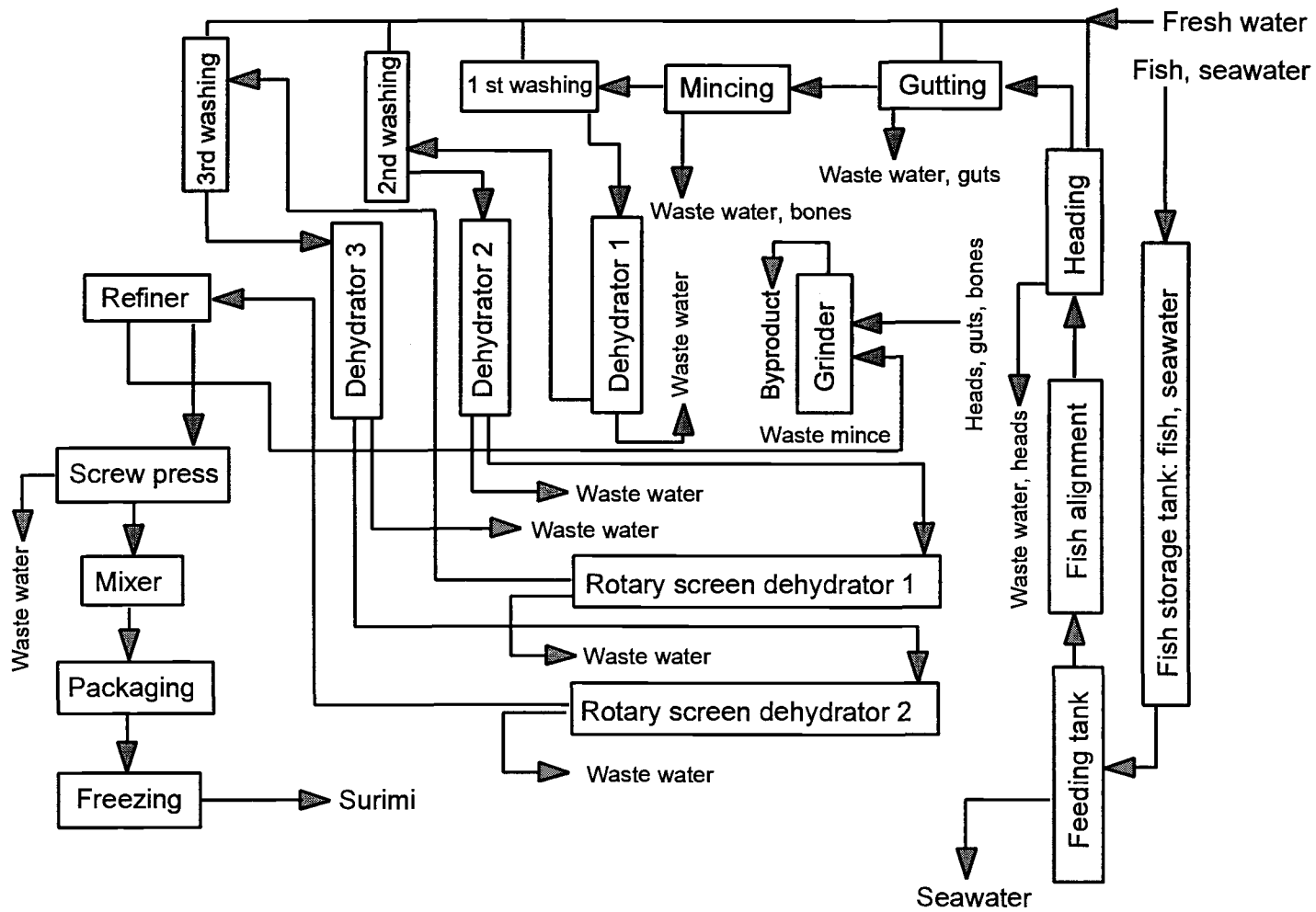
Fig. 32 Flow of materials and sources of waste water.
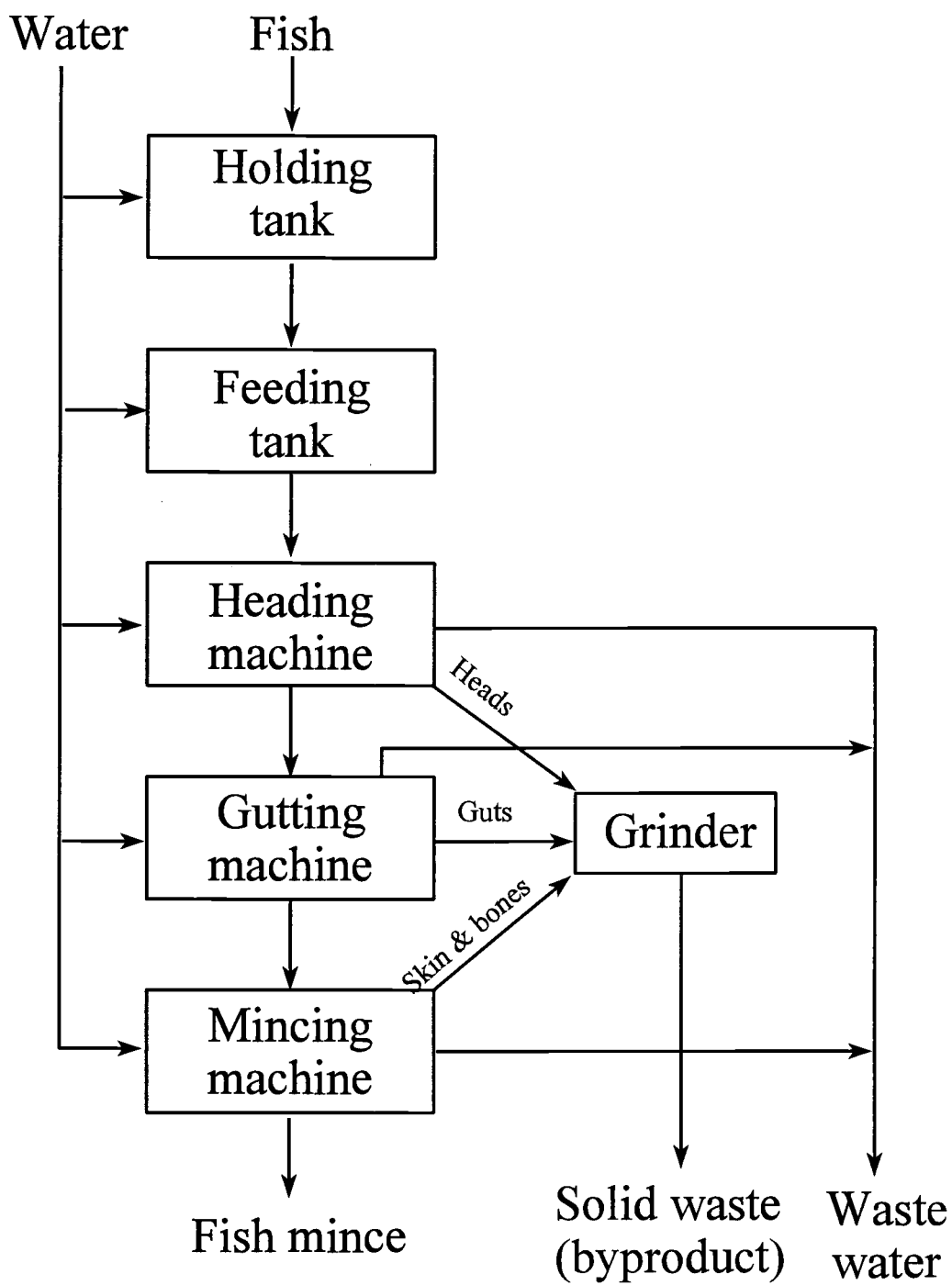
Fig. 33 Unit operations in Subsystem 1

117
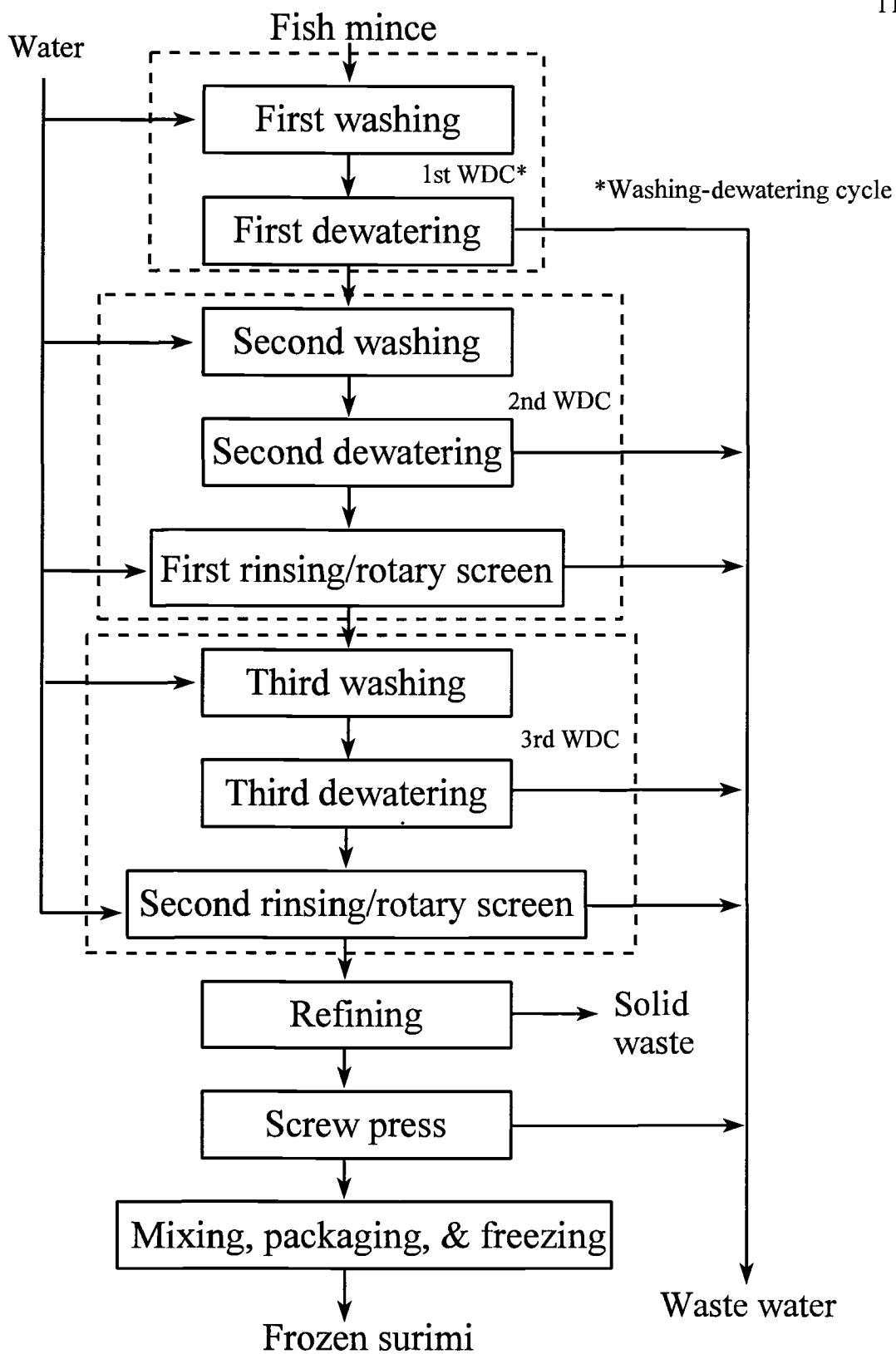
Fig. 34 Unit operations in the 2nd subsystem

fish bodies. The gutting machine removed the fish guts. The mincing machine removed skins and bones while mincing took place.

In the heading, gutting, and mincing operations, water was supplied to the machines to perform two functions. Water streams were injected to the cutting blades to clean the blades and to provide lubrication for smooth operations. Running water was used to flush the separated fish body parts (heads, guts, and skins) out of the machines. Estimated fish mince production rate was 29.1 kg/min, which was about 32% of the total fish fed into the production line. This value was very close to the published values (Babbitt et al., 1985; Lee, 1986).

5.1.1.2 Subsystem 2 - surimi processing

This subsystem contained three washing, three dewatering, two rinsing, one refining, one screw pressing, and one final product preparing (including mixing, packaging, and freezing) operations (Fig. 34). Fish mince received from Subsystem 1 went through three washing-dewatering cycles (WDC) in the plant, and was finally processed into frozen surimi. A more detailed explanation of each unit operation functions can be found in Lee (1985), Regier et at. (1985), Swafford et al. (1985), and Toyoda et al. (1992). In refining and screw pressing operations, the solid waste was pumped to the grinder in Subsystem 1.

Sequential batch operations were used in Subsystem 2. Surimi processing started with a batch of fish mince received from Subsystem 1, and continued sequentially in the processing line. Each unit operation was operated in an "on-off" manner controlled by

the process logic controller. When fish mince was pumped to the machines, an operation (such as washing and dewatering) was accomplished ("on" mode), and after that machines remained inactive ("off" mode) until the next batch of fish mince entered the machines. A continuous operation in Subsystem 2 was achieved with many sequential batch operations working at the same time (Fig. 2).

5.1.2 Water and waste water audit

5.1.2.1 Subsystem 1

Table 10 lists flow rates and characteristics of the waste water in the subsystem. The flow rates of solid wastes (COD, BOD_5, and TS) are listed in Table 11. These two tables show that gutting and mincing operations generated most of the waste water in Subsystem 1. The gutting operation contributed to the majority (>65%) of solid wastes. Although the flow rate of the waste water discharged in transferring the fish guts was not the highest due to high concentration of solids in the waste water, the flow rates of solid wastes (COD, BOD_5, and TS) were the highest among all the waste water sources in Subsystem 1. This is reasonable since the body fluid from the broken internal organs contained soluble materials that could be easily dissolved in the water. COD/BOD_5 of the waste water was approximately 2. In the mincing operation, part of the injected fresh water became wash water in the first washing tank. Only transferring water was discharged from the mincing operation. Since all fresh water entering this subsystem became waste water, the flow rate of fresh water was equal to that of waste water (192.3

Table 10 Flow rates and characteristics of waste water generated in Subsystem 1[1]

Unit operations		Flow rate (L/min)	COD (g/L)	BOD$_5$ (g/L)	TS (g/L)
Heading	CB[4]	14.9[2] ± 1.3[3]	6.54 ± 0.07	4.43 ± 0.07	3.97 ± 0.19
	T[5]	8.94 ± 0.96	6.47 ± 0.31	2.75 ± 0.18	3.78 ± 0.07
Gutting	CB	58.7 ± 12.4	5.42 ± 0.16	2.11 ± 0.33	3.81 ± 0.15
	T	30.4 ± 5.9	36.57 ± 1.93	18.89 ± 0.44	23.92 ± 0.30
Mincing	T	79.4 ± 14.7	6.54 ± 0.58	3.54 ± 0.45	5.30 ± 0.22
Subtotal		Waste water flow rate = 192.3 ± 20.2 (L/min)			

[1] Assuming that the operations were not interrupted.
[2] Averaged value
[3] Standard deviation
[4] Water injected to the cutting blades
[5] Water used to transfer heads, guts, and skins out of the machines

Table 11 Averaged solid waste flow in the waste water generated in Subsystem 1

Unit operations		COD (kg/min)	BOD$_5$ (kg/min)	TS (kg/min)
Heading	CB	0.097 ± 0.009	0.066 ± 0.006	0.059 ± 0.006
	T	0.058 ± 0.007	0.025 ± 0.003	0.034 ± 0.004
Gutting	CB	0.318 ± 0.068	0.124 ± 0.033	0.223 ± 0.048
	T	1.112 ± 0.224	0.574 ± 0.112	0.727 ± 0.141
Mincing	T	0.519 ± 0.107	0.281 ± 0.063	0.421 ± 0.080
Subtotal		2.10 ± 0.25	1.07 ± 0.13	1.46 ± 0.16

± 20.2 L/min). High variations in the waste water flow rates could be explained by the variations in feeding machine operators.

The feeding rate of raw fish to the heading machines was measured as 91.9 ± 18.0 kg/min. Approximately 2 kg of waste water was generated for every kg of raw fish processed in the heading, gutting, and mincing stage. For every kg of raw fish processed, the estimated amount of COD, BOD_5, and TS generated would be 0.023 ± 0.005, 0.012 ± 0.003, and 0.016 ± 0.004 kg/kg fish, respectively. Amount of water used for transferring solid wastes (heads, guts, skins, and bones) increased significantly as the operation proceeded (Table 11). Among the three operations, the smallest amount of fresh water ($\approx$ 15 L/min) was used to flush fish heads (the largest in physical size) out of the heading machine, while the mincing operation consumed the largest amount of water ($\approx$ 90 L/min). Considerable amount of water could be saved if the water used for transferring solid wastes is reduced in gutting and mincing operations.

5.1.2.2 Subsystem 2

Minced fish was sequentially transferred through several stages of washing and dewatering before feeding to the screw press. The first washing operation was a continuous process, and all the other unit operations were sequentially operated in batch style. To maintain a continuous operation in the production line, different numbers of washing tanks were involved in the second and third washing processes (Table 12). The washing time increased as washing cycles progressed (Table 13). Dehydration (dewatering) times were relatively consistent in the second and third dewatering operations

Table 12 Number of units in washing-dewatering operations in Subsystem 2

WDC*	Washing tank	Dehydrator	Rotary screen dehydrator
1	1	1	0
2	2	1	1
3	4	1	1

* Washing and dewatering cycle

Table 13. Time distribution in washing-dewatering operations in Subsystem 2

WDC	Washing tank		Dehydrator		Rotary screen dehydrator	
	t_a* (min)	t**(min)	t_a (min)	t (min)	t_a (min)	t (min)
1	2.29 ± 0.16	2.29 ± 0.16	0.88 ± 0.03	2.30 ± 0.06	0	0
2	3.43 ± 0.09	8.41 ± 0.46	2.26 ± 0.10	6.61 ± 0.88	2.50 ± 0.28	6.61 ± 0.88
3	8.44 ± 0.13	13.33±0.35	2.14 ± 0.30	5.13 ± 0.95	2.30 ± 0.01	5.13 ± 0.95

* t_a represents the fraction of time in a cycle of a batch needed to complete a function such as washing, dehydrating, or rinsing..

** t represents the time needed to complete a cycle in a batch operation.

(both in high speed dehydrators and rotary screen dehydrators). In each washing operation, water to fish mince ratio was approximately 3 to 1. Averaged water consumption was the highest in the first washing operation, followed by the second and third washing. Water streams were continuously injected to the rotary screen dehydrators, even when these units were in the "off" mode, leading to increased water consumption. If water streams were injected to the rotary screen dehydrators only when fish mince was pumped, a considerable amount of water (about 90 L/min) could be saved. Since two rotary screen dehydrators were used in the third WDC, more water was used to rinse the fish mince (Table 14).

The high speed dehydrator in the second WDC generated the highest flow of waste water, followed by those in the first and third WDCs (Table 15). Due to continuous water streams injected to the rotary screen dehydrators, averaged waste water flow rates were higher than those generated in the high speed dehydrators. The levels and amount of COD, BOD_5, and TS were the highest with the waste water generated from the first high speed dehydrator (Tables 16 and 17). Among three WDCs, more than 50% of the solid wastes (COD, BOD_5, and TS, kg/min) were generated in the first high speed dehydrator. Although relatively high in the concentrations of COD, BOD_5, and TS generated in the final screw press (Table 18), averaged flow rates of waste water and solid waste (kg/min) were not very high when compared with waste waters generated in the three preceding WDCs.

The total waste water generated from Subsystem 2 was 328.8 ± 21.9 L/min. If 50% of fish mince was processed into frozen surimi (9.7 kg/min), then about 34 L of

Table 14 Water consumption in a single washing and rinsing operation

WDC	Washing		Rotary screen dehydrator	
	$Q_{H2o,a}$ (L/min)	$Q_{H2O, avg}$ (L/min)	$Q_{H2o,a}$ (L/min)	$Q_{H2o, avg}$ (L/min)
1	89.1 ± 5.5	89.1 ± 5.5	0	0
2	447.1 ± 2.3	68.0 ± 3.7*	34.7 ± 4.7	34.7 ± 4.7
3	447.1 ± 10.6	23.1 ± 0.8*	58.9 ± 5.6	58.9 ± 5.6
Subtotal	317.5± 9.8		93.6 ±7.3	

* Averaged water flow rate based on one washing tank.

Table 15 Waste water flow rate in dewatering and rinsing operations

WDC	Dehydrator		Rotary screen dehydrator	
	$Q_{WH2o,a}$ (L/min)	$Q_{WH2o,avg}$ (L/min)	$Q_{Wh2o,\ a}$ (L/min)	$Q_{WH2o,\ avg}$ (L/min)
1	98.7 ± 2.7	37.8 ± 1.4	0	0
2	160.9 ± 13.2	55.0 ± 8.9	76.8 ± 4.5	63.7 ± 7.1
3	55.1 ± 10.2	23.0 ± 6.8	135.3 ± 11.5	119.6 ± 13.5

Table 16 Characteristics of waste water released in dewatering and rinsing operations

WDC	Dehydrator			Rotary screen dehydrator		
	COD (g/L)	BOD_5 (g/L)	TS (g/L)	COD (g/L)	BOD_5 (g/L)	TS (g/L)
1	32.35±1.41	15.68±1.73	28.39± 1.41	N/A	N/A	N/A
2	13.97±0.63	9.53 ± 0.78	12.34±0.28	13.94±0.63	8.14 ± 0.77	11.02±0.00
3	21.91±1.40	7.17 ± 0.39	14.17±0.38	13.60±0.58	5.36 ± 0.91	9.84 ±0.07

Table 17 Averaged solid waste generated in dewatering and rinsing operations

WDC	Dehydrator			Rotary screen dehydrator		
	COD (kg/min)	BOD_5 (kg/min)	TS (kg/min)	COD (kg/min)	BOD_5 (kg/min)	TS (kg/min)
1	1.39 ± 0.08	0.67 ± 0.08	1.22 ± 0.08	N/A	N/A	N/A
2	0.34 ± 0.06	0.23 ± 0.04	0.30 ±0.05	0.16 ± 0.02	0.09 ±0.02	0.13± 0.02
3	0.24 ± 0.06	0.08 ± 0.02	0.15 ± 0.04	0.36 ± 0.07	0.14 ± 0.04	0.26±0.05

Table 18 Characteristics of waste water and solid waste flow from final screw press*

Name of waste	Concentration (g/L)	Flow rate (kg/L)
COD	20.50 ± 0.08	0.08 ± 0.02
BOD_5	14.53 ± 0.42	0.06 ± 0.01
TS	13.20 ± 0.14	0.05 ± 0.01

* t_a = 7.8 ± 2.2 (min), t = 10.1 ± 2.2 (min), $Q_{WH2o,\ a}$ = 38.5 ± 3.1 (L/min), $Q_{WH2o,\ avg}$ = 29.7 ± 10.9 (L/min)

waste water was generated to make 1 kg of surimi from fish mince. Estimated solid waste (COD, BOD_5, and TS) generated would be 0.27, 0.13, and 0.21 kg/kg of surimi, respectively. Overall, the BOD_5 generated was about 50% of COD. If the processing was not interrupted, 473 m^3 of waste water was generated in Subsystem (Table 19).

Table 19 Summary of waste generation in Subsystem 2

Name of waste	Flow rate
Waste water	328.8 ± 21.9 L/min
COD	2.57 ± 0.14 kg/min
BOD_5	1.27 ± 0.10 g/min
TS	2.06 ± 0.12 kg/min

5.2 Treatment of surimi wash water by ohmic heating

The relationship between heating time and temperature (Fig. 35) followed a second order polynomial model, which can be expressed as

$$T = 11.1 + 0.0499t + 4.639 \times 10^{-5} t^2, \quad (R^2 = 0.995). \tag{73}$$

This result is in agreement with a similar study in which frozen fish mince wash water was used as the research subject (Huang et al., 1996). The constant term in Eq. 73 is related to the initial temperature of the samples. This model also suggests a linear heating rate (dT/dt) during the heating process, which may vary with the feed and applied voltage.

Electrical conductivity (σ) of wash water samples increased linearly with the heating temperature (Fig. 36). The relationship between electrical conductivity (σ) and temperature T was best fitted with a linear model (Eq. 74). An increase in σ is attributed to reduced electrical resistance at elevated temperatures. The intercept of this equation represents the electrical conductivity at 0°C, and slope is the rate (dσ/dt) at which σ changes with temperature.

$$\sigma = 0.353 + 0.0106 \, T \quad (R^2 = 0.993) \tag{74}$$

The initial concentrations of solids in wash water samples were 9.341 ± 0.137, 16.72 ± 0.22, 11.449 ± 0.090, and 1.366 ± 0.003 g/L, for protein, COD, TS, and TSS, respectively. After centrifugation (without heat treatment), these values dropped slightly to 8.948 ± 0.076, 16.17 ± 0.26, 10.875 ± 0.043, and 0.957 ± 0.079, for protein, COD, TS,
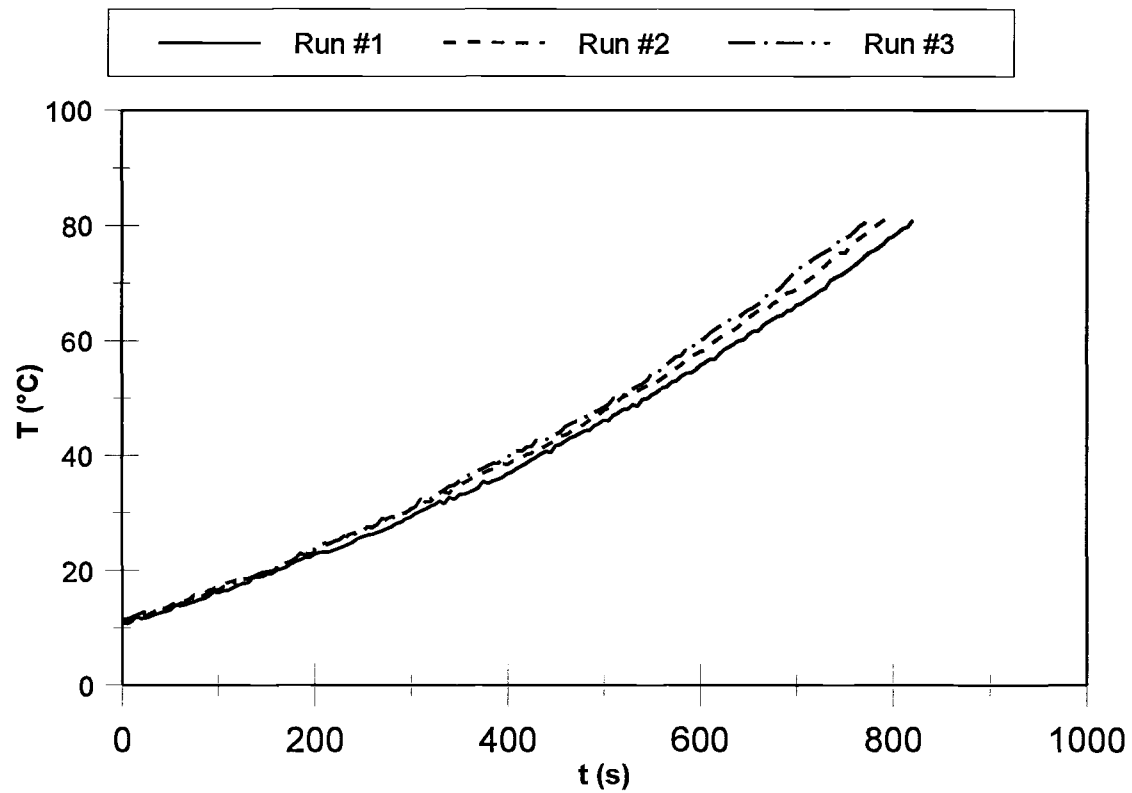
Fig. 35 Relationship between temperature and time during ohmic heating of surimi wash water

$$\sigma = 0.353 + 0.0106\ T, \quad R^2 = 0.993$$
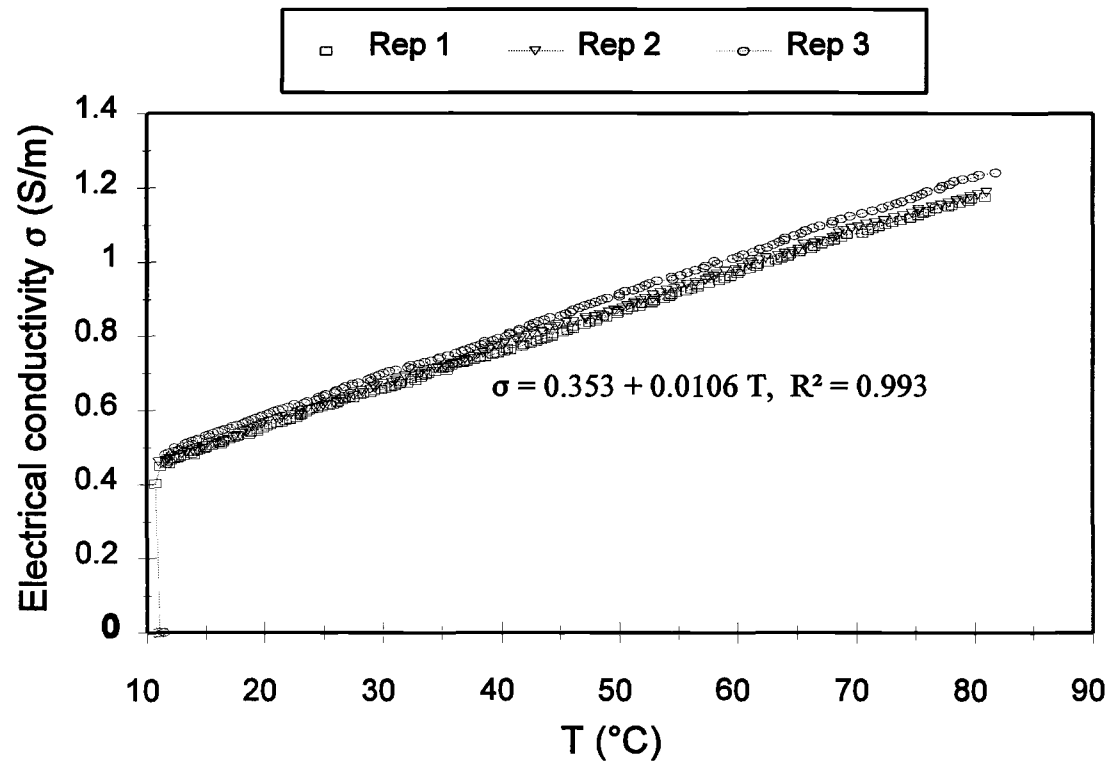
Fig. 36 Electrical conductivity increased linearly with temperature

and TSS, respectively. Heating to 30°C did not cause significant changes in solids concentration. At higher temperatures, heating caused heat-sensitive proteins to coagulate, leading to depletion of the solid concentration in the supernatants (Fig. 37). More than 80% TSS was removed at 40°C, indicating that larger particles are more sensitive to heat treatment and easier to precipitate by heat (Fig. 38). Above 60°C, more than 90% TSS was removed. Due to the presence of soluble solids such as minerals and other heat stable substances, reduction in TS was not as significant. Only slightly higher than 70% TS was removed at temperatures above 60°C while removal of proteins was observed higher than 80%. Reduction in protein concentration may be atttributed to coagulation and enzymatic degradation by the proteases during heating. The relationship between the residue solid concentration and heating temperature can be modelled by Eq. 75. Coefficients for each solid (protein, COD, TS, and TSS, respectively) can be found in Table 20.

$$ C = a_1 + a_2\ T + \frac{a_3}{T} \tag{75} $$

Effects of ohmic heating on the removal of proteins can be visually observed in the SDS-PAGE study (Fig. 39). Centrifugation without heat treatment and at low heating temperatures did not significantly affect the residual composition, since the SDS-PAGE band patterns are very similar between C and CT. When samples were heated to 50°C, two bands, one around 43,000 Dalton, and the other one between 20,000 and 30,000 Dalton began to disappear. At 60 °C, bands around 94,000, and in the ranges between 20,000 and 30,000 Dalton disappeared. At higher temperatures (>70°C), heat substantially
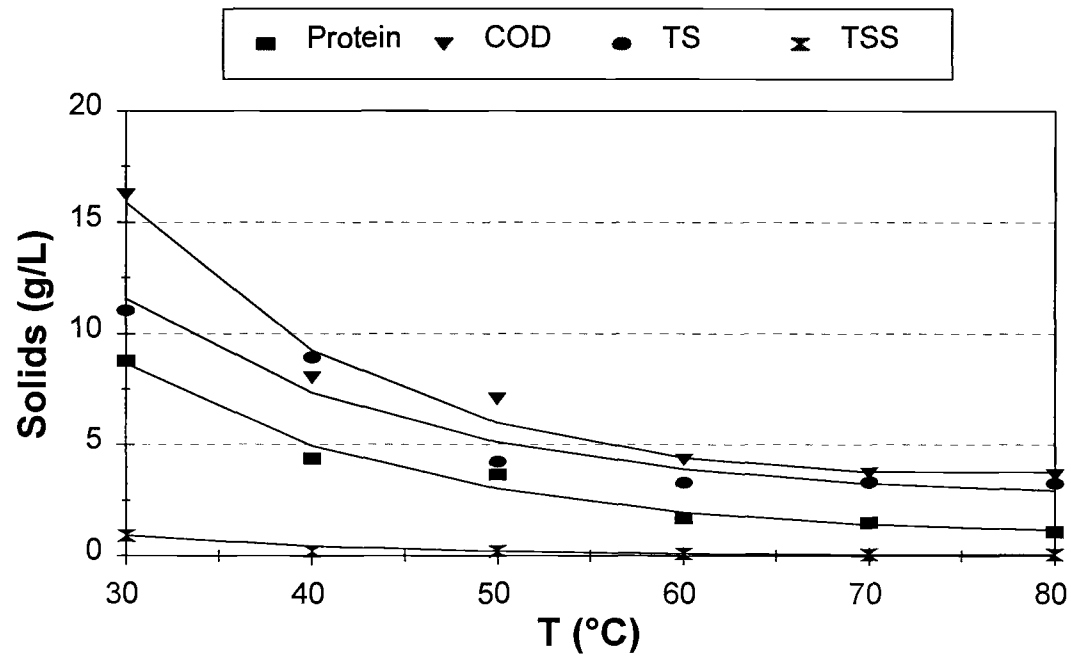
Fig. 37 Residual solids concentration decreased with temperature
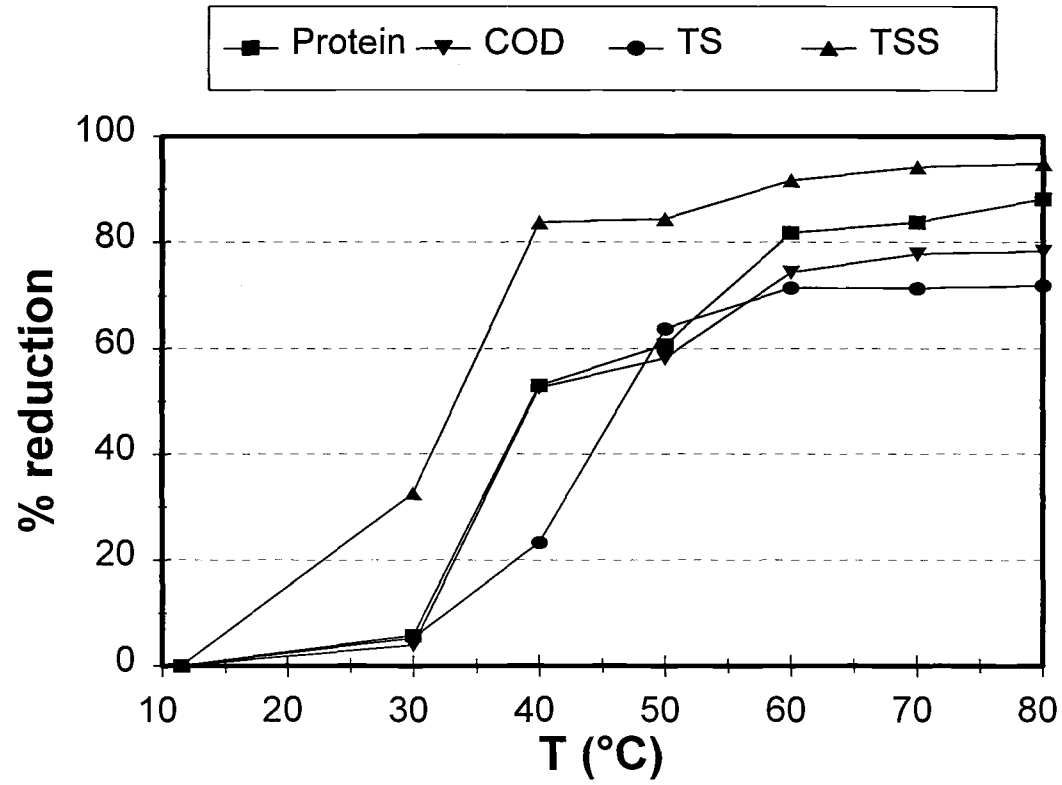
Fig. 38 Percent reduction of solids increased with temperature

Table 20 Coefficients for Eq. 75 for predicting the relationship between residual concentration and heating temperature

Solids	a_1	a_2	a_3	R^2
Protein	-11.0	0.0669	526	0.980
COD	-23.2	0.179	1012	0.975
TS	-10.83	0.0783	602.0	0.930
TSS	-2.56	0.0202	84.8	0.938

Low MW Std   High MW Std

	205 K
	116 K
94 K	97K
67 K	67 K
43 K	45 K
30 K	29 K
20 K	

C   CT   30   40   50   60   70   80   60'   70'   80'
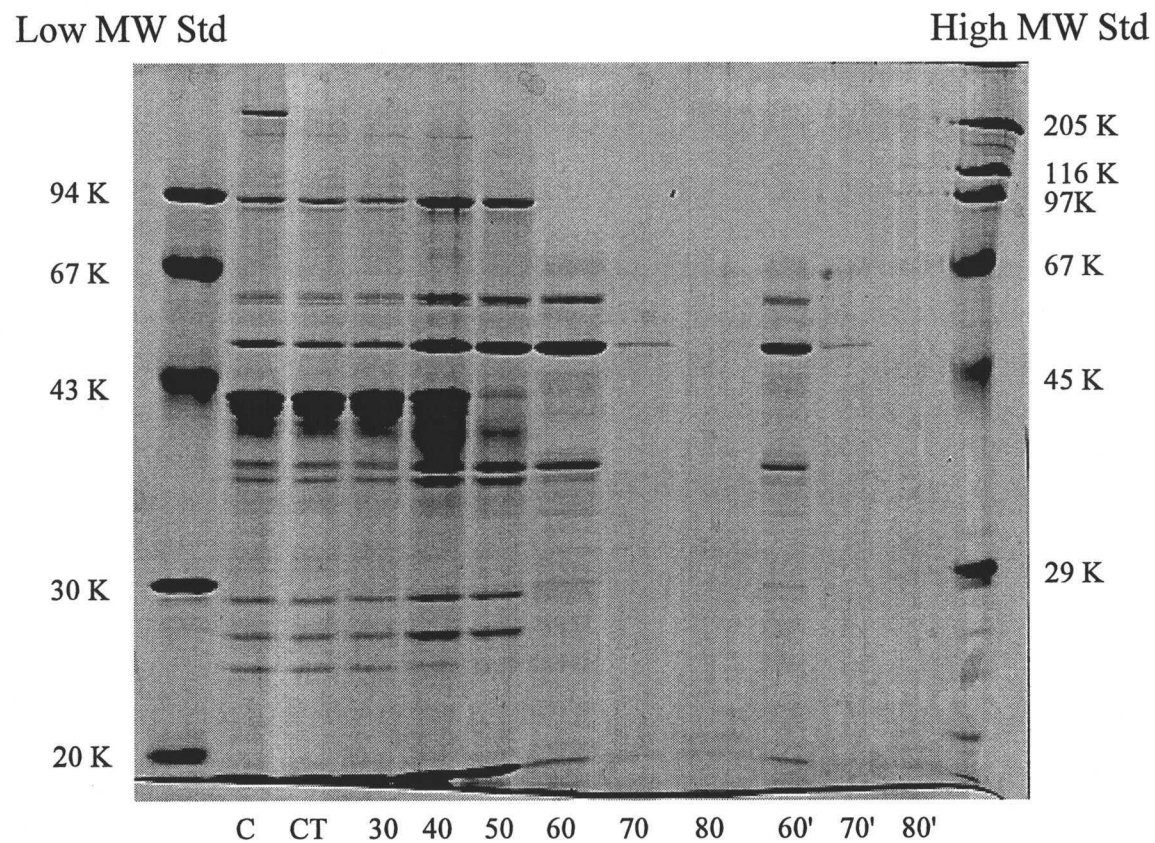
Fig.39   SDS-PAGE of ohmically treated surimi wash water samples..   C: Control; CT: Centrifuged; Lanes 30-80 are heating temperatures (sample load = 100 μg);   Lanes 60'-80' are the same as Lanes 60-80 with only 60 μg samples loaded.

damaged the proteins present in the samples, since only one band (45,000) is visible at 70°C, and essentially no clear protein bands are visible at 80°C. Although no protein bands are still visible after treatment at temperatures above 70°C, the presence of proteins was still detected by the Lowry method. A possible explanation to this observation is that these proteins were small molecules having molecular weights less than 20,000 Dalton. These results are in direct agreement with the previous research (Huang et al., 1996).

Protease activity (6.169 ± 0.002 nmol/min·mg) was found in the control samples. Since some enzymes may have been removed along with other solids in the samples after being centrifuged at 1700 x g without heat treatment and after heating to 30°C, a slightly decreased enzyme activity was observed (Fig. 40). However, at higher temperatures (>40°C), the enzyme activity began to increase. Between 30 and 60°C, the enzyme activity increased linearly with the temperature. At 70 and 80°C, low enzyme activity was observed since heat almost completely destroyed the proteins in the wash water. Enzyme activity of samples after heating to 60°C was almost 3 times that of the control. This should be the highest temperature that can be used to preserve the protease activity. When recovering proteolytic enzymes from the surimi waste water, heat coagulation can be used to preferentially remove contaminants, while preserving the heat stable proteases.
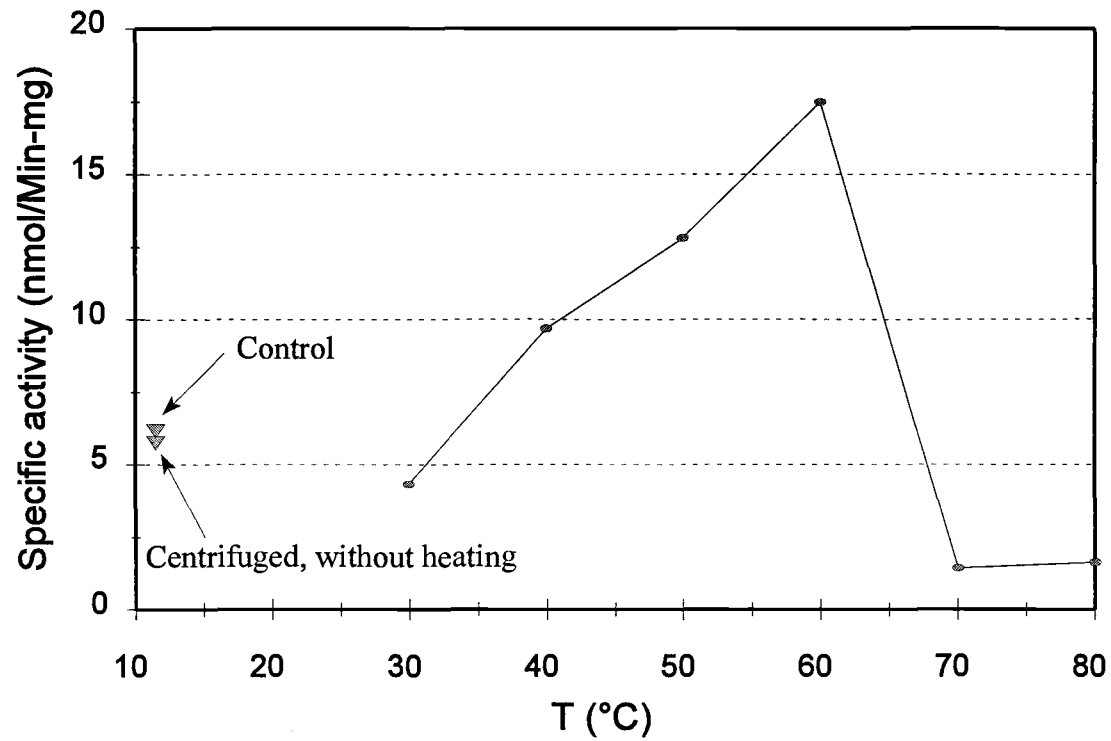
Fig. 40 Specific activity of proteolytic enzymes increased upon heating (<60°C) and decreased
dramatically at T > <60°C.

5.3 Microfiltration of surimi wash water

5.3.1 Effect of membranes on permeate flux and rejection coefficient

Microfiltration membranes may differ in pore sizes, pore size distribution, number of pores per unit area, and thickness. Macroscopically, the characteristics of membranes may be determined by filtering pure water through the membranes. Table 21 shows the characteristics of the membranes. Membranes with 0.45 μm pore size (S45 and H45) showed a higher specific flux and lower membrane resistance than the membrane with 0.20 μm pore size (S20 and H20). For the 0.45 μm membranes (S45 and H45), very little difference in J* and R_m was observed. However, pure water flux of S20 membranes had twice as much specific flux as that of H20 membranes, indicating that S20 membranes are higher in pure water permeability than H20 membranes.

Microfiltration of surimi wash water started with a high initial flux, and then the permeate fluxes declined rapidly with time, and finally a quasi-steady state filtration was observed (Fig. 41). The total volume of permeate accumulated rapidly in the first few minutes of filtration, and increased at a slower rate (Fig. 42). This process is typical for crossflow membrane filtration. The steady state permeate flux was around 20-22 L/m²hr for all membranes. Apparently, membranes with larger pore sizes (0.45 μm) had higher initial fluxes than the ones with smaller pores (0.20 μm), as shown in Fig. 41.

Since TSS was measured by passing the wash water samples through 1.0 μm glass fiber filters, while the pore size of membranes chosen in this study were smaller than 1.0 μm, no TSS was detected in the permeates. Except for the ash, concentrations of solids

Table 21 Characteristics of microfiltration membranes

Membranes[1]	Pore size (μm)	Specific flux J* (L/m^2-Pa)	Resistance R_m (m^2/L)
S20	0.20	$4.53 \times 10^{-5} \pm 7.52 \times 10^{-6}$	$2.29 \times 10^{7} \pm 3.68 \times 10^{5}$
S45	0.45	$7.73 \times 10^{-5} \pm 8.73 \times 10^{-6}$	$1.31 \times 10^{7} \pm 1.55 \times 10^{5}$
H20	0.20	$2.23 \times 10^{-5} \pm 4.60 \times 10^{-6}$	$4.60 \times 10^{7} \pm 6.26 \times 10^{5}$
H45	0.45	$7.86 \times 10^{-5} \pm 1.48 \times 10^{-5}$	$1.29 \times 10^{7} \pm 2.10 \times 10^{5}$

[1] S20 = Supor 20, S45 = Supor 45, H20 = HT 20, and H45 = HT 45
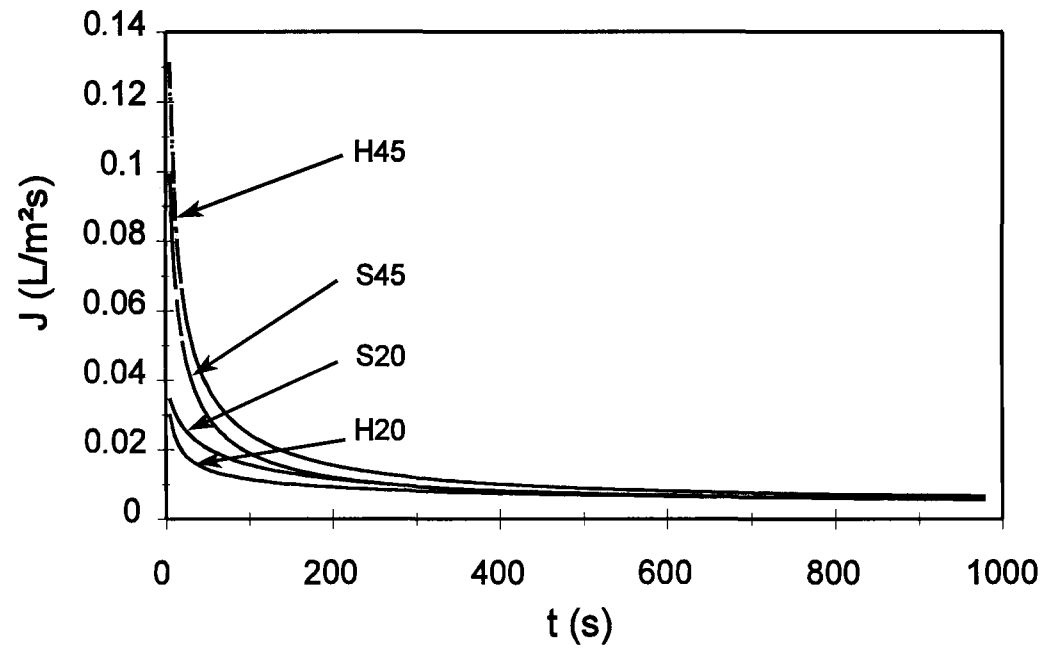
Fig. 41 Changes in permeate flux as a function of filtration time for four different types of microfiltration membranes
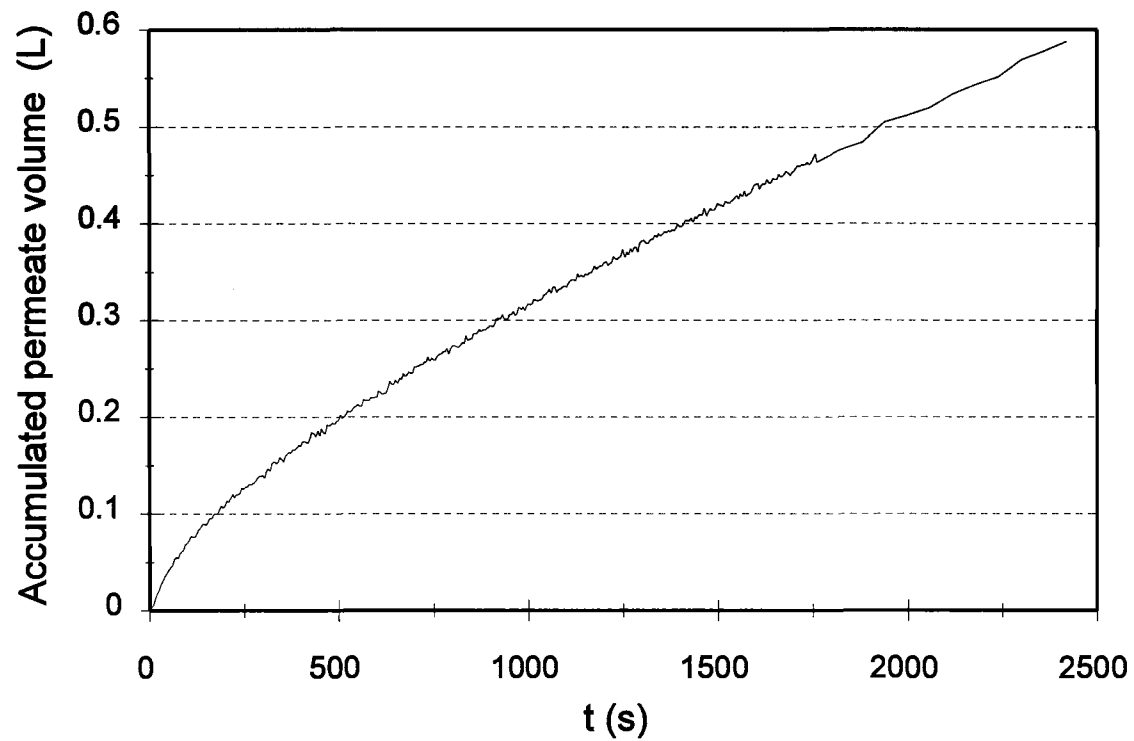
Fig. 42 The accumulated permeate volume increased rapidly at the first few minutes and then increased slowly with time.

in the permeates were reduced to different degrees (Table 22). H45 membranes show the smallest rejection coefficients (Table 23). To evaluate the effect of membrane materials and pore sizes on the permeate flux and apparent rejection coefficient, statistical analysis was conducted. The membrane pore sizes and materials had no significant effect ($p > 0.05$) on the steady state permeate fluxes (Table 24). However, rejection coefficients for the membranes with larger pore sizes were significantly smaller than the membranes with smaller membrane pore sizes ($p = 0.0206$). The effect of membrane materials on rejection coefficients was not statistically significant ($p = 0.4154$). Overall, microfiltration membranes were very permeable to the solids in the surimi wash water, as indicated by the small rejection coefficients (≈ 40-60% for proteins). Small rejection coefficients suggest that most soluble solids can be preferentially transmitted through the membranes, while only large particles (> pore sizes) are rejected by the membranes. This observation indicates that microfiltration may be suitable for recovering myofibrillar proteins (in suspended forms) from surimi waste water. Based on their capacity for rejection of proteins as shown in Table 23, S20 membranes showing the highest rejection to proteins were chosen for a detailed study.

Linear relationship between J and $Ln(r_a/(1-r_a))$ can be observed in Fig. 43 ($R^2 = 0.733$ and 0.717, for TS and TOS, respectively). The mass transfer coefficients for TS and TOS calculated from the slopes of the linear lines are 0.00258 ± 0.00052 and 0.00205 ± 0.00043 (L/m^{2}hr), respectively. The true rejection coefficients r_t calculated from the intercepts of the regressed linear lines in the vertical axis of Fig. 43 are 0.834 and 0.927, for TS and TOS, respectively. Since microfiltration membranes are completely permeable

Table 22 Concentrations of solids in raw wash water samples and permeates

ID	Run #	TS (g/L)		Protein (g/L)		Ash (g/L)		TSS (g/L)
		C_b	C_p	C_b	C_p	C_b	C_p	C_b
S20	1	10.599 ± 0.091	7.467 ± 0.045	8.895 ± 0.426	4.372 ± 0.072	2.160 ± 0.007	1.193 ± 0.023	0.985 ± 0.075
	2	11.011 ± 0.132	6.186 ± 0.123	9.429 ± 0.356	3.238 ± 0.088	1.896 ± 0.027	1.623 ± 0.048	2.272 ± 0.136
	3	11.153 ± 0.168	7.659 ± 0.580	10.064 ± 0.409	3.651 ± 0.127	2.156 ± 0.054	1.880 ± 0.043	1.749 ± 0.109
H20	1	10.479 ± 0.162	5.852 ±0.063	8.618 ± 0.770	4.722 ± 0.200	2.020 ± 0.032	1.404 ± 0.260	1.570 ± 0.154
	2	11.127 ± 0.205	6.586 ± 0.251	8.336 ± 0.346	3.616 ± 0.051	2.133 ± 0.061	1.649 ± 0.012	0.993 ± 0.262
	3	11.0193 ± 0.195	8.343 ± 0.048	7.889 ± 0.111	3.117 ± 0.076	2..583 ± 0.034	2.344 ± 0.001	0.802 ± 0.083
S45	1	10.524 ± 0.131	5.402 ± 0.064	7.888 ± 0.090	2.734 ± 0.056	2.047 ± 0.052	1.364 ± 0.017	1.378 ± 0.081
	2	8.725 ± 0.110	6.01 ± 0.016	6.497 ± 0.273	3.857 ± 0.378	1.631 ± 0.125	1.453 ± 0.011	0.849 ± 0.108
	3	10.094 v 0.078	6.376 ± 0.018	7.385 ± 0.405	3.239 ± 0.059	2.010 ± 0.041	1.705 ± 0.055	1.273 ± 0.127
H45	1	11.717 ± 0.102	9.267 ± 0.179	6.577 ± 0.124	3.866 ± 0.052	2.100 ± 0.010	1.960 ± 0.024	1.223 ± 0.088
	2	10.298 ± 0.235	8.331 ± 0.079	8.969 ± 0.248	5.583 ± 0.149	2.139 ± .0017	1.920 ± 0.037	1.023 ± 0.084
	3	11.126 ± 0.105	9.079 ± 0.102	7.422 ± 0.564	4.951 ± 0.087	2.160 ± 0.025	2.027 ± 0.018	1.180 ± 0.075

Table 23 Apparent rejection coefficients during microfiltration of surimi wash water using different membranes

ID	Run #	TS	Protein	TSS
S20	1	0.296	0.509	0.114
	2	0.438	0.657	0.144
	3	0.313	0.637	0.128
H20	1	0.487	0.653	0.334
	2	0.311	0.406	0.109
	3	0.368	0.561	0.152
S45	1	0.442	0.452	0.305
	2	0.408	0.566	0.227
	4	0.255	0.605	0.092
H45	1	0.209	0.412	0.067
	2	0.191	0.378	0.103
	3	0.184	0.333	0.062

Table 24 Statistical analysis* of effect of membrane materials and pore sizes on steady state flux and apparent rejection coefficients (r_{a**}) during microfiltration of surimi wash water

Factors		Mean J (L/m²s)	Mean r_a
Memrbaane material	Polysulfone (S)	0.00613[a]	0.339[b]
	Polyethersulfone (H)	0.00559[a]	0.303[b]
Pore size	0.20 μm	0.00547[d]	0.380[e]
	0.45 μm	0.00624[c]	0.261[f]

* Tukey's studentized test procedure was used to evaluate the contribution of different factors to the performance of different membranes. Statistical analysis was conducted using PC-SAS (Version 6.0). Means in a column within a factor not sharing the same superscript are different ($p < 0.05$)

** Based on total solids concentration
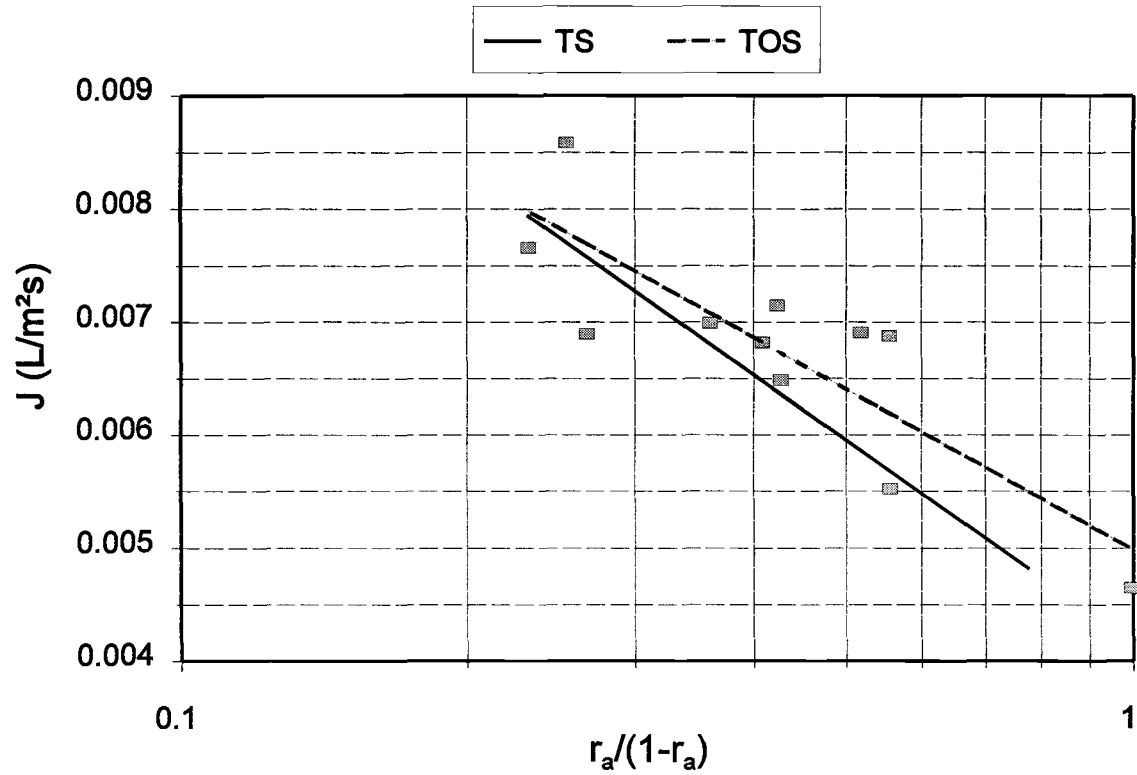
Fig. 43 Linear relationship between J and $Ln(r_a/(1-r_a))$

to the soluble salts included in TS, the true rejection coefficient r_t for TS is, therefore, smaller than that of TOS. The high true rejection coefficient of TOS may indicate the fouling of membranes by the organic substances in the wash water.

The SDS-PAGE shows that there is some similarity in the band patterns between the raw wash water samples and the permeates (Fig. 44), except around 205,000 Dalton (myosin heavy chain). The similarity in the bands is an indication that microfiltration membranes are permeable to smaller molecules such as sarcoplasmic proteins and retentive for larger particles. They are suitable for recovering myofibrillar proteins.

5.3.2 Mechanisms of membrane fouling

5.3.2.1 Pore blocking model

Linear relationship between $1/V$ and $1/t$ in Eq. 21 was observed in the early stage of filtration (at high $1/t$ values), as evidenced in Fig. 45 for the tests of different feed concentrations (TS). As filtration progressed, a nonlinear relationship developed as the slope of the curves began to quickly increase at $t>200$ s, depending on the feed concentration. As expressed in Eq. 21, slope K_1 is a linear function of $1/J_o$, and a fairly good linear relationship between K_1 and $1/J_o$ was found (Fig. 46). The filtration area estimated from the slope of Fig. 46 was 0.0320 m^2, which was very close to the actual filtration area of the membrane filter (0.03 m^2). This indicates that pore blocking had occurred during the early stage of microfiltration. Dependence of initial permeate fluxes on feed concentration was observed (Fig. 47).
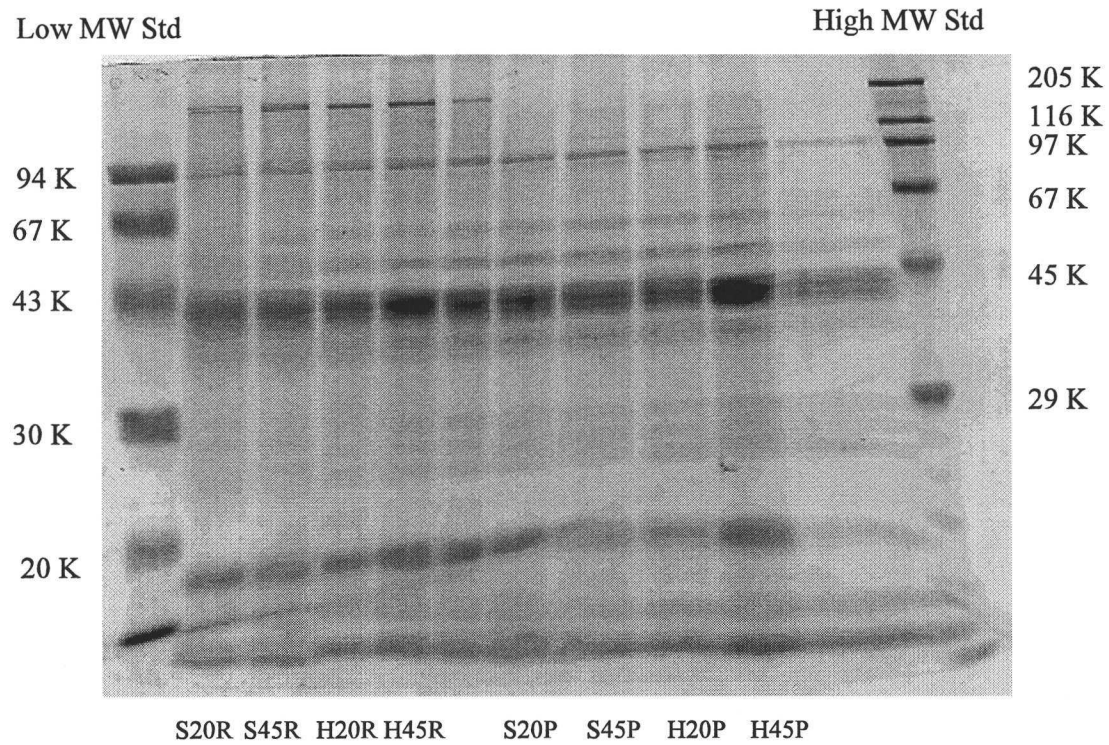
Fig. 44 SDS-PAGE of surimi wash water samples before and after microfiltratoon. Lane indexes ending with "R" are raw samples. Lane indexes ending with "P" are permeates.
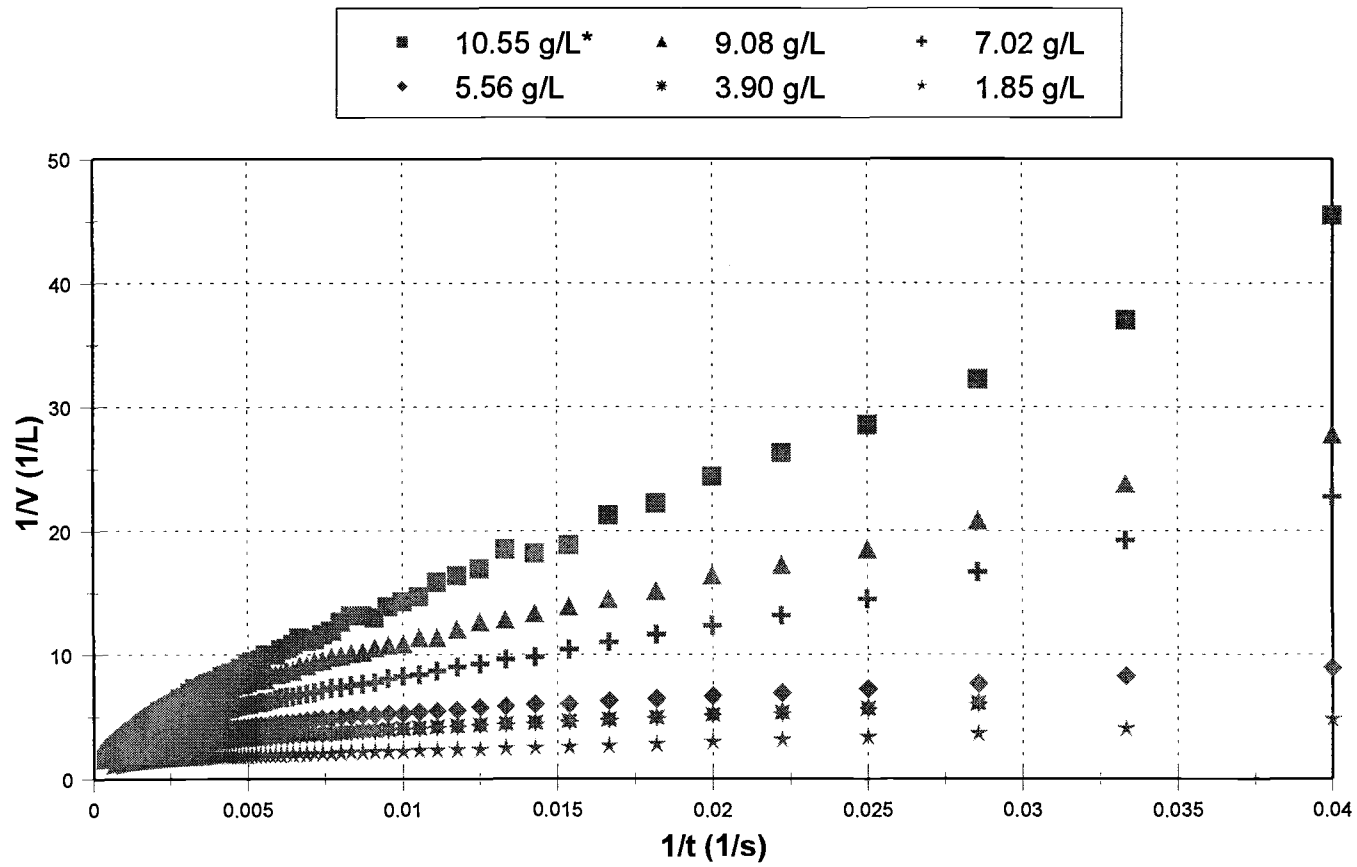
Fig. 45 Linear relationship between 1/V and 1/t at the initial stage of filtration
       * Total solid concentration
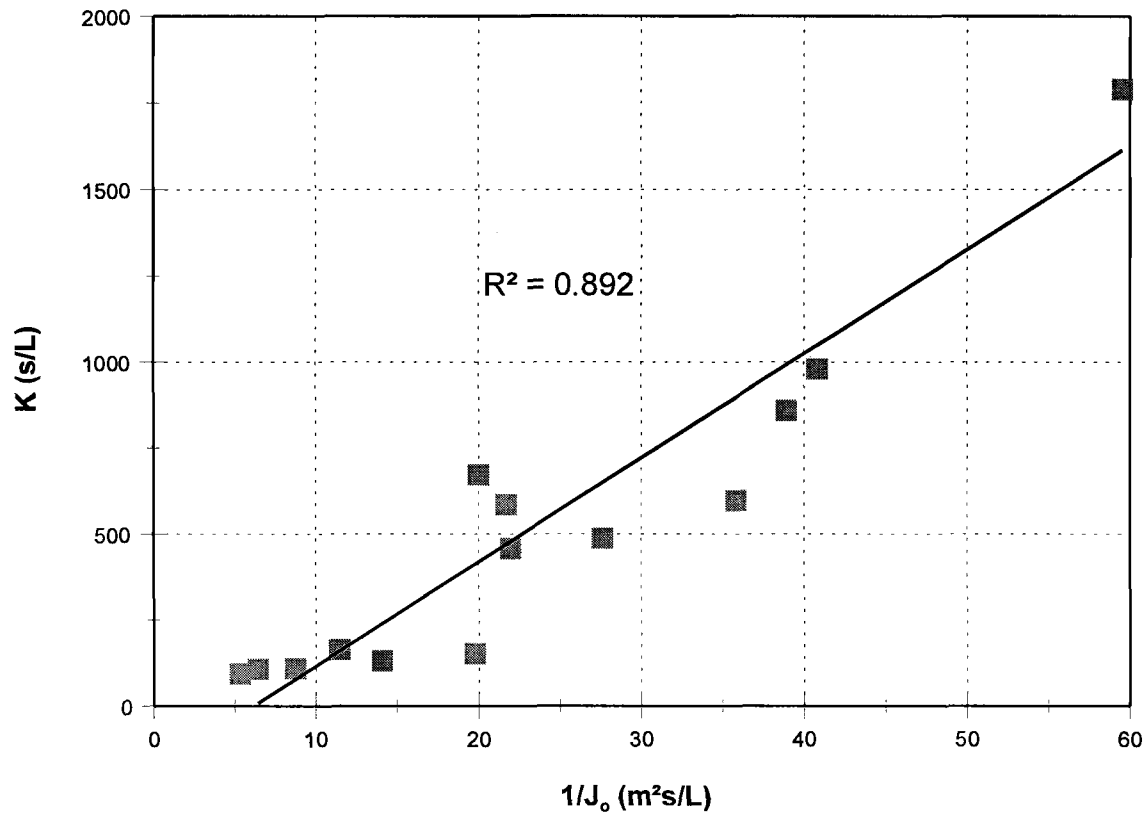
Fig. 46 Linear relationship between the slopes of the linear region of Fig. 45 and the initial flux
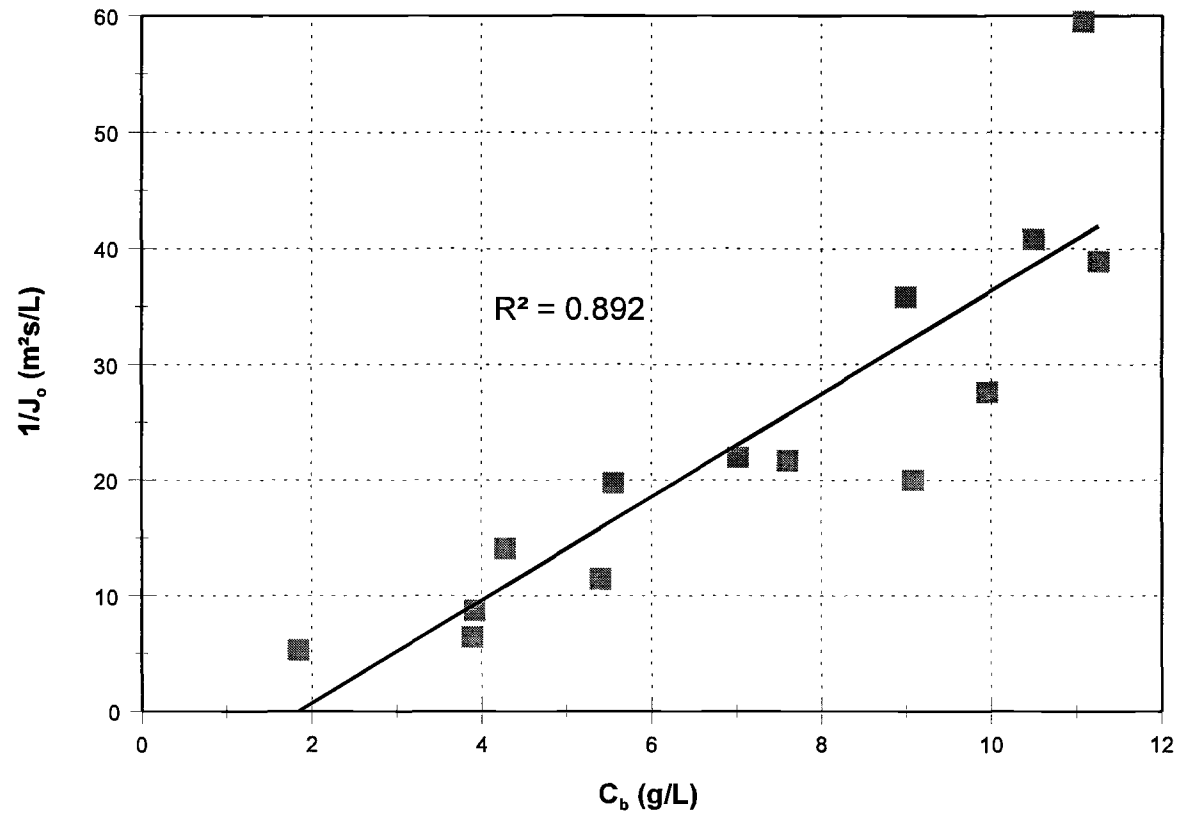
Fig. 47 Dependence of initial flux on feed concentration

The intercept in Eq. 21 is a function of membrane (initial pore volume V_{po}) and the property of the solids in the permeate is determined by the density (ρ) of the solids and the amount of solids (m_s) deposited on the inner pores per unit volume of permeate passing through the pores. If the physicochemical property of solids in the surimi wash water is relatively consistent, and the interactions between the proteinaceous solids and the inner walls of the membrane pores remains the same, the intercept should be affected by the concentration of the permeates. As depicted in Fig. 48, the intercept (B_1) increased exponentially with the permeate concentration (C_p).

Pore narrowing can be estimated from the Hagen-Poiseuille equation (Eq. 18) when the fluxes and pore sizes at the initial point and the end point of pore blocking are known. Generally, pore blocking was more severe when filtering low feed concentrations (Fig. 49). This observation was in agreement with Bowen and Hall (1995). At high feed concentrations, the surface cake may form easier and faster and the pore entrance may be blocked by the suspended solids.

Belfort et al. (1994) gave an excellent review of the process of membrane fouling during microfiltration of macromolecular solutions. They stated that membrane fouling was a five-phase process: 1) internal sorption of macromolecules, 2) build-up of first sublayer, 3) build-up of multisublayers, 4) densification of sublayers, and, 5) increase in bulk viscosity. Apparently, the first phase is related to the process of internal pore blocking at the initial stage. When a protein solution is pumped across the membrane surface, interaction between protein molecules and the membrane surface may occur immediately due to the amphoteric nature of protein molecules and the hydrophobic nature
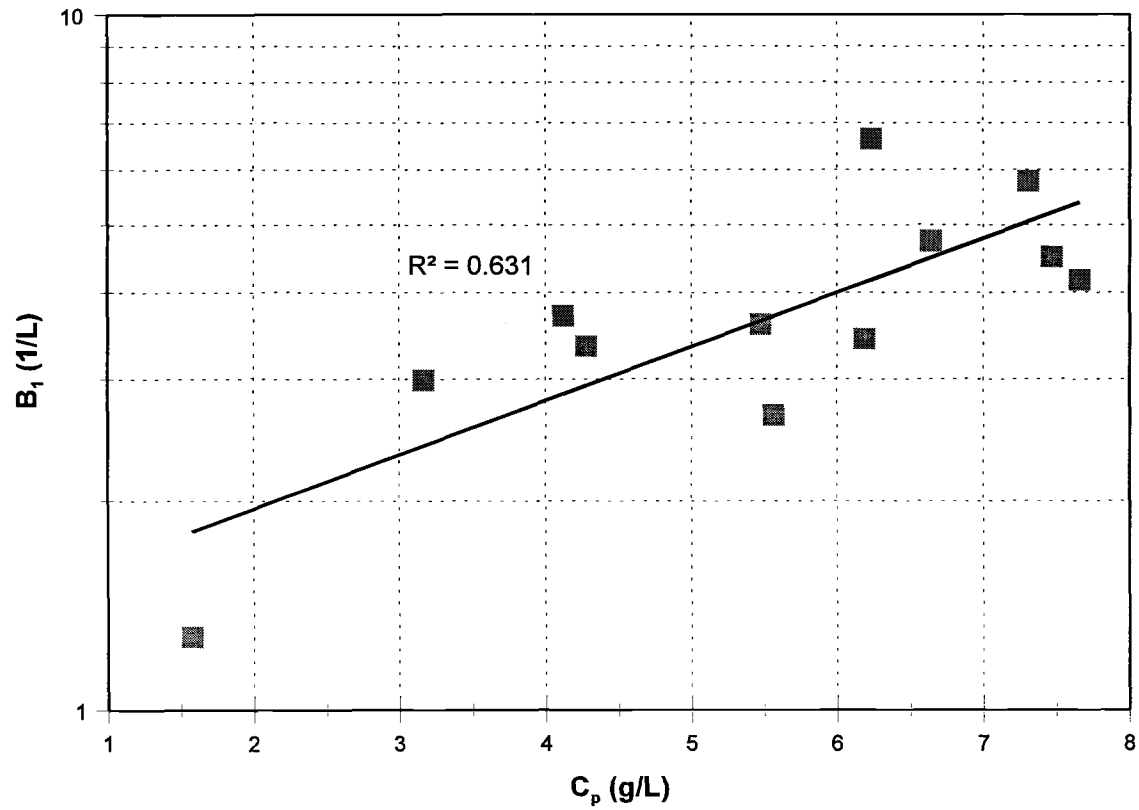
Fig. 48 B_1 increased exponentially with the permeate concentration
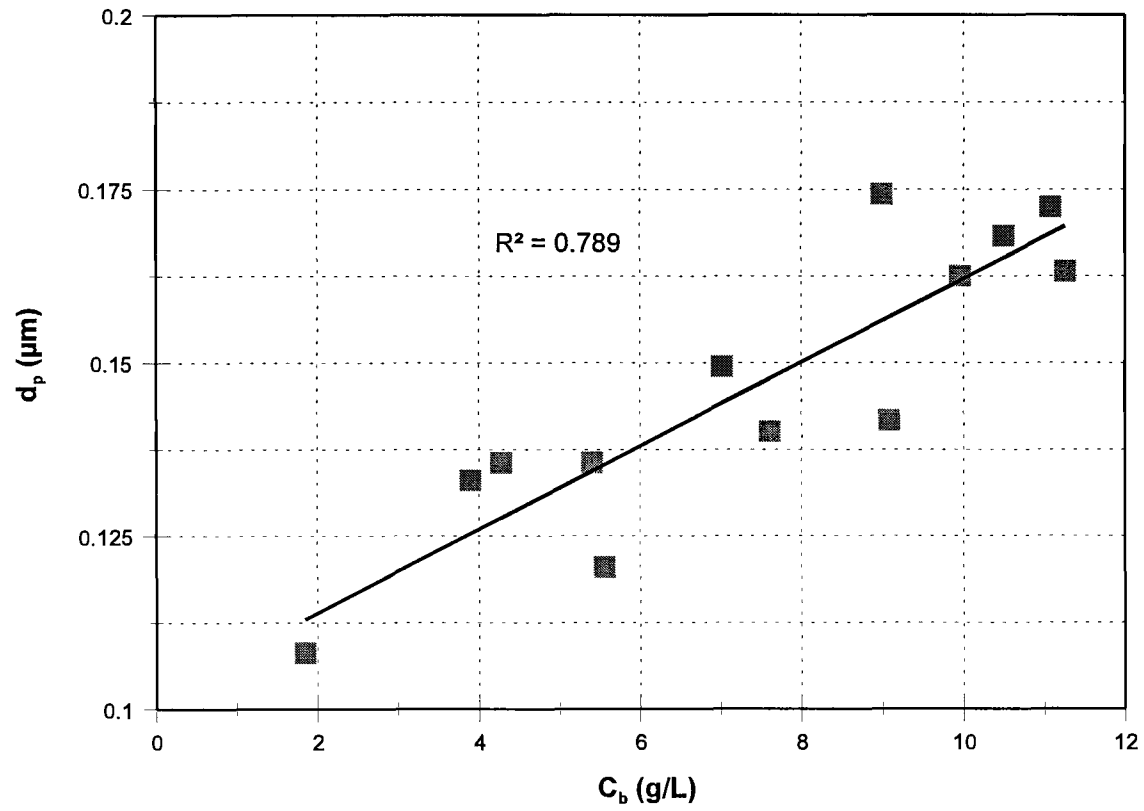
Fig. 49 Pore diameter at the end point of pore blocking decreased linearly with feed concentration

of the membrane material. According to Belfort et al. (1994), the build-up of first sublayer in the second phase is a slow process and the permeate flux is not affected during the formation of the first sublayer. Therefore, pore blocking is the dominating resistance during the first two phases of membrane fouling. The experimental data quantitatively verified these processes and our hypothesis.

5.3.2.2 Cake layer formation

As more protein is deposited on the membrane surface, the cake resistance increases dramatically and becomes the dominant resistance. Depending on the thickness of the cake layer, the membrane resistance may become insignificant if compared with the cake resistance. The mass transfer is mainly controlled by the cake layer when it is thick enough. A linear relationship between Ln $(V_t - V_c)$ and Ln $(t - t_c)$ was observed (Fig. 50), which verified the assumption in Eq. 24 that the resistance is a power-law function of the permeate volume. In Fig. 50, both slopes and intercepts were dependent upon the feed concentrations. As shown in Fig. 51, slope (α) actually increased linearly with the feed concentration, while the intercept ξ in Eq. 24 decreased linearly with the slope α (Fig. 52). The constant β was estimated as 1.94×10^{-10}, when the viscosity μ was assumed to be 0.0012 Pa.s.

The total filtration resistance was estimated using Eq. 12, and was found to vary with the filtration time (Fig. 53). When the cake resistance dominates, the Ln (R) should change linearly with Ln (t), which is verified in Fig. 53. The resistance values at the initial period of filtration (t<100 s) were found to be an order of magnitude smaller than
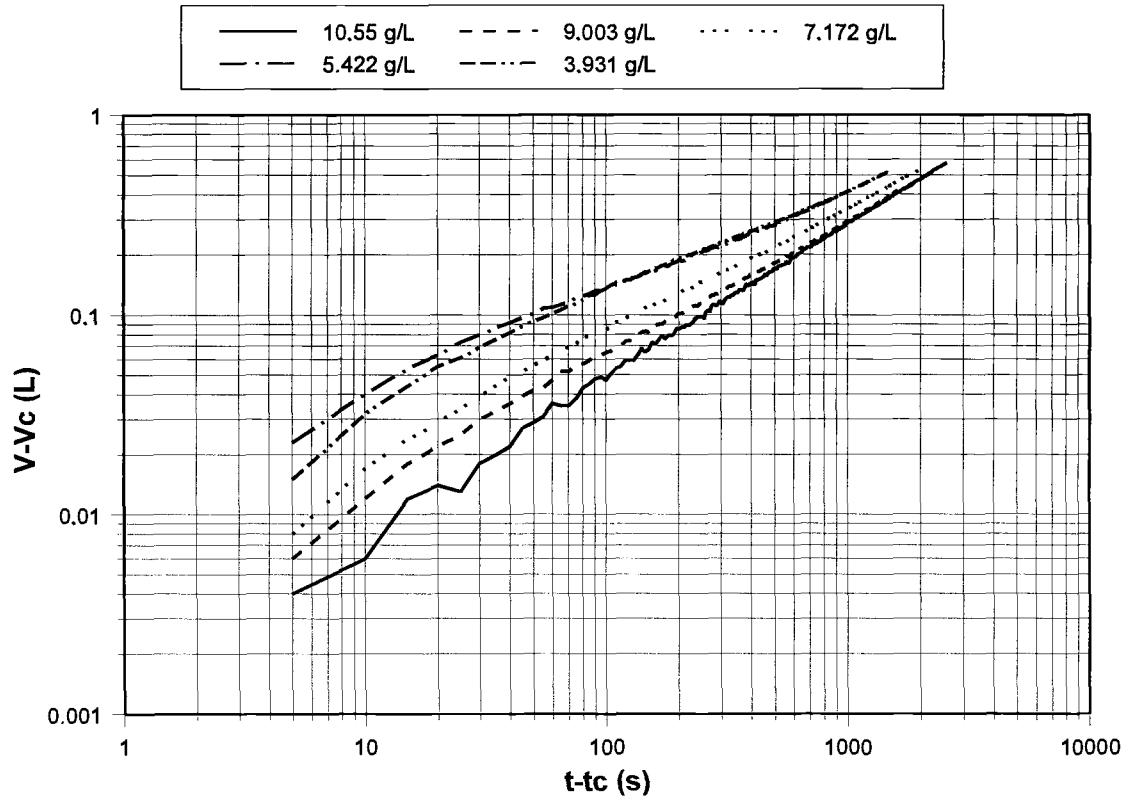
Fig. 50 Linear relationship between Ln(V-V$_c$) and Ln(t-t$_c$) during the continuous development of the cake layer
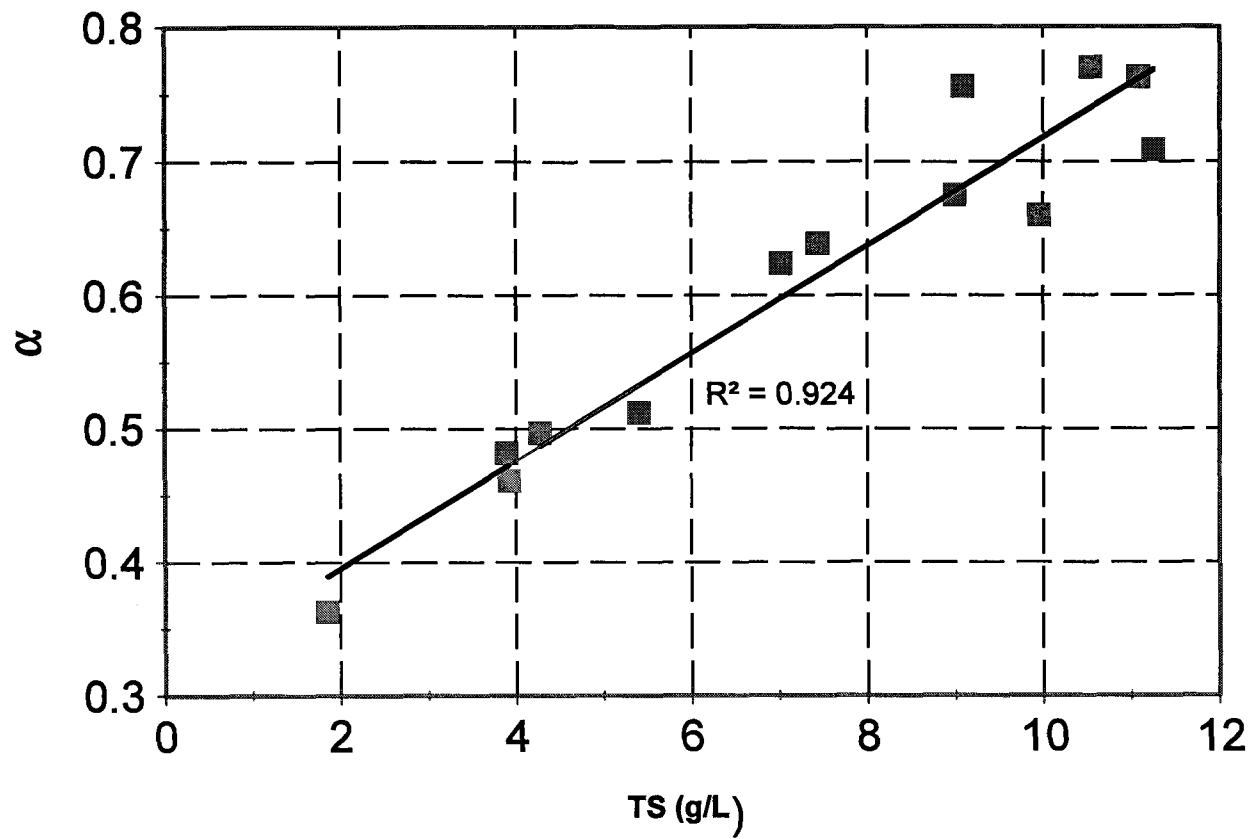
Fig. 51 The slopes in Fig. 50 increased linearly with the feed concentration.
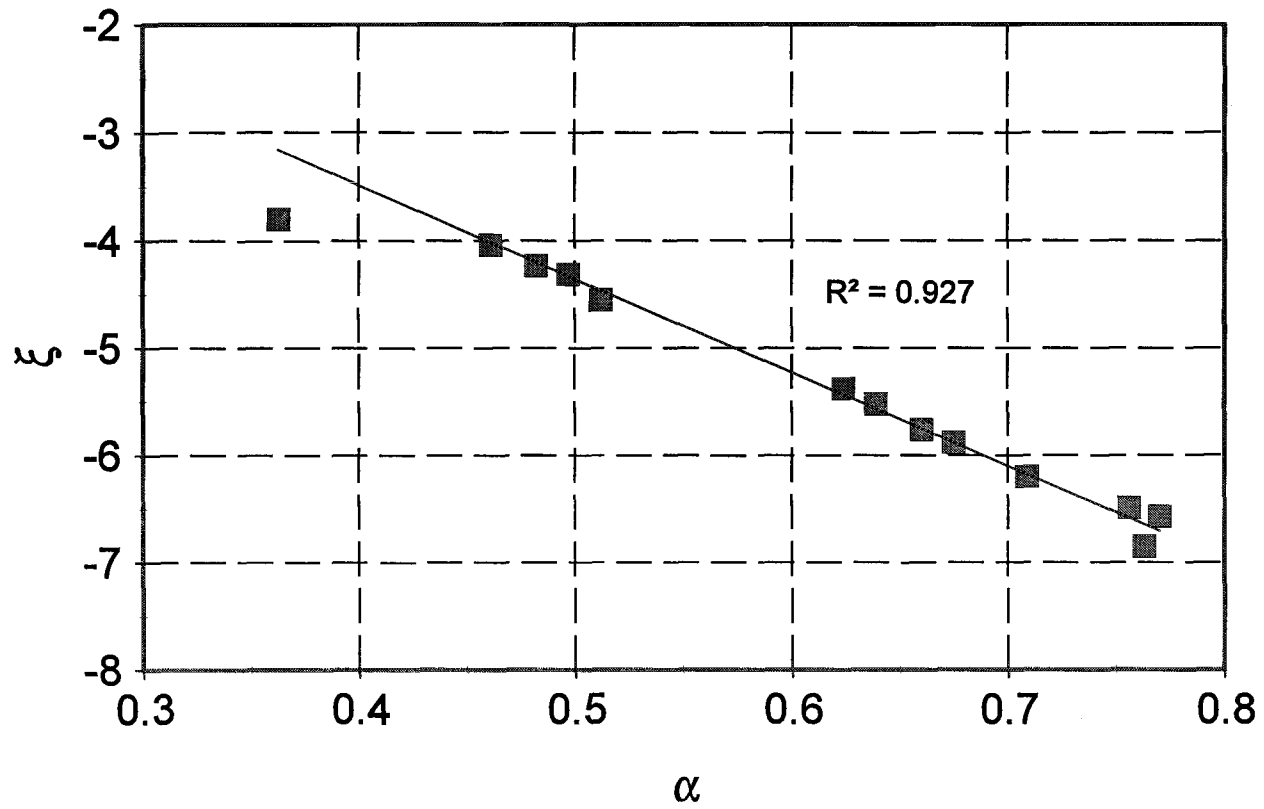
Fig. 52 The intercepts in Fig 50 decreased linearly with α
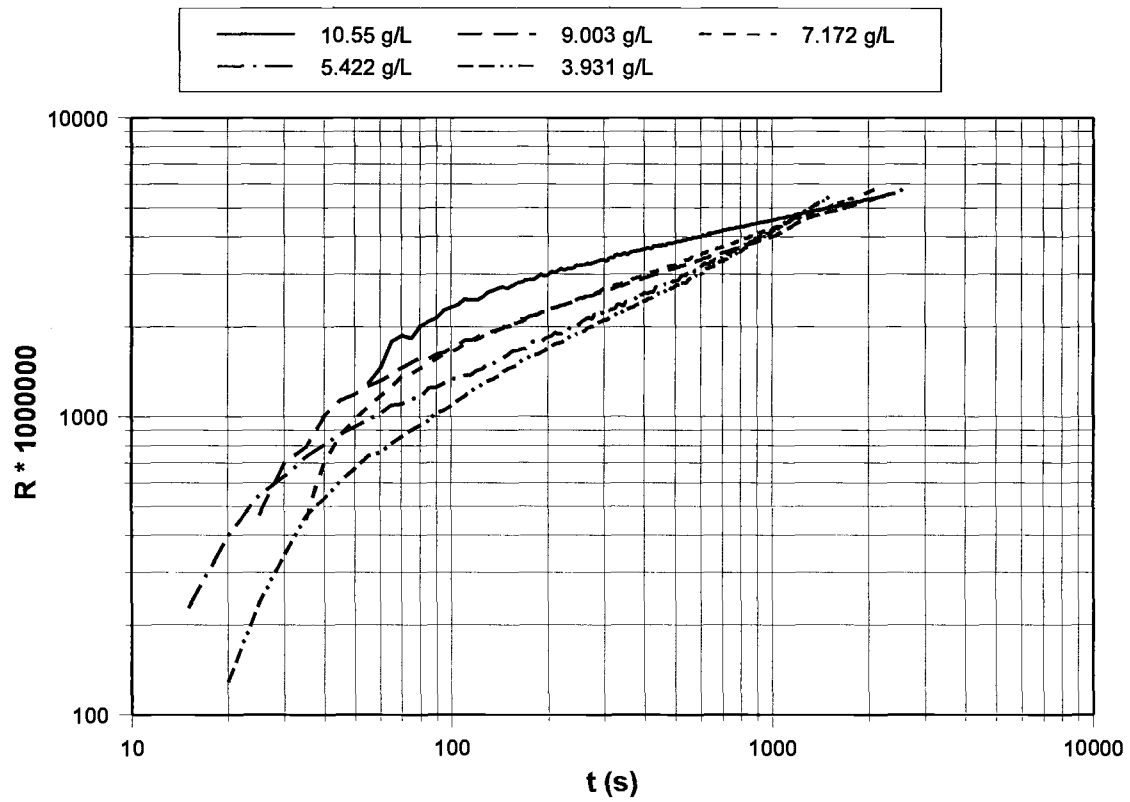
Fig. 53 Development of filtration resistance as a function of time

those of the linear range, presumably to be the cake resistance dominant range. As expected, the resistance increased with the feed concentration.

5.4 Finite element analysis of concentration polarization during ultrafiltration BSA

5.4.1 Finite element mesh generation

During membrane filtration of small protein molecules such as bovine serum albumin, the solutes in the solution are convected to the semipermeable membrane surface. Under positive pressure, the solvent is pushed out through the membrane matrix leaving the solutes behind. The accumulation of the solutes near the membrane surface causes the solutes to diffuse back into the main stream. At equilibrium, a very steep concentration gradient will develop as a result of this, leading to formation of a concentration boundary layer near the membrane surface. In the region outside the concentration boundary layer, the concentration is equal to that of the bulk feed solution. Concentration polarization occurs only in the vicinity of the membrane surface.

Due to the steep concentration gradient, denser meshes are needed in the vicinity of the membrane surface. As shown in Fig. 54, more grid points are distributed near the region close to the membrane surface. This treatment is similar to the finite difference method used by Kleinstreuer and Paller (1983) in which grid spacing was very fine near the membrane surface and relaxed toward the channel centerline.

Finite element analysis of concentration polarization in a radial crossflow device
Mesh generation

N

1.00

0.75

0.50

0.25

0.00

0.08333 < = R< = 1
0 <= Z <= 1

0.00   0.25   0.50   0.75   1.00

R

PdzOPlt09GridSa: St=3 Gr=1 err=0.000509
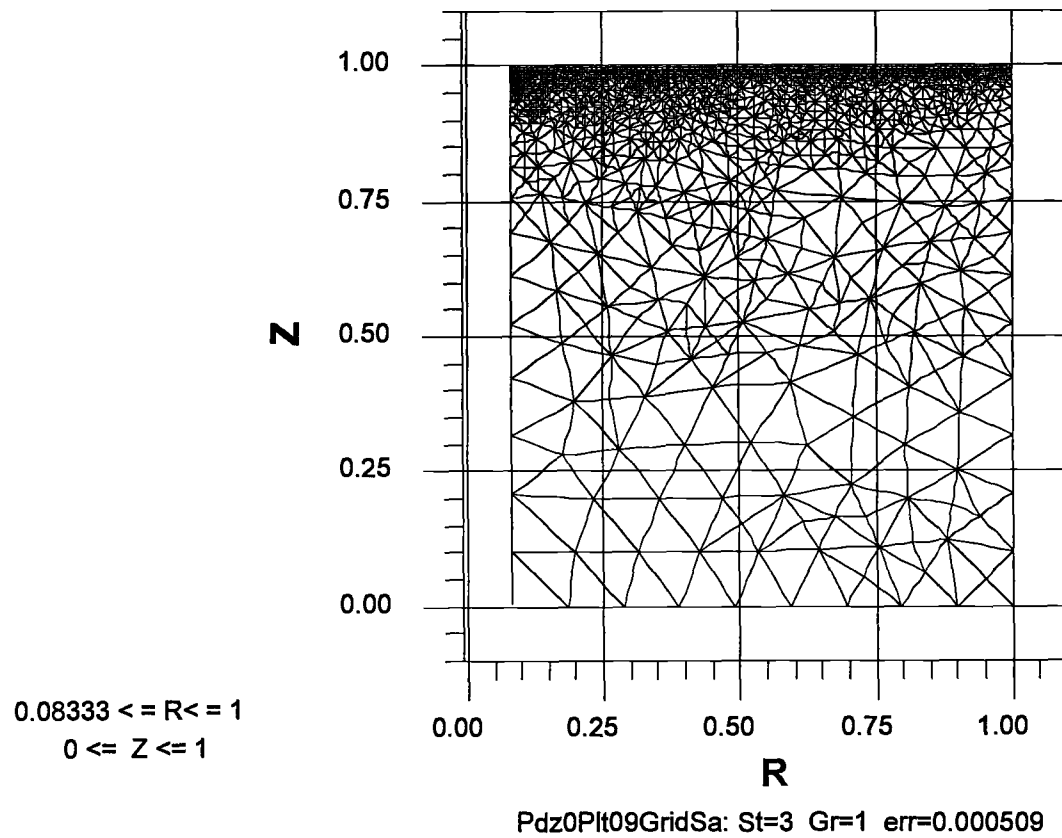
Fig. 54 Finite element mesh generation in the normalized fluid flow channel.

5.4.2 Effect of permeate flux on the velocity profiles within the membrane flow channel

The fluid flow in the membrane channel is governed by the continuity equation (Eq. 27). When the fluid flow is in the laminar region, the velocity component u is parabolic (Fig. 55). The withdrawal of solvent from the membrane will change the profiles of u and v in the flow channel. In the cross section at R=0.5, the curve with the dotted line represents the profile of u for the fluid flow in an impermeable (without membrane) channel. When pure water is filtered through the membrane, the u profile is considerably lower than that of the impermeable channel. When the BSA solution is filtered through the membrane, due to concentration polarization, the u profile is only slightly lower than that without permeate withdrawn from the flow channel (Fig. 55).

The concentration polarization has more impact on the v profiles (Fig. 56). In the cross section at R=0.5, the permeate flux (v at Z=1.0) for the BSA solution is significantly smaller than that of pure water.

In a radial cross flow filter, the fluid velocity changes with the radius and Z directions (Fig. 57 and Fig. 58). Velocity u is the highest at the entrance and in the centerline of the flow channel. Since the radius of the radial cross flow membrane filter was relatively small (1.75 cm or 0.69 inch), and the pressure drop along the radius direction was negligible, the variation of v at the membrane surface was considered negligible. The velocity v is more a function of Z rather than R (Fig. 58).
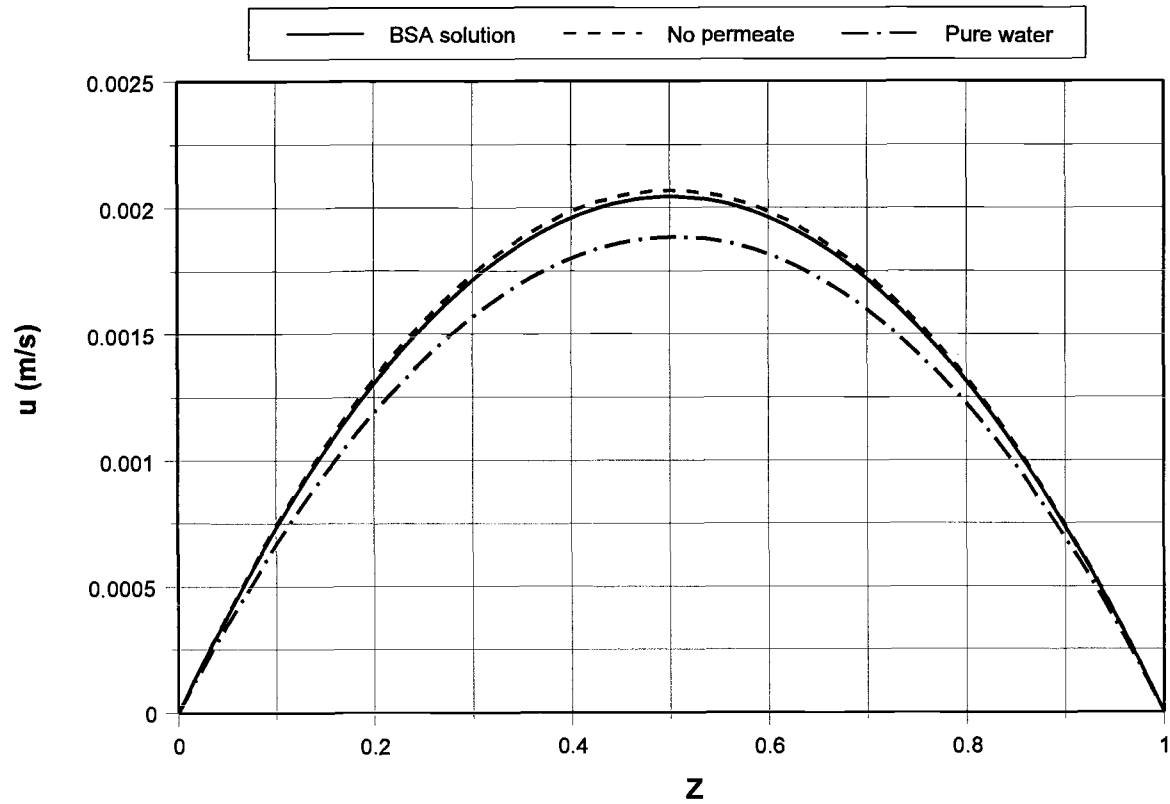
Fig. 55 The profile of velocity component u in the flow channel at R=0.5
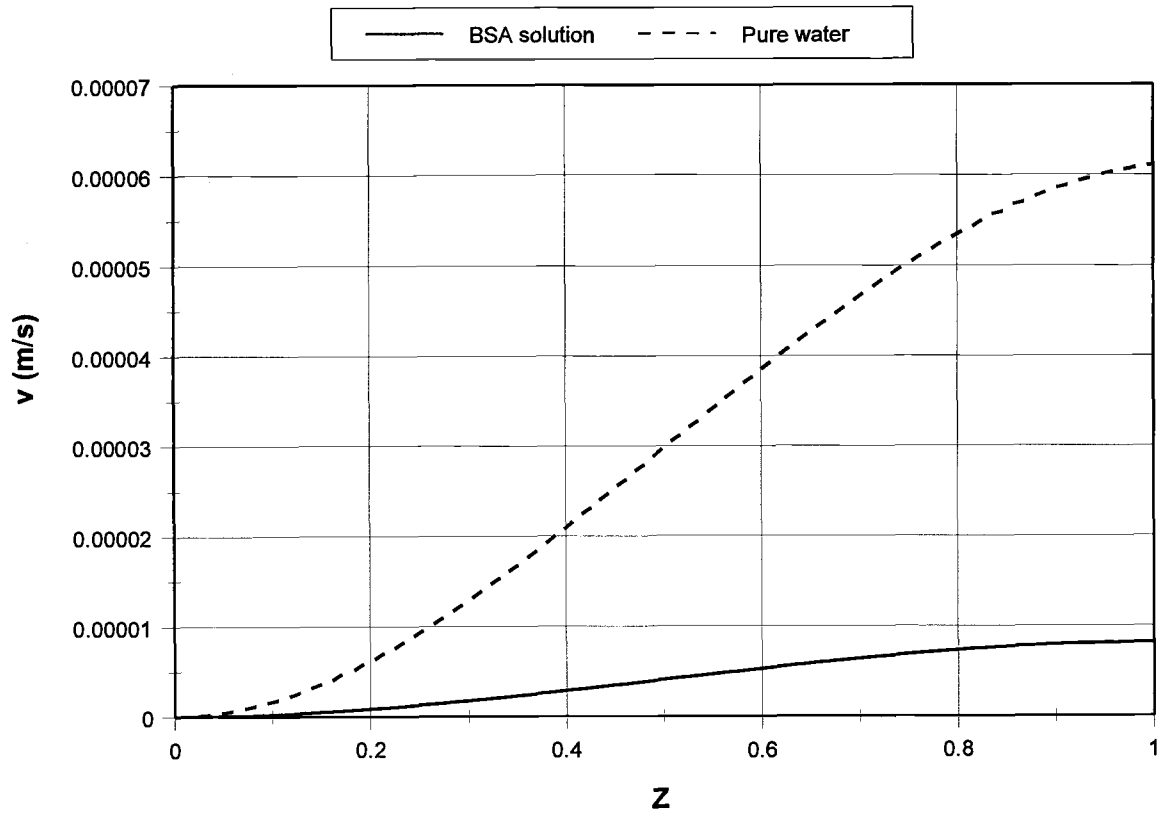
Fig. 56 The profiles of velocity component v at the cross section of R=0.5

Finite element analysis of concentration polarization in a radial crossflow device
Crossflow velocity

Z

X   Y

Crossflow velocity (u)

(10^-3)

7.5

2.5

0.00

0.20

0.40

0.60   R

0.80

Z

0.08333 <= R <= 1
0 < = Z <= 1
0 <= s(R, Z) <= 0.01238
Vol = 0.001729

Pdz0Plt12SurfSa: St=3 Gr=1 err=0.0008505
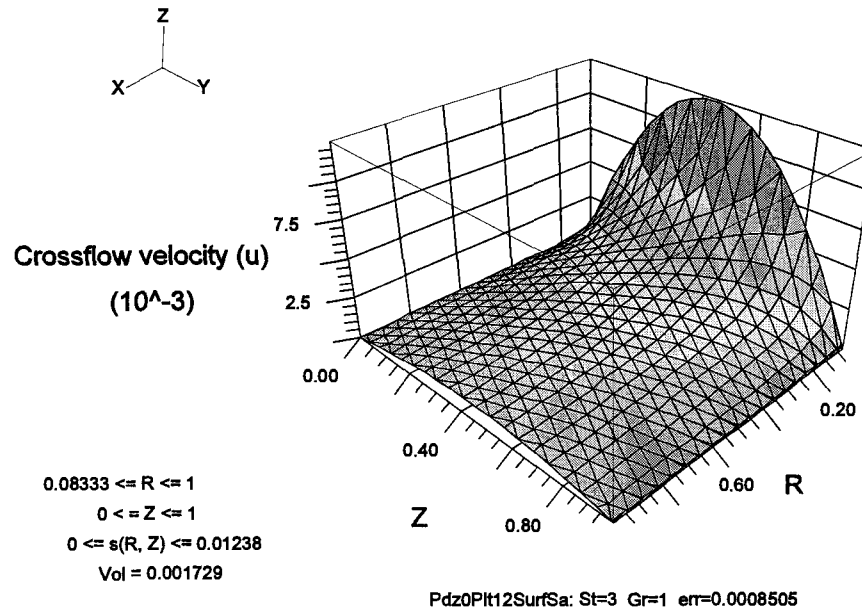
Fig. 57 Profile of velocity component u as a function of channel height Z and radius R

Finite element analysis of concentration polarization in a radial crossflow device

Transverse velocity (v)

Transverse velocity (v)
(10^-6)

8.0
6.0
4.0
2.0
0.00

0.08333 <= R <= 1
0 <= Z <= 1
0 <= s(R, Z) <= 8.17E-6
Vol=3.733E-6

0.20
0.40
0.60 R
0.80

Z

Pdz0Plt13SurfSa: St=3 Gr=1 err=0.0008505
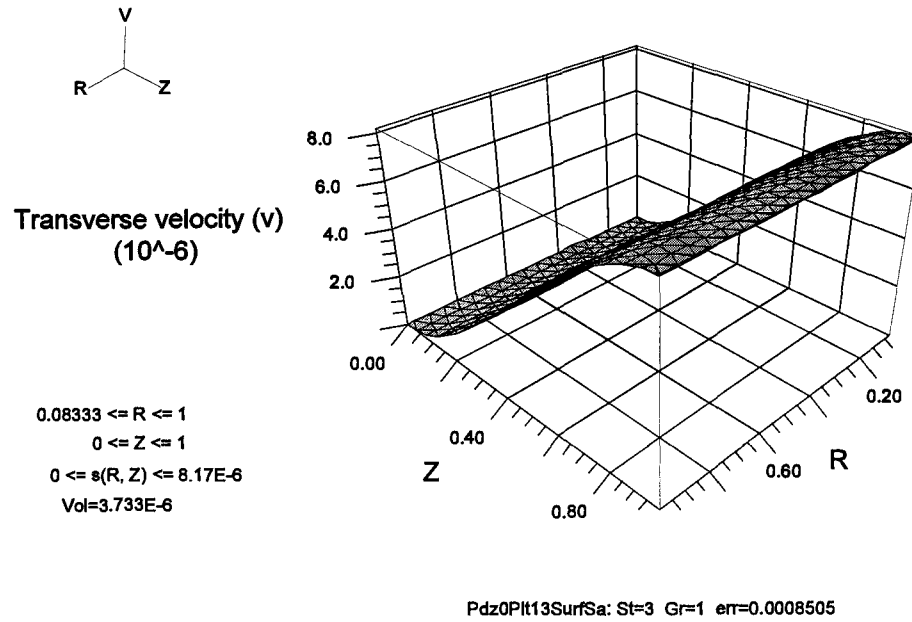
Fig. 58 Profile of velocity component v as a function of Z and radius R

5.4.3 Prediction of concentration polarization

A converged solution of Eq. 47 was obtained with 4137 nodal points and 2002 cells using the input data listed in Table 25. The error for the finite element analysis was 8.505 x 10^{-4}. In Fig. 59, at the cross section of R=0.5, the concentration profile as a function of Z is shown. The highest concentration was found right on the membrane surface, and was equal to 248.2 g/L. This value is very close to the interfacial BSA concentrations in the published literature (Cheryan, 1986; Viker et al., 1984; Li, 1984; Porter, 1979). The C_m estimated from Eq. 1 is 224.5 g/L, very close to the one predicted by the finite element method. Concentrations predicted by the finite element analysis agreed closely with the calculation from Eq. 1 for the runs under different hydrodynamic conditions (Table 26).

Concentration polarization within the flow channel only occurs in a small vicinity near the membrane surface, as illustrated in a three dimensional surface plot of C as a function of both horizontal and vertical positions (Fig. 60). The concentration polarization developed shortly after the feed flowed into the membrane channel (Fig. 61).

For the same average permeate flux, the magnitude of selected effective diffusion coefficients affects the thickness of the concentration boundary layer. According to the osmotic pressure model (Eq. 1), the interfacial solute concentration C_m is affected by the permeate flux. If the permeate flux remains the same, the mass transfer coefficient k (=D/δ) in the boundary layer is determined by both thickness (δ) and D (Eq. 1). The calculated thickness of the concentration boundary layer δ was affected by D (Fig. 62). A linear relationship between D and δ was found (Fig. 63). The mass transfer coefficient

Table 25 Input data for the finite element analysis

Parameters	Value
Channel height (m)	4.76×10^{-3}
Effective flow radius (m)	1.75×10^{-2}
Fluid flow rate (m^3/s)	3.96×10^{-7}
Average transmembrane pressure (Pa)	4.82×10^{4}
Diffision coefficient (m^2/s)	3.6×10^{-10}
Average permeate flux (m/s)	8.17×10^{-6}
Feed concentration (g/L)	0.25
Membrane permeability (1/m)	1.15×10^{-6}

Finite element analysis of concentration polarization in a radial crossflow device

Concentration

Curves:

a: C
Area: 2.357

0.08333 <= Z <= 1
0.2408 <= f(Z) <= 242.8
From (0.5,0) to (0.5,1)

04/06/97 - 18:55:14

Pdz0Mon07Elev
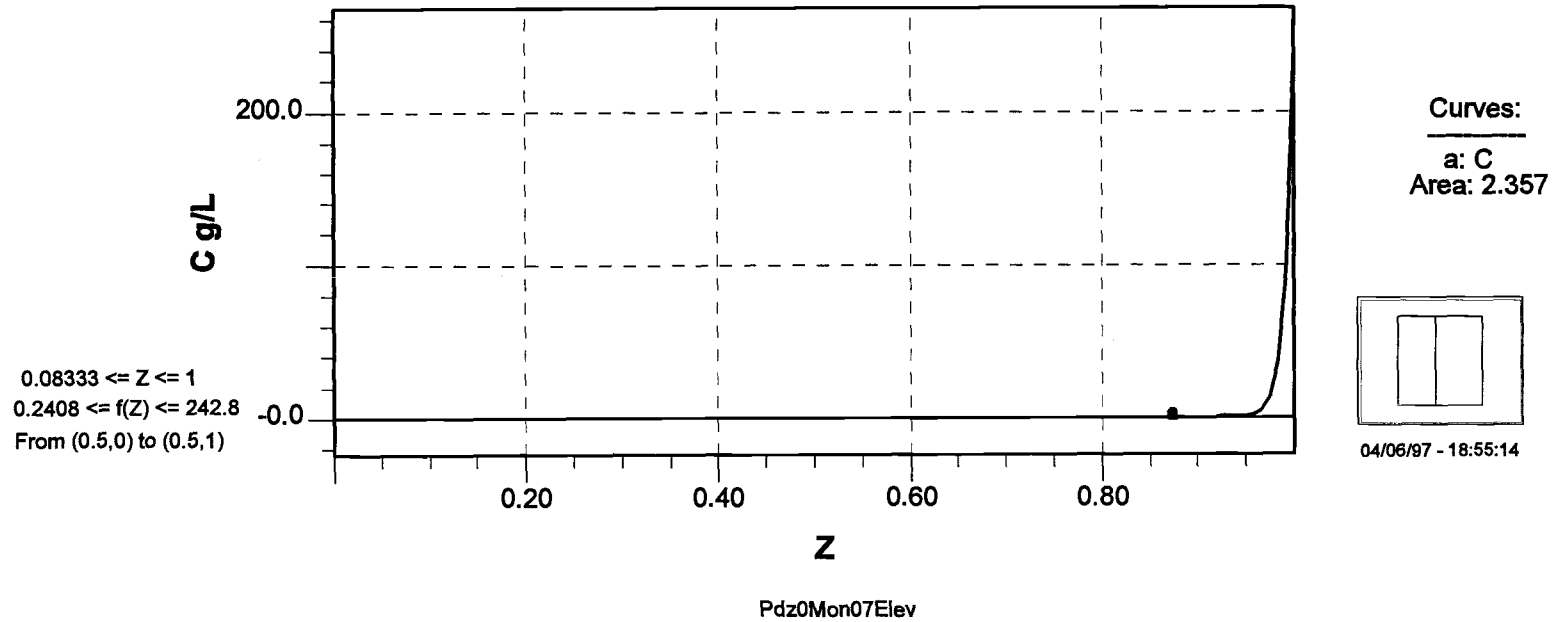
Fig. 59 Concentration as a function of Z at the cross section of R=0.5

Table 26. Comparisons of concentrations predicted by finite element analysis and calculated from Eq. 1

Run #	C_{mp} (g/L)*	C_{mc} (g/L)**	C_{mp}/C_{mc}
1	242.8	224.5	1.081
2	256.2	231.0	1.109
3	283.0	271.0	1.045

* Cm predicted by finite element analysis.
** Cm calculated from Eq. 1.

Finite element analysis of concentration polarization in a radial crossflow device

Concentration profile

C (g/L)

200.0

150.0

50.0

0.00

C

R   Z

0.08333 <= R <= 1

0< = Z <= 1

0.2208 <= s(R, Z) <= 242.8

Vol= 2.096

0.20

0.40

0.60   R

Z   0.80

PdzOPlt15SurfSa: St=1 Gr=3 err=0.0008519
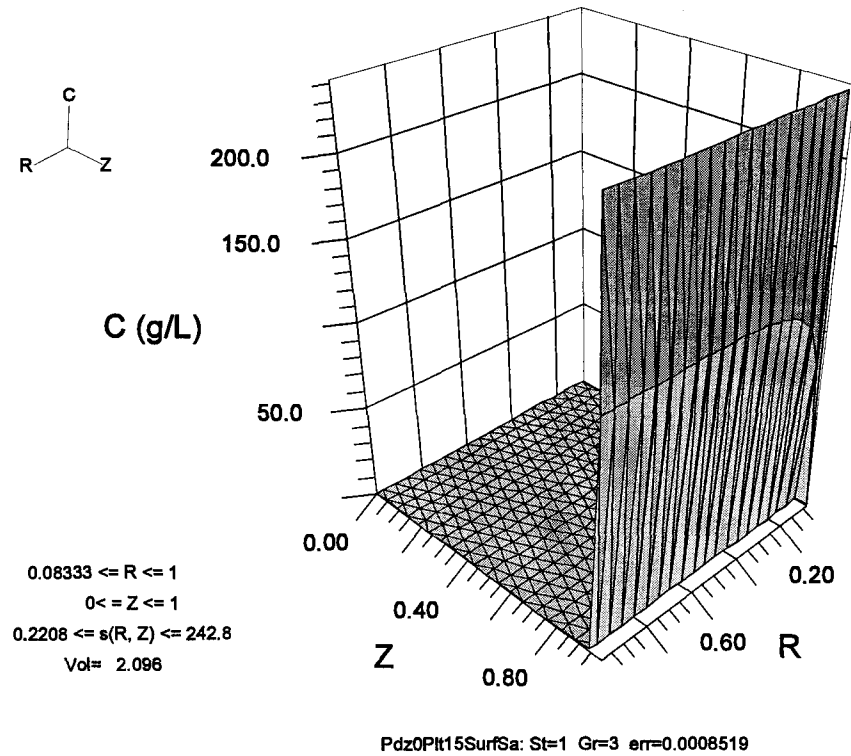
Fig. 60 Concentration profile in the membrane flow channel as a function of both horizontal and vertical positions
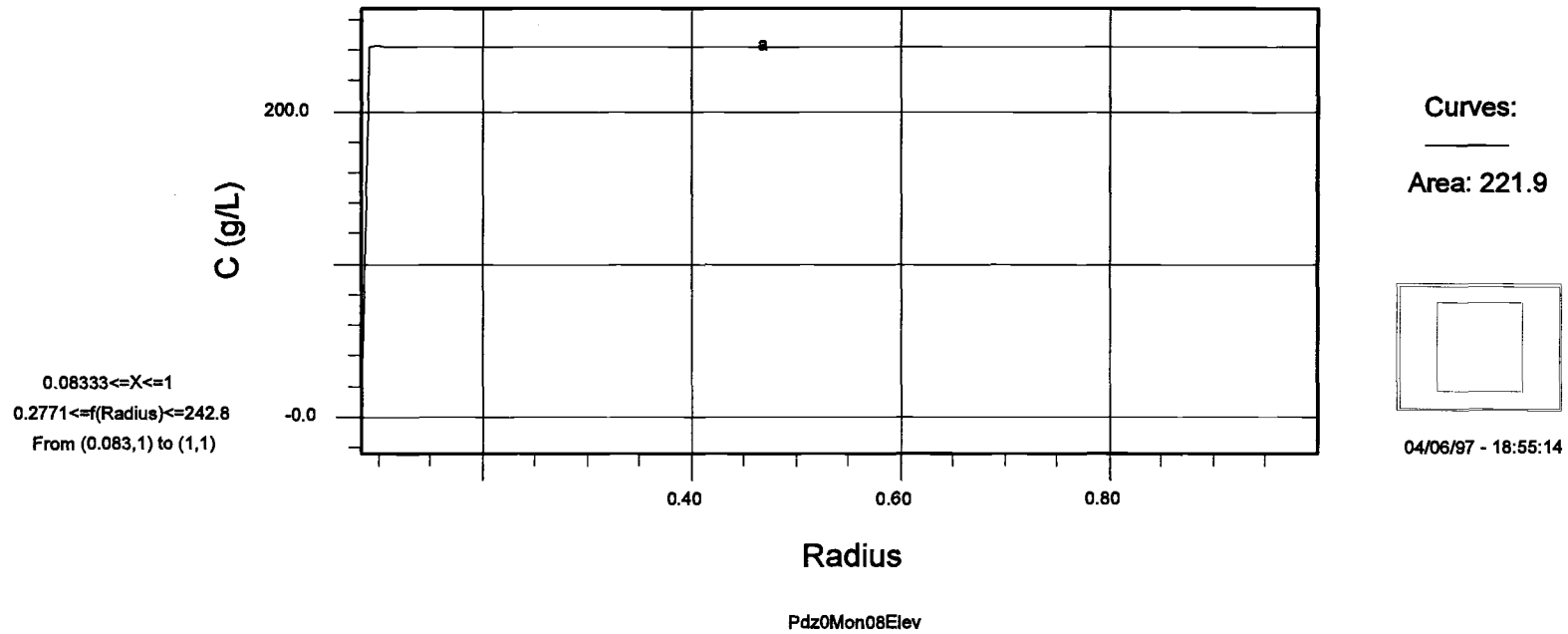
Fig. 61 Development of concentration polarization along the radius direction.
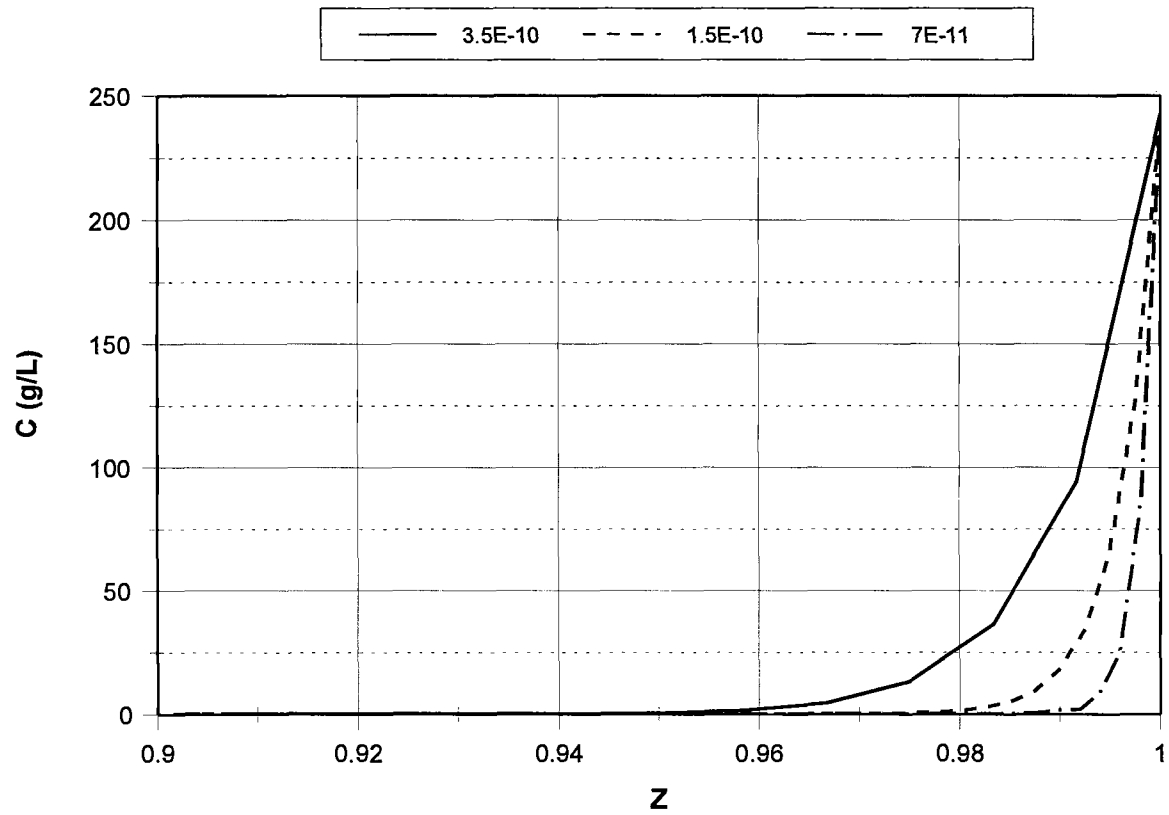
Fig. 62 Effect of effective diffusion coefficient on the thickness of the concentration boundary layer
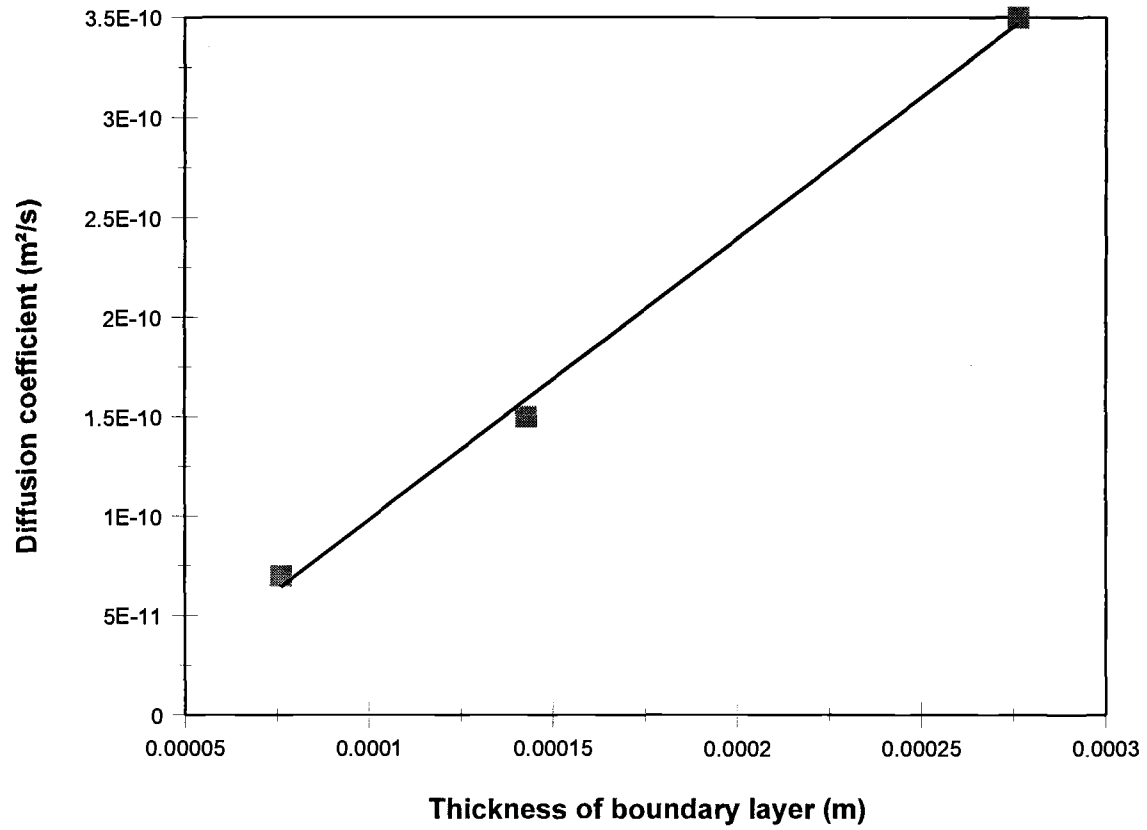
Fig. 63 Linear relationship between the calculated boundary layer thickness and diffusion coefficient

(1.410 x 10^{-6}) can be determined from the slope of Fig. 63 and is compared favorably with the one (1.19 x 10^{-6}) calculated with Eq. (3) using C_m obtained by the finite element analysis. Using the mass transfer coefficient and the value for C_m predicted in the finite element analysis, the permeate flux calculated from Eq. (3) is 9.70 x 10^{-6} m/s.

However, when a very small diffusion coefficient D is used, the concentration boundary layer becomes very thin. More meshes are needed in the vicinity of the membrane surface to obtain a quick and converged solution (Fig. 64). For a diffusion coefficient of 7.0 x 10^{-11} m^2/s, Eq. 47 was numerically solved using 21762 nodal points and 10653 cells.

In summary, based on the physical property of the solutes in the feed solution, the finite element method can accurately simulate the development of concentration polarization within the fluid flow channel and predict the BSA concentration (C_m) on the membrane surface. This method can be used to estimate the mass transfer coefficient and thickness of the concentration layer. It can also be used in the engineering analysis and design of ultrafiltration processes, and should provide useful information for designing a membrane filtration system.

Finite element analysis of concentration polarization in a radial crossflow device

Mesh generation for a small D

0.08333 <= R <= 1
0< = Z <= 1

Pdz0Plt07Grid: Gr=6 err=0.0006507
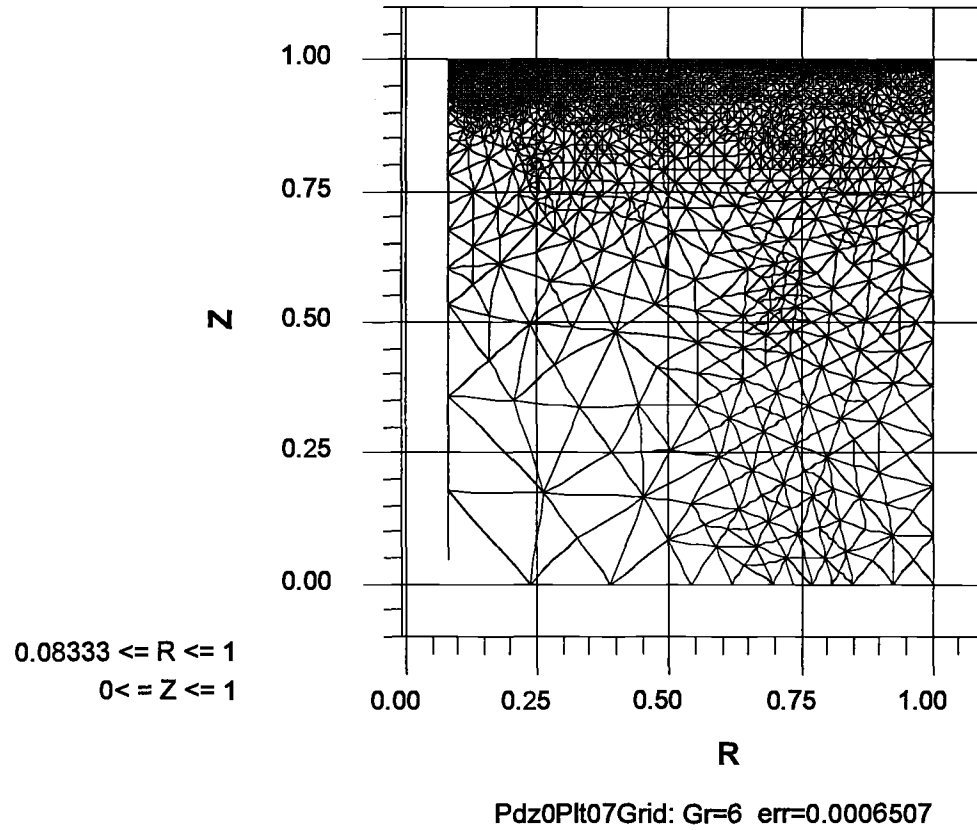
Fig. 64 Mesh generation for D = 7.0 x 10^{-11} m²/s

6. CONCLUSIONS

6.1 Audit of water consumption and waste water generation

The flow rates of waste water and the contribution of waste loads varied, depending on the sources in the surimi processing line. Waste water from the gutting operation and the first high speed dehydrator were the two major contributors of COD, BOD_5, and TS in the waste water. Although these two operations generated around 24% of the total waste water, 60% of the total solid waste was generated in these two operations. Overall, from the raw material stage to the frozen surimi stage of the processing, for each kg of fish processed, approximately 5.7 L of waste water was generated. About 0.051, 0.025, and 0.038 kg of COD, BOD_5, and TS, respectively, were generated for each kg of fish processed into frozen surimi. Although the waste water generated in Subsystem 2 was almost twice as much as that in Subsystem 1, the flow rates of solid wastes were similar. The total waste water generated in the processing plant was 750 m^3 per day, with 473 m^3 generated in the washing-dewatering processes.

6.2 Ohmic heating of surimi wash water

The ohmic heating study demonstrated the applicability of ohmic heating to coagulate fish proteins and partially purify proteolytic enzymes from surimi wash water. The study showed that temperature was a critical factor in controlling the degree of fish protein coagulation and in preserving the activity of the proteases. The relationship between temperature and heating time can be expressed using a second order polynomial

model, which indicates a linear heating rate (dT/dt) during ohmic heating. The electrical conductivity of the wash water was predicted as 0.353 S/m, which increased linearly with the heating temperature at a rate of 0.0106 S/m·°C. After heating and centrifuging, the residual solids (proteins, COD, TS, and TSS) concentration was found to follow Eq. (37). Suspended solids were more susceptible to heat. At 40°C, more than 80% TSS were removed, and at 60°C more than 90% TSS were removed. Reduction of protein concentration was more than 80% at 60°C. Heating did not cause a complete coagulation of proteins at 80°C. Some heat stable proteins, mainly those with molecular weights below 20,000 Dalton, remained in the supernatant. Due to coagulation of the heat sensitive fish proteins between 30 and 60°C, the specific activity of heat stable proteases increased linearly with the heating temperature. At 60°C, the protease activity was approximately 3 times that of the control, indicating that a partial purification of the enzymes was achieved at this temperature. At temperatures above 60°C, a significant loss of enzyme activity was observed due to heat denaturation. This temperature (60°C) may be the highest at which the activity of the proteases is preserved, while coagulating the majority of the fish proteins.

6.3 Microfiltration of surimi wash water

Microfiltration of surimi wash water started with high initial permeate fluxes, and rapidly reached a steady state with permeate fluxes ranging from 20 to 22 L/m²hr, which was twice the values reported by Jaouen et al.(1989 & 1990) and Jaouen and Quemeneur (1992). Although the characteristics of microfiltration membranes differed from each

other, no statistical differences were found for the effects of membrane materials or pore sizes on the steady state permeate fluxes. The microfiltration membranes were very porous for the surimi wash water with rejection coefficients between 40-60%. Membranes with large pore sizes (0.45 μm) showed smaller rejection coefficients than the ones with smaller pore sizes. Small rejection coefficients suggested that soluble proteins could be transmitted through the membrane pores, while larger particles were rejected by the membrane. Polysulfone microfiltration membranes with a pore size of 0.20 μm showed the highest rejection coefficient.

The process of microfiltration of surimi wash water can be modeled using the thin film theory. The estimated mass transfer coefficient 0.00258 ± 0.00052 and 0.00205 ± 0.00043 (L/m^{2}hr) for TS and TOS. Although the apparent rejection coefficient for TS was around 30-40%, the true rejection was 83.4%, indicating deposition of the protein layer on the membrane surface.

Analysis of experimental data from microfiltration of surimi wash water containing both soluble and suspended solids showed that the development of membrane fouling was a dynamic process starting with pore blocking at the initial stage of filtration, and followed by a continuous cake layer formation. At the initial pore blocking stage, the process can be modeled by the standard pore blocking law. The process of cake formation seemed to follow a newly proposed power law model:

$$J = \frac{1}{A}\frac{dV}{dt} = \frac{\Delta P \alpha \beta}{\mu} \frac{1}{V^{\frac{1}{\alpha}-1}}, \tag{76}$$

where α is a linear function of feed concentration, and β is a constant.

Although microfiltration membranes can be used to recover myofibrillar proteins, the permeate flux is very low due to pore blocking and cake formation. The low permeate flux may be an obstacle for a large scale application of microfiltration technology to recover myofibrillar proteins from a large volume of industrial surimi wash water. However, when ultrafiltration is used to treat the raw surimi wash water, the presence of large particles may cause a rapid development of membrane fouling due to the much higher pressure used in ultrafiltration (Cheryan, 1986). A pretreatment with microfiltration or other technologies is necessary prior to ultrafiltration.

6.4 Finite element analysis of ultrafiltration of diluted BSA solutions

Finite element analysis with Pdease2D® can be used to simulate the development of concentration polarization in the membrane flow channel during ultrafiltration of diluted BSA solutions. The predicted BSA concentration (C_m) on the membrane surface agreed with the theoretical value calculated based on the osmotic pressure model and the values in the published literature.

Selection of effective diffusion coefficients affects the thickness of the concentration boundary layer, but does not affect the prediction of C_m on the membrane surface for a given permeate flux. When a very small diffusion coefficient is used in finite element analysis, more meshes must be concentrated in the near vicinity of the membrane surface to cope with the steep concentration gradient. For a given permeate flux, linear relationship between diffusion coefficient and thickness of the concentration boundary layer was observed, which is in agreement with the theory.

Finite element analysis can be used to predict the mass transfer coefficient, which is an important parameter in engineering design and analysis of a membrane filtration (RO/UF) process.

6.5 Summary and recommendations for future research

The objectives of this research project were accomplished. Detailed information of water usage and waste water generation was gathered from a shore-based surimi processing plant and the results can be applied to other shore-based surimi operations. Water saving could be achieved by reducing the water supply in some unit operations, such as heading, gutting, mincing. More studies are needed to improve the fish mince washing efficiency.

The ohmic heating study has demonstrated its potential in coagulating fish proteins and purifying proteases from Pacific whiting surimi wash water. More than 80% of fish proteins could be removed from the wash water at temperatures above 60 °C. A 3-fold increase in the protease activity was found in the wash water after heating to 60°C. More studies should be done in applying this technology in extracting and purifying proteases from Pacific whiting wash water.

Microfiltration was used to recover myofibrillar proteins from surimi wash water. Under the test conditions, the permeate fluxes ranged from 20-22 L/m^{2}hr for four different membranes regardless of the different pore size and membrane materials. This study demonstrated that membrane fouling, which dramatically reduced the permeate flux, was caused by initial pore blocking and continuous cake formation. The cake resistance was

dominant throughout the pseudo-steady state filtration. A new continuous cake formation model was proposed and verified. Future studies are needed to develop an innovative membrane filtration process that can substantially reduce the cake formation on the membrane surface.

A new computer simulation method based on finite element analysis was used to accurately predict the mass transfer coefficient and solute concentration on the membrane surface during ultrafiltration of a single component protein solution. This method could be used in engineering design and analysis of membrane filtration process (ultrafiltration and reverse osmosis).

7. NOMENCLATURES

A_e effective electric conducting area of the electrodes (m^2)

A_m effective membrane filtration areas (m^2)

B   constant

B1   constant ($m_s/V_{po}\rho$), 1/L

BOD   biological oxygen demand (g/L)

C   solids (protein, COD, TS, and TSS) concentration (g/L)

C_b feed concentration (g/L)

C_m solute concentration on membrane surface (g/L)

C_p permeate concentration (g/L)

COD   chemical oxygen demand (g/L)

d   pore diameter (μm)

d_o initial pore diameter (μm)

d_p diameter of particles (m)

d_t pore diameter at time t (μm)

D   solute diffusion coefficient (m^2/s)

h   thickness of membrane (m)

H   height of a plate-and-frame membrane filter (m)

I   electric current (A)

J   permeate flux (L/m^2s)

J_o initial permeate flux (L/m^2s)

J_t permeate flux at time t (L/m^2s)

k	mass transfer coefficient (m/s)
K	constant, equal to $1/(J_o A_e)$
K_c	effective ohmic heating device coefficient
L_c	thickness of cake layer, m
L_e	distance between two electrodes (m)
m_s	amount of solids deposited on the internal walls of pores (kg/L)
N	total number of pore of membrane
p	pressure (Pa)
P	pressure (Pa)
Q	flow rate of water or waste water (L/s)
r	radius (m)
r_a	apparent rejection coefficient
r_t	true rejection coefficient
R	radius of a radial crossflow membrane filter (m)
R_c	cake layer resistance (1/m)
Re	Reynolds number (1/m)
R_m	resistance of a clean membrane (1/m)
R_{sc}	specific cake resistance ($1/m^4$)
R_t	total resistance (1/m)
Sc	Schmidt number
Sh	Sherwood number
t	filtration time (s)

t_c	reference time point at which flow stabilized (s)
T	heating temperature at time t (°C)
TS	total solids (g/L)
TSS	total suspended solids (g/L)
u	horizontal velocity component (m/s)
v	vertical velocity component (m/s)
V	permeate volume (L)
V_c	permeate volume at t_c, (L)
V_{po}	initial pore volume (m^3)
V_e	electric voltage (V)
α	constant, linear function of C
β	constant
δ	thickness of concentration polarization (m)
ε	porosity of membrane
γ	shear rate (1/s)
λ	dimensionless vertical distance
μ	viscosity of the feed (Pa.s)
π	osmotic pressure (Pa)
ρ_s	density of solids deposited on the pore walls (kg/m^3)
σ	apparent electrical conductivity (S/m)
τ	tortuosity of membrane
ξ	constant

REFERENCES

Anonymous. 1994. Industrial sewer account - monthly billing report. City of Albany, Oregon.

An, H., Peter, M. Y., Seymour, T. A., and Morrissey, M. T. 1995. Isolation and activation of Cathepsin L- commplex from Pacific whiting (*Merluccius productus*). J. Agric. Food Chem. 43, 337-330.

An, H., Weerasinghe, V., Seymour, T. A., and Morrissey, M. T. 1994a. Cathepsin degradation of Pacific whiting surimi proteins. J. Food Sci. 59, 1013-1017, 1033.

An, H., Seymour, T. A., Wu, J, and Morrissey, M. T. 1994b. Assay systems and characterization of Pacific whiting. J. Food Sci. 59, 277-281.

AOAC, 1995. AOAC Official Method 938.08. In *Official Methods of Analysis of AOAC International, 16th Edition*, (P. Cunniff, ed). AOAC International, Arlington, VI.

Babbitt, J., Repond, K., Hardy, A., Zetterling, T., and Swafford, T. C. 1985. Effect of washing on the composition and functional stability of minced pollock flesh. *In Proceedings of International Symposium on Engineered Seafood Including Surimi. Nov. 19-21, 1985. Seattle, WA*, R. E. Martin and R. L. Collette (Eds), National Fishery Institute, Washington, DC, p 117-128.

Baker, A. J. and Pepper, D. W. 1991. *Finite Elements 1-2-3*. McGraw-Hill, Inc. New York.

Belfort, G. Davis, R. H. and Zydney, A. L. 1994. The behavior of suspensions and macromolecular solutions in crossflow microfiltration. J. Memb. Sci. 96: 1-58.

Benjakul, J., Seymour, T. A., Morrissey, M. T., and An, H. A. 1996. Proteinase in Pacific whiting surimi wash water: identification and characterization. J. Food Sci. 61: 1165-1170.

Berman, A. S. 1953. Laminar flow in channels with porous walls. J. Applied. Phys. (24): 1232-1235.

Bhattacharyya, D., William, M., Ray, R. J., and McCray, S. B. 1992. Chapter 23 Design. In *Membrane Handbook*, (W. S. W. Ho and K. K. Sirkar, eds), Van Nostrand Reinhold, New York.

Biotol, 1992. Product Recovery in Bioprocess Technology, published on behalf of Open Universiteit and Thames Polytechnic, Butterworth-Heinemann Ltd.

Biss, C. H., Coombes, S. A. and Skudder, P. J. 1989. The development and application of ohmic heating for the continuous processing of particulate food stuffs. In *Process Engineering in the Food Industry*, (R. W. Field and J. A. Howell, eds), p. 17-27, Elsevier, London.

Blanpain, P., Hermia, J., and Lenoel, M. 1993. Mechanisms governing permeate flux and protein rejection in the microfiltration of beer with a Cyclopore membrane. J. Membrane Sci. (84): 37-51.

Blatt, W. F., David, A., Michaels, A. S., and Nelson, L. 1970. Solute polarization and cake formation in membrane ultrafiltration: Causes, consequence, and control techniques, In *Membrane Science and Technology*, (J. E. Flinn, ed), Plenum Press, New York.

Bouchard, C. R., Carreau, P. J., Matsuura, T., and Sourirajan, S. 1994. Modeling of ultrafiltration: prediction of concentration polarization effects. J. Membrane Sci. (97) 215-229.

Bough, W. A., Landles, D. R., Miller, J, Young, C. T., and McWhorter. 1975. Utilization of chitosan for recovery of coagulated by-products from food processing wastes and treatment systems. In *Proceedings of the Sixth National Symposium on Food Processing Wastes*, April 9-11, 1975. Madison, WI.

Bowen, W. R. 1993. Understanding flux patterns in membrane processing of protein solutions and suspensions. Trends in Biotech. (11): 451-460.

Bowen, W. R. and Gan, Q. 1991. Properties of microfiltration membranes: flux loss during constant pressure permeation of bovine serum albumin. Biotech. and Bioeng. (38): 688-696.

Bowen, W. R. and Gan, Q. 1992. Properties of microfiltration membranes: the effects of adsorption and shear on the recovery of an enzyme. Biotech. And Bioeng. (40): 491-497.

Bowen, W. R. and Hall, N. J. 1995. Properties of microfiltration membranes: mechanisms of flux loss in the recovery of an enzyme. Biotech. And Bioeng. (46): 28-35.

Brian, P. L. T. 1965. Concentration polarization in reverse osmosis desalination with variable flux and incomplete salt rejection. Ind. Eng. Chem. Fundam. (4) 439-445.

Brian, P. L. T. 1966. Mass transport in reverse osmosis. In Desalination by Reverse Osmosis, (U. Merten, ed), MIT Press, Cambridge, MA.

Chao, A. C., Machemehl, J. L., and Galarrange, E. 1980. Ultrafiltration treatment of seafood processing wasterwaters. In *Proc. 35th Industrial Waste Concerence*, Purdue University, p 560-570.

Chao, A. C., Tzou, L, and Young, C. T. 1983. Recovery and application of solids from crab-processing wastewater. In *Proc. 38th Industrial Waste Conference*, Purdue University, p 829-838.

Chao, A. C. , Tzou, L., and Green, D., 1984. Modeling of ultrafiltration for treating fishery wastewaters. In *Proc. 39th Industrial Wastes Conference*, Purdue University, p 555-563.

Cheftel, J. C., Cuq, J. L., and Lorient, D. 1985. Amino acids, peptides, and proteins. In *Food Chemistry*, (O. R. Fennema, ed), Marcel Dekker, Inc., p. 245-369.

Cheryan, M. 1986. Ultrafiltration Handbook. Technomic Publishing Co, Inc. Lancaster, PA.

Cheryan, M. And Merin, U. 1980. A study of the fouling phenomena during ultrafiltration of cottage cheese whey. In *Ultrafiltration membranes and Applications*, (A. R. Cooper, ed), Pleunum Press, New York, p. 619.

CH2M Hill. 1993. Reviews of environmental management options at Inland Quick Freeze Albany Oregon. Prepared for Pacific Power & Light Company.

Cocci, A. A., Wilson, D. R., and Landine, R. C. 1991. Anaerobic treatment of clam processing wastewater. In *Proceedings of Seafood Environmental Summit- A Portion of the Seafood and the Environment Symposium*, Raleigh, NC.

Colton, C. K., Henderson, L. W. Ford, C. A. 1975. Kinetics of hemodiafiltration. I. In Vitro transport characteristics of a hollow-fiber blood ultrafilter. J. Lab. Clin. Med. 85: 355

Cowan , J. A. C., MacTavish, F., Brouckaert, C. J. and Jacobs, E. P. 1992. Membrane treatment strategies for red meat abattoir effluents. Water. Sci. Tech. 25(10): 137-148.

Dalrymple, C. W. 1994. Use of electrocoagulation for wastewater treatment. In: Wastewater Technology Conference and Exhibition. Conference Proceedings. Hotel Vancouver, Vancouver, British Columbia, Canada.

de Alwis, A. A. P., and Fryer, P. J. 1990. The use of direct resistance heating techniques in the food industry. J. Food Eng. 11, 3-27.

Drukker, W., Parsons, F. M., and Maher, J. F. 1983. Replacement of renal function by dialysis. Martinus Nijhof, Boston.

Dziezak, J. D. 1990. Membrane separation technology offers processors ultimated potential. Food Tech. (9): 108-113).

Eckstein, E. C., Bailey, D. G., and Shapiro, A. H. 1977. Self-diffusion of particles in shear flow of a suspension. J. Fluid. Mech. 79: 191.

Edwards, R. H. and Kohler, G. O. 1981. Heating of proteinaceous liquids. US. Patent No 4,421,682.

Forsht, E. H. 1974. Development document for effluent limitation guidelines and new sources performance standards for the catfish, crab, shrimp and tuna segment of the canned and preserved seafood processing source categories. EPA-44071-74-0290-1, U.S. Environmental Protection Agency, Washington, DC.

Fresenius, W., Schneider, W., Bohnke, B., and Poppingaus, K. 1989. Waste water technology - origin, collection, treatment and analysis of waste water. Springer-Verlag, Berlin and Heidelberg, Germany.

Ganguly, S. And Bhattacharya, P. K. Development of concentration profile and prediction of flux for ultrafiltration in a radial cross-flow cell. J. Membrane Sci. (97): 185-198.

Gekas, V. And Hallstrom, B. 1987. Mass transfer in the membrane concentration layer under turbulent flow. J. Membrane Sci. 30: 153.

Gibbs, C. R. 1979. Introduction to chemical oxygen demand. Technical information series - Booklet No. 8. Hach Chemical Co. Loveland, Co.

Goel, V., Accomazzo, M. A., Dileo, A. J., Meier, P., Pitt, A., and Pluskal, M. 1992. Dead-end microfiltration: application, design, and cost. In *Membrane Handbook*, (W. S. W. Ho and K. K. Sirkar, eds), Van Nostrand Reinhold, New York.

Greenberg, A. E., Trussell, R. R., Clesceri, L. S. 1980. Standard methods for the examination of water and waste water. 15th Edition. APHA (American Public Health Association), AWWA (American Pollution Water Works Association), and WPCF (Water Pollution Control Federation). Washington, D.C.

Harrison, T. D., Boardman, G. D., and Flick, G. J., 1992. Characterization and treatment of wastes from blue crab processing facilities. In *Proc. 42th Industrial Waste Conference*, Purdue University, p 775-788.

Hopkins, K. 1983. Case histories: pretreatment of poultry processing wastewater. In: *Proc. 38th Industrial Waste Conference*, Purdue University, West Lafayette, Indiana.

Huang, L. Chen, Y., and Morrissey, 1996. Coagulation of fish proteins from frozen fish mince wash water by ohmic heating. J. Food Proc. Eng. (In press).

Huang, L. and Morrissey, M. T. 1997a. Application of ohmic heating to coagulate proteins and partially concentrate proteolytic enzymes in surimi wash water. Submitted to J. of Aquatic Food Product Technology.

Huang, L. And Morrissey, M. T. .1997b. Fouling of membranes during microfiltration of surimi wash water: roles of pore blocking and surface cake formation. Submitted to J. of Membrane Science.

Huang, L. Santos, M. Singh, P. R., and Morrissey, M. 1997. Characterization of waste water from the surimi processing industry. To be submitted to J of Aquatic Food Product Technology.

Hultin, H. O. 1985. Characteristics of muscle tissue. In *Food Chemistry*, 2nd edition, (O. R. Fennema, ed). Marcel Dekker, Inc. New York and Basel.

Ingham, K. C., Busby, T. F. Sahlestrom, Y., and Castino, F. 1980. Separation of macro molecules by ultrafiltration: Influence of protein adsorption, protein-protein interaction and concentration polarization, In *Ultrafiltration membranes and Applications*, (A. R. Cooper, ed), Pleunum Press, New York, p. 141.

Iritani, E., Hayashi, T., and Murase, T. 1991. Analysis of filtration mechanism of crossflow upward and downward ultrafiltration. J. Chem Eng. Japan (24): 39-44.

Ismond, A. 1994. How to do a seafood processing plant water, waste, and wastewater audit. Aqua-Terra Consultants. Seattle, WA.

Ismond, A. 1997. Personal communication. Aqua-Terra Consultants. March 1997. Seattle, WA.

Jaouen, P., Bothorel, M., and Quemeneur, F. 1989. Recovery of soluble proteins by membrane separation process: Performances and membrane cleaning. In *Preprints: 6th International Symposium on Synthetic Membranes in Science and Technology*, September 4-8, 1989, Thubingen, Germany.

Jaouen, P., Bothorel, M., and Quemeneur, F. 1990. Treatment of seafood processing effluents through microporous membranes - applications and prospects. In *Proc. of International Congress on Membranes and Membrane Process*. Chicago, USA.

Jaouen, P. and Quemeneur, F. 1992. Membrane filtration for waste-water protein recovery. In *Fish Processing Technology*, (G. M. Hall, ed), Blackie Academic & Professional, published in North America by VCH Publishers, Inc., New York.

Johnson, H. M. 1996. 1996 Annual report on the United States Seafood Industry. H. M. Johnson & Associates.

Johnson, R. A. and Gallanger, S. M. 1984. Use of coagulants to treat seafood processign wastewaters. J. Water. Pollution Control Federation (56):970-976.

Kasper, D. R. and Reichenberger, J. C. 1983. Use of polymers in the coagulation process. In *Proc. of AWMA Seminar on Use of Organic Polyelectrolytes in Wate Treatment*, Las Vegas, NE.

Kawakatsu, T., Nakao, S., and Kimura, S. 1993. Effect of size and compressibility of suspended particles and surface pore size of membrane on flux in crossflow filtration. J. Membrane Sci. (81): 173-190.

Kleinstreuer, C. and Paller, M. S. 1983. Laminar dilute suspension flows in plate-and-frame ultrafiltration units. AICHE Journal (28) 529-533.

Knorr, D. 1991. Recovery and utilization of chitin and chitosan in food processing waste management. Food Tech. (1): 114-122.

Kolff, W. J. and Berk, H. T. 1944. The artificial kidney: a dialyzer with a great area. Acta Med. Scan. 117:121-134.

Laemmli, U. K. 1970. Cleavage of structural protein during the assembly of the head of bacteriophage T4. Nature 227: 680-685.

Lebrun, R. E., Bouchard, C. R., Rollin, A. L., Matsuura, T., and Sourirajan, S. 1989. Computer simulation of membrane separation processes. Chemical Eng. Sci. (44) 313-320.

Lee, C. M. 1984. Surimi process technology. Food Tech. (11): 69-80.

Lee, C. M. 1985. A pilot plant study of surimi-making properties of red hake. Paper No. 20., presented at International Symposium on Engineered Seafood Including Surimi, Seattle, WA., Nov 19-21.

Lee, C. M., 1986. Surimi manifacturing and fabrication of surimi-based products. Food Tech. (3):115-124.

Lee, D. N. and Merson, R. L. 1975. Examination of cottage cheese whey protein by scanning electron microscopy: Relationship to membrane fouling during ultrafiltration. J. Dairy Sci. 48(10) 1423.

Li, N. N. 1984. Membrane processes. In *Perry's Chemical Engineers' Handbook*, (R. H. Perry, D. W. Green, and J. O. Maloney, eds). McGraw-Hill chemical engineering series. McGraw-Hill, Inc., New York.

Lin, T. M., Park, J. W., and Morrissey, M. T. 1995. Recovered protein and reconditioned water from surimi processing waste. J. Food Sci. 50(1):6-9.

Lin, T. M. 1996. Solubility and structure of fish myofibrillar proteins as affected by processing parameters. Doctoral Thesis. Department of Food Science and Technology, Oregon State University. Corvallis, OR.

Lind, C. 1995. A coagulant road map. Public Work (3):36-38.

Longsdale, H. K. 1983. Reverse osmosis. In *Synthetic Membranes: Science, Engineering and Application*, (P. M. Bungay, H. K. Longsdale, and M. N. De Pinho, eds). NATO ASI Series. Series C, Mathematical and physical sciences; Vol. 181.

Lowry, O. H., Rosebrough, N. J., Farr, A. L., and Randall, R. J. 1951. Protein measurement with Folin phenol reagent. J. Biol. Chem. (193):256-257.

Ludlow, M. 1997. Personal communication. Natural Biopolymers, Inc. January 1997. Raymond, WA.

Madsen, R. F. 1977. *Hyperfiltration and Ultrafiltration in plate-and-frame systems.* Elsevier Scientific Publishing Co.

Mannapperuma, J. D., Mate, J. I., and Singh, R. P. 1993. Reduction of environmental impact and energy use through water recycling and by-product recovery in food processing, final report prepared for the California Institute for Energy Efficiency. Department of Agricultural Engineering, University of California, Davis. Davis, CA.

Marshall, A. D., Munro, P. A., and Tragardh, G. 1991. The effect of protein fouling inmicrofiltration and ultrafiltration on permeate flux, protein retention and selectivity: A literature review. Desalination 91: 65-108.

Martin, D. W. 1983. Membranes. In *Harper's Review of Biochemistry*, 19th edition, (D. W. Martin, Jr., P. A. Mayes, and V. W. Rodwell, eds), Lange Medical Publications, Los Altos, CA.

Mate, J. I. 1992. Accounting and simulation of waste water use and recycling in food processing. M.S. Thesis. Department of Agricultural Engineering. University of California, Davis. Davis, CA 95616.

Matsumoto, J. J. 1978. Minced fish technology and its potential for developing countries. In *Proceedings on Fish Utilization Technology and Marketing*, Vol. 18, Sec III, p. 267. Indo-Pacific Fishery Commision. Bankok. Thailand.

Matthiasson, E. 1983. The role of macromolecular adsorption in fouling of ultrafiltration membranes. J. Membrane Sci. 16: 23-36.

Mikkelson, K. A. And Lowery, K. W. 1992. Desogning a sequential batch reactor system for the treatment of high strength meat processing wastewater. In *Proc. 47th Industrial Waste Conference*, Purdue University, West Lafayette, Indiana.

Mir, L., Michael, S. L., and Goel, V. 1992a. Crossflow microfiltration: application, design, and cost. In *Membrane Handbook*, (W. S. W. Ho and K. K. Sirkar, eds), Van Nostrand Reinhold, New York.

Mir, L., Michael, S. L. Goel, V., and Kaiser, R., 1992. Crossflow microfiltration: applications, design, and cost. In *Membrane Handbook*, (W. S. W. Ho and K. K. Sirkar, eds), Van Nostrand Reinhold, New York.

Miyata, Y. 1984. Concentration of protein from the wash water of red meat fish by ultrafiltration membrane. Bull. of the Japan. Soci. of Sci. Fish. 50 (4): 659-663.

Mohr. C. M., Engelgau, D. E., Leeper, S. A., and Charboneau, B. L. 1989. Membrane applications and research in food processing. Noyes Data Corp. Park Ridge, NJ.

Muhuriji, M., Faggard, G., Van Der Mast, V., and Iamai, H. 1989. Jeddah I RO plant - Phase I 15 MGD reverse osmosis plant. Desalination 76: 75.

Mulder, M. 1990. *Basic Principles of Membrane Technology*. Kluwer Academic Publishers. The Netherlands.

Murase, T., Ohn, T., and Kimtat, K. 1995. Filtrate flux in crossflow microfiltration of dilute suspension forming a highly compressible fouling cake-layer. J. Membrane Sci. (108): 121-128

Nakao, S. Wijmans, J. G., and Smolders, C. A. 1986. Resistance to the permeate flux in unstirred ultrafiltration filtration of dissolved macromolecular solutions. J. Membrane Sci. (26): 165-178.

Nilson, J. L. 1990. Protein fouling of UF membranes: causes and consequences. J. Membrane Sci. 52: 121-142.

Ninomiya, K., Ookawa, T., Tsuchiya, T., and Matsumoto. 1985. Recovery of water soluble protein in waste wash water of fish processing plants of Ultrafiltration. Bull. of the Japan. Soci. of Sci. Fish. 51(7): 1133-1138.

Okada, M. 1992. History of surimi technology. In *Surimi Technology*, (T. C., Lanier and C. M., Lee, eds), Marcel Dekker, Inc. New York, pp. 3-39.

Pacheco-Aguilar, R., Crawford, D. L., and Lampila, L. E. 1989. Procedures for the efficient washing of minced whiting (Merluccius products) flesh for surimi production. J. Food Sci. 54: 248-252.

Palaniappan, S. and Sastry, S. K. 1991a. Electrical conductivity of selected solid foods during ohmic heating. J. Food Process Eng. 14, 221-236.

Palaniappan, S. and Sastry, S. K. 1991b. Electrical conductivity of selected juices: Influences of temperature, solids content, applied voltage, and particle size. J. Food Process Eng. 14, 247-260.

Park, J. W. 1997. Personal communication. March 1997. Oregon State University Seafood Laboratory, Astoria, OR.

Paulson, D. J., Wilson, R. L., and Spatz, D. D. 1984. Crossflow membrane technology and its applications. Food Tech. (12): 77-111.

Pearce, R. J. 1992. Whey protein recovery and whey protein fractionation. In *Whey and lactose processing*, (J. G. Zalow, ed)., Elsevier Science Publishing Co. Inc., New York.

Perry, R. H., Green, D. W., and Maloney, J. O. 1984. Perry's Chemical Engineers' Handbook. McGraw-Hill, Inc., New York.

Peters, G. 1997. Personal communications. Alyeska Seafoods. Dutch Harbor, Alaska.

Petersons, L. D. 1990. Product recovery from surimi wash water. In *Making Profits out of Seafood Wastes: Proceedings of the International Conference on Fish By-Product*, (S. Keller, ed), Anchorage, Alaska.

Porter, M. C. 1972. Concentration polarization with membrane ultrafiltration. Ind. Eng. Chem. Prod. Res. Dev, 11: 234.

Porter, M. C. 1979. Membrane filtration. In *Handbook of Separation techniques for Chemical Enggineers*, (P. A. Schweitzer, ed). McGraw-Hill

Radtke, H. 1995. Windows on Pacific whiting: An economic success story for Oregon's fishing industry. Oregon Coastal Zone Management Association, Newport, OR.

Rautenbach, R. And Albrecht, R. 1989. Membrane Process. John Willey & Sons.

Redkar, S. G. and Davis,R. H. 1993. Crossflow microfiltration of yeast suspensions in tubular filters, Biotechnol. Prog. (9) 625-634.

Regier, W. L., Ernst, R. C., and Hale, M. B. 1985. Processing requirements for the preparation of minced intermediates or surimi from menhaden. In *Proceedings of the International Symposium On Engineered Seafood Including Surimi. November 19-21, 1985. Seattle, WA*, R. E. Martin and R. L. Collette (Eds), National Fisheries Institute, Washington, D.C., pp 129-140.

Renner, E. and Abd EI-Salam, M. H. 1991 *Application of Ultrafiltration in the Dairy Industry*. Elsevier Science Publishers Ltd.

Rusten, B., Eikebrokk, B., and Thorvaldsen, G. 1990. Coagulation as pretreatment of food industry wastewater. Wat. Sci. Tech. 22 (9): 1-8.

Sandu, C., and Singh, R. K. 1991. Energy increase in operation and cleaning due to heat exchanger fouling in milk pasteurization. Food Tech. 45(12), 84-91.

Sastry, K. S. and Palaniappan, S. 1992. Ohmic heating of liquid-particle mixtures. Food Tech. 46(12), 64-67.

Seymour, T. A., Morrissey, M. T., Peters, M. Y., and An, H. 1994. Purification and characterization of Pacific whiting proteases. J. Agric. Food Chem. 42, 2421-2427.

Shoji, T., Nakajima, M., Nabetani, H., Ohtani, T., and Watanabe, A. 1988. Effect of pore size of ceramic support on the self-rejection characteristics of the dynamic membrane formed with water soluble proteins in waste water. Nippon Nogeikagaku Kaishi 62 (7): 1055-1060.

Singh,R. And Laurence, R. L. 1979. Influence of slip velocity at membrane surface on ultrafiltration performance: I. Channel flow system. Int. J. Heat Mass Transfer (22) 721.

Stirling, R. 1987. Ohmic heating - a new process for the food industry. Power Eng. J. 6, 365-369.

Suki, A., Fane, A. G. F., and Fell, C. J. D. 1984. Flux decline in protein ultrafiltration. J. Memb. Sci. 21: 269-283.

Swafford. T. C., Babbitt, J, Reppond, K., Hardy, A., Riley, C. C., and Zetterling, T. K. A. 1985. Surimi process yield improvement and quality contribution by centrifuging. In *Proceedings of the International Symposium On Engineered Seafood Including Surimi. November 19-21, 1985. Settle, WA*, R. E. Martin and R. L. Collette (Eds), National Fisheries Institute, Washington, D.C., pp483-496.

Tanaka, T., Kamimura, R., Itoh, K., and Nakanishi, K. 1993. Factors affecting the performance of crossflow filtration of yeast cell suspensions. Biotech. And Bioeng. (41): 617-624.

Toyoda, K., Kimura, I., Fujita, T., Noguchi, S. F., and Lee, M. 1992. The surimi manufacturing process. In: *Surimi Technology*, T. C., Lanier and C. M., Lee (Eds), Marcel Dekker, Inc. New York, pp. 79-112.

U.S. Environmental Protection Agency 1967. Evaluation of Waste Disposal Practices of Alaskan Seafood Processors. Office of Enforcement, EPA-33012-75-001, Washington.

Van den berg, G. B. And Smolders, C. A. 1988. Flux decline in membrane processes. Filtration & Filtration (March/April): 115-121.

Viker, V. L., Colton, C. K., and Smith, K. A. 1981. The osmotic pressure of concentrated protein solutions: Analysis of concentration polarization and solution pH dependence for bovine serum albumin in saline solution. J. Colloid Interface Sci. (79) 548.

Viker, V. L., Colton, C. K., Smith, K. A., and Green, D. L. 1984. The osmotic pressure of concentrated protein and lipoprotein solutions and its significance to ultrafiltration. J. Membrane Sci. (20) 63.

Watanabe, T. 1974. Treatment of waste solutions containing animal blood. Japan Kokai No. 74, 79,052.

Watanabe, H., Takai, R., Sekigawa, A., and Hasegawa, H. 1982. An estimation of the amount of protein lost in the effluent from frozen surimi manufacture. Bull. Jap. Soc. Fish. 48: 869.

Watanabe, A., Ohtani, T., Horikita, H., Ohya, H., and Kimura, S. 1986. Recovery of soluble protein from fish jelly processing with self-rejection dynamic membrane. In *Food Engineering Process Applications*, (L. Le Maguer and P. Jelen, eds), Vol 2. P. 225-236.

Watanabe, A., Shoji, T., Nakajima, M., Nabetani, H., and Ohtani, T. 1988. Electronmicroscopic observation of self-rejection type dynamic membrane formed with water soluble proteins in waste water from fish paste process. Nippon Nogeikagaku Kaishi 62 (7) 1061-1066.

Wojcik, C. 1983. Desalination of water in Saudi Arabia by reverse osmosis performance study. Desalination 46:17.

Zydney, A. L. And Colton, C. K. 1986. A concentration polarization model for the filterate flux in cross-flow microfiltration of particulate suspensions. Chem. Eng. Commun. 47: 1-21.